Distribution Agreement

In presenting this thesis or dissertation as a partial fulfillment of the requirements for an advanced degree from Emory University, I hereby grant to Emory University and its agents the non-exclusive license to archive, make accessible, and display my thesis or dissertation in whole or in part in all forms of media, now or hereafter known, including display on the world wide web. I understand that I may select some access restrictions as part of the online submission of this thesis or dissertation. I retain all ownership rights to the copyright of the thesis or dissertation. I also retain the right to use in future works (such as articles or books) all or part of this thesis or dissertation.

Signature:

Patrick Reeves 11/15/09

_____ _____

Date

Disabling Poxvirus Pathogenesis

By

Patrick M. Reeves
B.S.

Advisor: Daniel Kalman, Ph.D.

An abstract of

A dissertation submitted to the Faculty of the Graduate School of Emory University in partial fulfillment of the requirements for the degree of

Doctor of Philosophy

in Microbiology and Molecular Genetics

2009

Abstract

Disabling Poxvirus Pathogenesis

Patrick Reeves

This work focuses on the molecular mechanisms by which viruses utilize host factors to spread from one cell to another. These investigations focus the poxviruses vaccinia, variola, and monkeypox. Vaccinia serves as the vaccine against variola, the cause of smallpox. Following replication and maturation, *Poxvirinae* virions travel to the cell surface along microtubules and fuse with the plasma membrane to form cell-associated enveloped virions (CEV). CEV can either form actin tails and move towards apposing cells or detach to form extracellular enveloped virions (EEV). The formation of actin tails is thought to mediate intra-tissue spread, while EEV are thought to be important for inter-tissue dissemination. The role of tyrosine kinases in actin motility and release of EEV was investigated using cell lines lacking particular kinases or with small molecules that inhibit kinase activity. Experiments presented demonstrate that Src- and Abl-family tyrosine kinases mediate actin motility, whereas release of infectious EEV depends upon Abl-family tyrosine kinases. Moreover, the utilization of these kinases by vaccinia, variola, and monkeypox is highly conserved. One inhibitor, Gleevec, blocks Abl-family tyrosine kinases and is FDA approved to treat patients with chronic myelogenous leukemia. In mice, Gleevec reduces viral load of vaccinia and protects from a lethal challenge whether administered as a prophylactic or in a therapeutic context. Together, these experiments support the role of EEV in dissemination and pathogenesis of poxviruses *in vivo.* Moreover, these data suggest a means to develop therapeutic strategies based on an understanding of the molecular mechanisms underlying host-pathogen interactions.

Disabling Poxvirus Pathogenesis

By

Patrick M. Reeves

B.S.

Advisor: Daniel Kalman, Ph.D.

A dissertation submitted to the Faculty of the Graduate School of Emory University in partial fulfillment of the requirements for the degree of

Doctor of Philosophy

in Microbiology and Molecular Genetics

2009

Table of Contents

Chapter 1. Background……1

Background References……28

Background Figures…….....40

Chapter 2. Disabling poxvirus pathogenesis by inhibition of Abl-family tyrosine kinases……44

Chapter 2 References……71

Chapter 2 Figures……...79

Chapter 3. Variola and monkeypox utilize conserved mechanisms of virion motility and release that depend on Abl- and Src-family tyrosine kinases……...106

Chapter 3 References……..130

Chapter 3 Tables/Figures……133

Chapter 4. Future Directions……...……...146

Chapter 4 References…...…….....152

Chapter 4 figures…...……...154

Chapter 5. Conclusion……159

Chapter 5 References……..……170

List of Figures

Chapter 1

Figure 1. Vaccinia virus replication cycle

Figure 2. Actin polymerization cascade

Figure 3. Domain diagram of Src, Abl, and BCR-Abl

Chapter 2

Figure 1. Abl and Src-family tyrosine kinases localize in VV actin tails

Figure 2. VV actin motility persists in cell lines lacking Abl and Src family kinases

Figure 3. Redundant Abl and Src-family tyrosine kinases are sufficient for VV actin tail formation

Figure 4. Redundant Abl and Src-family tyrosine kinases are required for cell-to-cell spread

Figure 5. Redundant Abl-family kinases are required for EEV release

Figure 6. STI-571 reduces number of viral genomes and promotes survival in VV-infected mice

Supplementary Figure 1. Protein sequences surrounding phosphorylation sites in VV A36R and enteropathogenic E. coli Tir

Supplementary Figure 2. Identification of VV-infected cells

Supplementary Figure 3. Structures of PD-166326 and STI-571

Supplementary Figure 4. Characterization of kinases sufficient for VV actin motility

Supplementary Figure 5. Effects of tyrosine kinase inhibitors on VV plaque formation

Supplementary Figure 6. Viral yield assays of VV on 3T3 cells

Supplementary Figure 7. Distinguishing the effects of Abl and Arg on EEV and IMV.

Chapter 3

Figure 1. VarV and MPX form actin tails

Figure 2. Actin tails formed by VarV and MPX require Abl and Src-family tyrosine kinases

Figure 3. VarV and MPX recruit host cell factors required for actin polymerization

Figure 4. Comet Assays

Figure 5. EEV & CAV Assay

Figure 6. Effects of tyrosine kinase inhibitors on VacV infection in mice

Supplementary Figure 1. Localization of proteins on tips of MPX actin tails

Supplementary Figure 2. BMS-354825 blocks VacV actin tails

Supplementary Figure 3. MPX & VacV comet assay

Supplementary Figure 4. CMC Plaque Assay

Supplementary Figure 5. BMS-354825 In Vivo

Chapter 5

Figure 1. F13L Phosphorylation

Figure 2. F13L Mutant Growth and EEV Production

Figure 3. F13L Mutant Plaque Phenotypes

Figure 4. F13L Mutant Microscopy

Acknowledgements

To all of my teachers and mentors, many thanks for your patience and skill as you taught me and allowed me to learn on my own. Without your individual efforts, large and small, I simply would not have been prepared for all the opportunities and adventures that have come along the way. An additional thanks is due to Dr. Jennifer Smith and Dr. Elliot Altman, who introduced me to laboratory life and helped to develop and strengthen my scientific curiosity, thinking and skill.

Thank you to my labmates and classmates for all of your support, colleagiality, and for providing a wonderful environment. A large measure of appreciation and gratitude is owed to my thesis advisor, mentor, and friend Dr. Daniel Kalman. Thank you continuing to shine the light as we searched for a way forward, bringing me along as your colleague as we learned together. I cherish the lessons learned together with our conversations and explorations and look forward to many more in the future.

To my family and friends, thank you for being a source of levity, inspiration and stability. To Analise, your support, counsel and grace have been instrumental in the completion of my dissertation. To my parents, thank you for your guidance and support and for instilling your enthusiasm for education. To my family, thank you for your kindness and encouragement throughout and for reminding me what we are really working to achieve. Without your kindness, help, and encouragement the journey would be impossible and in your absence no achievement or acknowledgement would bring any satisfaction.

Chapter 1

BACKGROUND

Poxvirus Structure and Organization

Poxviruses are large (~250x350nm, ~130-250kb) double-stranded DNA viruses (54). Poxvirinae virions consist of a DNA filled core and adjacent lateral bodies encased by a lipid-bilayer containing membrane (69). The genomes of poxviruses are linear and possess inverted terminal repeats (ITRs) to form hairpin-loops at both ends. Association of ITRs with their cognate at both ends of the genome induces the genome to assume a tube-like structure. This conformation permits the genome to assume a compact S-shaped structure within the core (54). The genome is ordered with highly conserved genes towards the center and the more variable elements located at the distal ends. Generally, convention assigns poxvirus genes a number based on their position relative to the ends of the genome. However, orthopoxvirus gene nomenclature predates the advent of sequencing and thus is less intuitive. Orthopoxvirus gene names are derived from HindIII digestion of the genome; each fragment is designated with a letter(54). Gene names are assigned based on their fragment, order (from the end) and direction of the ORF (left or right), e.g. B5R.

Poxvirus gene expression is well described and can be divided into three sequential steps, early, intermediate and late (21, 54). Early gene transcription occurs prior to genome replication and accounts for ~50% of all gene expression. Early genes are associated with viral DNA replication, immune-modulatory products, and factors for intermediate gene transcription. The initiation of intermediate gene production coincides with the termination of DNA replication.

Intermediate genes often are associated with virion assembly and maturation as well as products necessary for late gene expression. Factors produced by both early and intermediate genes are involved in late gene expression. Products of late gene expression generally are factors necessary for the initiation of early gene expression and are packaged into the virion. Some genes are expressed continuously throughout replication, while the amount of transcript produced may vary from stage to stage. Taken together, orthopoxviruses as a family share a high degree of homology in terms of virion structure, genome organization and gene expression (21, 54). Despite the range of similarities, poxvirinae exhibit large variety in regards to tropism and pathogenesis. Indeed, the 11 genera of poxviruses are divided into two sub-families: those capable of infecting invertebrates (*entomopoxvirinae*) and vertebrates (*chordopoxvirinae*). Four genera of chordopox are of particular interest, in light of their ability to cause disease in humans: parapox, yatapox, molluscipox, and orthopox.

Poxvirus Human Infections

While parapox, yatapox, molluscipox, and orthopox may all infect humans, the source, mode of transmission and pathogenesis are varied. Parapoxviruses typically infect cattle and sheep and are distinguished by the spiral appearance of their outer coat (21). Human infections often are associated with the handling of infected animals or tissues. Often undiagnosed in humans, parapox infections usually have no long-term clinical impact and abate within 6-8 weeks. Similarly, yatapoxviruses rarely result in long-term sequelae (75). There are three putative yatapoxvirus members: Yaba monkey tumor virus, Tanapox and Yaba-like disease virus. While the reservoir is unknown, typically yatapox are found in the monkeys of central Africa. It is thought that insect vectors mediate infection of monkeys and humans, which can occasionally result in the formation of skin tumors called histiocytomas. Infection of humans is rare. When infected, lesions often spontaneously resolve and are seldom malignant (75). By contrast, the molluscipoxvirus, molluscum contagiosum, is not infrequent and most often molluscum contagiosum is seen in children. *Molluscum contagiosum* is transmitted by contact with infected skin or contaminated surfaces and infection results in pearly lesions, which persist for 9-24 months. After resolving the infection, individuals do not exhibit acquired immunity and thus are susceptible to re-infection. In contrast to all other poxvirinae, *Molluscum contagiosum* is an obligate human pathogen; a feature shared only by the orthopoxvirus variola (11, 21).

Historically, of all poxviruses, the orthopoxviruses have exerted the greatest impact on humans and thus are the focus of intense study. Some orthopoxvirinae, although not associated with human disease can still adversely affect human well-being. Both camelpox and buffalopox infect livestock and affect humans indirectly by disrupting livelihoods and food supplies (27). Camelpox, like variola, has a single host(27). Similarly, the rabbit virus myxoma is species restricted and is not associated with human disease. However, work with myxoma has significantly contributed to our understanding of viral tropism and innate immune responses to infection (18, 52). Further, important insights into virology, host pathogen interactions, and immunology have resulted from the study of the clinically relevant orthopoxvirinae: cowpox, monkeypox, vaccinia and variola.

Clinically Relevant Poxvirus Infections

The most notorious of the poxviruses is variola, the causative agent of smallpox. Infection with variola can occur when as few as 10 plaque-forming units (pfu) are absorbed into respiratory or alimentary tracts (32, 82). Once infected, patients follow a well characterized disease progression (13). Soon after infection, variola spreads from initial site of infection to the proximal draining lymph nodes. There, during a 4-17 day latent period, the virus multiplies within the lymphatic phagocytic cells, primarily macrophages and monocytes contained within the connective tissue. The latent period concludes with a brief viremia followed by the onset of prodromal symptoms: fever, malaise, aches, and occasional vomiting. During this time the virus moves from the lymph nodes into mucous membrane of the mouth and pharynx as well as the capillaries of the dermal layer. Typically 2-4 days following onset of the prodrome stage, a rash appears leading to the formation of lesions first in the mouth followed by centrifugal diffusion to the face, arms and legs. The papules become pus filled and take on the distinctive of appearance of a pock: opaque with a depressed center. Soon thereafter, fever returns and papules burst to form lesions which become scab covered. Individuals are most infectious when the rash first appears and remain so until all scabs have fallen off and lesions are healed. Approximately 30% of individuals exposed to variola develop smallpox. Of those infected, between 5% and 40% succumb to the disease (7). The two subtypes of variola account for the wide variance in morbidity: the major and minor strains.

Variola major exhibits more extensive morbidity and mortality of 10-40%, typically 30%. Variola minor infection produces all diagnostic features of smallpox, though the disease may be decreased in severity with mortality of <4%, typically <1% (7, 13).

The first description of monkeypox was in 1958 and stemmed from serological surveys conducted as part of the WHO campaign. Rodents are the likely reservoir for monkeypox. Infection usually occurs after contact with an infected rodent or primate. Usually, monkeypox infection resembles a mild variola infection (10). Notably, the lymph nodes are often enlarged with monkeypox infections, unlike variola (10, 22). The mortality rate of monkeypox is highest in young children, ~10% and <5% in adults (10, 22). Previously monkeypox was confined to western central Africa, until appearing in United States in 2003 (12). Recent evidence suggests that monkeypox may be re-emerging and gaining prevalence in western Africa (33, 55). Vaccination against variola is cross protective for monkeypox and cessation of the WHO smallpox vaccination campaign may be a contributing factor in the re-emergence of monkeypox (10, 33).

The last natural incidence of smallpox was a case of variola minor in Somalia in 1977, preceded by the last natural variola major case in 1975. The last death from smallpox occurred in 1978, following a laboratory incident. As a result of this accidental exposure all known stocks were destroyed or transferred to the Centers for Disease Control and Prevent (CDC) in Atlanta, GA or to State

Research Center of Virology and Biotechnology (VECTOR) in Koltsovo, Russia. Shortly thereafter, the World Health Organization (WHO) declared smallpox eradicated on May 8, 1980, concluding a campaign begun in 1958. To date smallpox remains the only eradicated human disease, an accomplishment made possible by the discovery of vaccination nearly 200 years prior by Edward Jenner.

In 1796 Edward Jenner inoculated a young boy named James Phipps with cowpox to protect him from variola virus, the cause of Smallpox (2). However, the procedure was not novel. Variolation, the use of dried smallpox scabs to inoculate naïve individuals against variola, dates back to at least 10th century China. However, Jenner's innovation demonstrated for the first time the possibility of utilizing a benign proxy source of antigen (cowpox) to protect against another infection (variola). This approach, further refined by Pasteur, Cohn, Koch and others, gave rise to the field of immunology. So successful was Jenner's method that it remained virtually unchanged until near the conclusion of the WHO eradication campaign. Towards the end of the WHO campaign an alternative to live vaccinia inoculation was developed. Vaccinia inoculation, while much safer than variolation, is not without complications and potential risks including: progressive vaccinia, fetal vaccinia, and other adverse reactions (14). Thus in 1976 Anton Mayr and colleagues produced an attenuated strain of vaccinia called: Modified Vaccinia Ankara (MVA)(51). The virus was attenuated by 571 serial passages in chicken embryo fibroblasts. MVA lacks ~10% of the

parental genome and is no longer capable of replicating in mammalian cells (53). The safety profile of MVA is greatly improved and has seen widespread adoption as a potential vaccine vector. However, MVA never displaced vaccinia as the agent of choice for protection against variola. Interestingly, at some stage subsequent to Jenner's work, a transition from cowpox to vaccinia as the predominate vaccinating agent occurred. It is unclear if the change resulted from necessity, experimentation, or a confluence of these and unknown factors.

Even more obscure are the origins of vaccinia virus. It is clear that shortly following Jenner, others used cowpox and horsepox interchangeably to conduct vaccinations (66). There is some evidence of regional preferences for either horsepox (France) or cowpox (England). Some hypothesize that vaccinia is a now extinct strain of horsepox, while others suggest it is a highly attenuated variola minor strain; removed from a patient and alternately passed in humans and cattle (2-4). A third suggestion: hybrid strains were generated by the co-infection of cattle intended as reservoirs from which to vaccinate (such was tissue culture in the 18th and 19th century)(3). To date, DNA sequence studies cannot provide a definitive conclusion (27, 79). Indeed all accounts may represent scenarios that likely existed at one point in time or another. Interestingly, the closet homolog to variola by sequence is camelpox, though no evidence exists of camels infected by smallpox nor of humans infected by camelpox (27). Although, inoculation of camels with variola can vaccinate them against camelpox infection(27). How does vaccination with vaccinia provide robust and long lasting

protection? Especially while similar poxviruses persist for much longer periods and yet elicit no immune memory (molluscum contagiousum)? These are interesting trivia from a historical or biological perspective. However, within these puzzles are clues as to how microbes adapt to their current and potential new hosts and how in turn hosts respond to infection both in the short term and in anticipation of re-exposure. Nevertheless, today vaccinia is the prototypical poxvirus and the subject of extensive work describing the replication, pathogenesis and immunology of poxviruses (21, 54).

Poxvirus Lifecycle & Dissemination

Extensive studies with vaccinia have generated detailed models of the poxvirus lifecycle and modes of dissemination (21, 54) (Figure 1). The receptor for poxviruses remains an open area of investigation. It is likely that several cellular proteins can serve as the receptor, including EGFR (epidermal growth factor receptor) (52). Further, receptor identity and preference likely differs between various cell and virus types. Following binding, virions fuse with the plasma membrane and enter through a low pH-dependent mechanism, leading to the formation of a juxta-nuclear replication center (43). There, concatemeric genomes are produced and resolved into crescent shaped individual units. Crescents associate with a matrix of viral proteins and replication factors and form membrane bound immature virions (IV). Subsequently, IV condense through a poorly understood process involving proteolysis of numerous viral proteins to form the now infectious mature virions (MV). Indeed, the composition and manner of the membrane assembly remain open and contentious areas of investigation. Some MV then move on microtubules towards an early-enodosomal/golgi compartment. There, MV acquire two additional membranes to form intracellular enveloped virions (EV). From there, the triple membraned EV traffic on microtubules to the cell surface, where they then merge their outer-most membrane. The result is a cell-associated extracellular virion (CEV), which is tethered to the host-plasma membrane via a complex of host and viral proteins.

From this stage the virus can now spread to a new cell where the entire process can begin again.

Viral spread is mediated through at least three distinct mechanisms(69). Upon lysis MV are released into the milieu and *in vivo* MV are thought to mediate spread between hosts. Prior to lysis virions located on the plasma membrane are either released directly from the surface of the cell to form Extracellular Enveloped Virions (EEV) or CEV can move towards uninfected cells on the tips of actin tails, filipodia-like actin-filled protrusions. While EEV and CEV represent a small fraction (<5%) of total progeny, they are important to viral dissemination (69). The release of EEV is thought to mediate dissemination to distal sites within the host, while actin-tails facilitate intra-tissue spread(5, 69, 76). EEV are particularly well suited for this role as they maintain a low antigenic profile through their low abundance, as well as their host complement control proteins and little viral antigen (81). The addition of EEV neutralizing antibody or vaccination with EEV specific proteins can attenuate disease in mice (34, 45). Similarly, mutations that eliminate the formation of actin tails reduce plaque size *in vitro* and also attenuate disease *in vivo* (84). Taken together, these observations demonstrate that poxviruses have developed a multi-faceted and sophisticated pathogenic program.

Use of Actin by Pathogens

Actin polymerization is often achieved through pathways linked to Arp2/3, a protein central to actin nucleation (Figure 2). Arp 2/3 mediated actin polymerization is utilized in mammals, amoebas (*Dictyostelium discoideum*), and plants (*Arabidopsis*) (37, 50). The binding of an extracellular ligand induces receptor activation/dimerization and initiates a signaling cascade to activate the Arp2/3 complex. Following ligand binding, receptor activation recruits SH2/SH3 adapter proteins such as Nck and Grb2. In turn, Nck/Grb2 recruitment can lead to activation GTPases such as Rho, Rac, or CDC4. Activated GTPases can bind to and stimulate one of several Wiskott-Aldrich syndrome (WASP) or Suppressor of Camp Receptor (SCAR) family members such as Wave and N-WASP. WASP/SCAR-family proteins, once activated bind both to actin and Arp2/3 to form an actin nucleation core. Arp2/3 binds to extant actin filaments and directs the nucleation of additional actin to modify the actin cytoskeleton. Arp2/3 mediated actin polymerization contributes to a variety processes including: endocytosis, pinocytosis, as well as cell motility through the formation of lamellapodia and filopodia. Several pathogens usurp the Arp2/3 linked pathways to achieve actin polymerization as part of their pathogenic program (25).

Numerous microbes usurp host actin polymerization as part of their pathogenic program including the bacteria *Listeria*, *Shigella*, and enteropathogenic *E. coli* (EPEC)(25). *Shigella* induces actin polymerization both to enter and exit cells (59). During entry *Shigella*, through its Ipa proteins,

induces Rho/Rac/Cdc42 activation leading to the formation actin filled extensions and eventual phagocytosis. After escaping the phagosome and following replication, *Shigella* mimics host-proteins to stimulate actin polymerization and exit host cells. The *Shigella* protein IcsA activates N-WASP much like CDC42, leading to actin nucleation beneath the bacteria (15, 24).

Coxsackie virus, like *Shigella*, induces a signaling cascade to achieve an actin mediated invasion scheme (17). Following binding Coxsackie virions activate the host tyrosine kinase Abl leading to Rac activation. The subsequent actin remodeling enables Coxsackie to move towards the tight-junctions of adjacent cells. There, the virions bind their cognate receptor, which activates another tyrosine kinase, Fyn. Activation of Fyn enables the virions to enter through caveolin-associated vesicles. Conversely, the food-borne intracellular pathogen *Listeria*, exits cells through a mechanism similar to *Shigella*. Through the protein ActA, *Listeria* emulates WASP protein signaling to activate Arp2/3 directly (47, 83). The polar distribution of ActA enables Listeria to polymerize actin on one end; the now motile bacterium then is pushed towards and into neighboring cells (16, 83). In contrast, the attaching and effacing pathogen EPEC remains extra-cellular throughout infection and employs a different strategy to induce actin remodeling. After attaching loosely to the surface of a cell, EPEC forms a Type-III secretion pilus and translocates several effector proteins including. Among these is Tir (translocated intimin receptor), which interacts with the bacterial surface protein Intimin to secure the bacteria to the plasma

membrane. Subsequently, phosphorylation of Tir by any of several host tyrosine kinases begets recruitment of N-WASP and Arp2/3 leading to actin polymerization (38, 39).

Vaccinia induces actin polymerization in a manner highly analogous to EPEC (23). The formation of actin tails beneath the virion results from the phosphorylation of the viral protein A36R by either Src- or Abl-family tyrosine kinases(67). Subsequently, actin-polymerizing factors are recruited beneath the virion and include: N-WASP, Arp2/3, Nck, and Grb2. The phosphorylation of A36R on its two tyrosine residues Y112 and Y132 leads to the recruitment of Nck and Grb2 respectively(71). While both residues are phosphorylated, each serves a distinct purpose for actin tail formation. Mutation of Y112 prohibits the formation of tails, while Y132 mutants exhibit shortened protrusions. This suggests that phosphorylation of Y112 and Nck localization are necessary for actin tails. While, Y132 and Grb2 recruitment act to stabilize the actin tail structure. Vaccinia actin tails are vital to dissemination: mutants unable to form actin tails produce small plaques *in vitro* and are attenuated *in vivo*.

Importantly, both EPEC and Vaccinia localize any of several host tyrosine kinases beneath the microbe within the actin pedestal or tail (67, 77). Either Tec- or Abl-family kinases can localize or phosphorylate the EPEC protein Tir(6, 77). Similarly, the vaccinia protein A36R can be phosphorylated by Src- or Abl-family kinases(67). Further, using tests for redundancy, both EPEC and vaccinia demonstrate the capacity to utilizing kinases in a redundant manner (67, 77).

Tyrosine Kinases

The study of tyrosine kinases has its roots in the work Peyton Rous. In an effort to identify the factor responsible for a transmissible cancer in Plymouth Rock Hens, Rous extracted the tumor and exposed naïve animals to a series of filtered lysates. From these experiments Rous concluded that a “virus” must be the responsible factor. Later, Rous Sarcoma Virus (RSV) was determined to be a retrovirus. Subsequently, work by Martin and others using temperature sensitive alleles determined that RSV contained the transforming factor in its genome and that virus lacking this sequence did not induce cancer. The transforming sequence or oncogene was dubbed v-Src, derived from sarcoma. Further studies by Bishop and Varmus identified mammalian homologues of v-Src and other related genes including Fyn, Yes and Lck, which together comprise the Src family. Additionally, dysregulation of a variety of cellular, cytoplasmic, and receptor tyrosine kinases including EGFR, c-Kit, and c-Abl can alter cellular processes and result in various cancers, including chronic myelogenous leukemia (CML) (28).

The example of Abl and CML illustrates the oncogenic potential of tyrosine kinase dysregulation. In healthy cells c-Abl is associated with a variety of cellular functions: cell-cycle regulation, differentiation, actin remodeling, and embryogenesis (35, 80). While various domains of c-Abl have been crystallized, to date a complete crystal structure is not available. However, homologues of

human c-Abl identified in drosophila and mice have facilitated investigation into the mechanisms of activity and regulation.

Abl derives its name from the transforming activity within Abelson Leukemia Virus (ALV). Like RSV, ALV contains a viral homolog (v-Abl) of a host tyrosine kinase (c-Abl). The dysregulation of Abl leads to hyperactive signaling which drives cells to proliferate and results in CML. Dysregulation of c-Abl in CML often results from a translocation involving a portion the breakpoint cluster region (BCR) of chromosome 22 and c-Abl on chromosome 9 designated as the t(9;22)(q34;q11) chromosomal translocation, the so-called Philadelphia chromosome.

In 1960, using cytogenetic analysis, Nowell and Hungerford, identified the Philadelphia chromosome in samples from two patients with CML (61). Later Rowley identified the breakpoint and Schtivelman was able to clone BCR-Abl (70, 73). Together these observations demonstrated that through a N-terminal translocation of BCR, Abl can become dysregulated and lead to CML. Similar mutations are associated with acute myeloid leukemia (AML) and acute lymphoblastic leukemia (ALL)(44). Through the removal of the N-terminus from c-Abl or other mutations, the auto-inhibitory capacity of c-Abl is reduced. Thus the dysregulated Abl-kinase activity allows cell proliferation to proceed in cytokine independent manner, resulting in leukemia.

Kinase regulation

How do these mutations within a kinase result in leukemia? To answer this question, it is necessary to discuss the structure and regulation of c-Abl. To date a complete crystal structure has not been elucidated. However crystal structures of several c-Abl domains and other closely related kinases are available (57, 58, 74).

The structure of c-Abl is illustrated in Figure 3. While the precise mechanism(s) of Abl regulation remains an active area of investigation, several components are thought to be well understood and have been recently reviewed by Hantschel and Superti-Furga (29). The c-Abl protein assumes distinct conformational arrangements based on its activation status. The inactive form assumes a “closed” state and once activated, the conformation opens to expose the various domains. Recent work demonstrates that the N-terminal domain is necessary for c-Abl to maintain its closed or inactive state (62). In addition, the C-terminus region contains sequences associated with nuclear localization signals, as well as binding sites for Crk, Nck, and p53 and actin. Between the two termini lie the SH3, SH2, and kinase domains. The Src Homology (SH3, SH2) domains also contribute to the inter-protein as well as intra-protein interactions of Abl. The SH3 domain preferentially binds to proline rich sequences of potential substrates containing the consensus pxxp motif (42). The SH2 domain recognizes and binds specific sequences that contain phosphorylated tyrosine residues and resemble the consensus pYEEI (42). Additionally, the SH3 and SH2 domains together can

interact with the Abl kinase domain, contacting the N- and C-terminal domain ends respectively. The SH3-SH2/kinase domain interaction creates a cap, which is stabilized by the N-terminus. Together the SH3/SH2 cap and N-terminus latch act to prevent access to the active site and block kinase activity. Thus, Abl is capable of auto-regulation through the function of its various domains.

Activation of the kinase requires disruption of the SH3-SH2 interaction with the kinase domain. Disruption of the SH3-SH2 cap occurs when the SH2 domain encounters and recognizes an appropriate phosphorylated sequence. It is likely those phospho-proteins capable of interacting with and destabilizing SH3-SH2 cap result from basal Abl activity or pathway crosstalk. Recent work demonstrates that the N-terminus is “unlatched” in 0.5% of c-Abl molecules at any given moment (85). However, unlatching of the n-terminus and disassociation of the SH3-SH2 domains from the active site must be followed by phosphorylation of the activation loop.

Inactive kinase contains an un-phosphorylated activation loop that occupies a portion of the active site. However, phosphorylation of the activation loop induces a conformation change, which in turn produces an open active site. With the kinase now in an active conformation and the active site no longer occluded, the kinase is free to associate with and phosphorylate substrate. Activated Abl may act in *trans* on the activation loop of other c-Abl proteins. Trans activation, together with the increase of phospho-substrates to potentially

destabilize the SH3-SH2 domain inhibition, can work to generate a positive-feedback loop.

Does the proto-oncogene from RSV, Src behave in an analogous manner? Both Src- and Abl-family kinases are closely related. Thus, it is not surprising that the structure and regulation of c-Src resembles c-Abl. However, there are some important distinctions. The variable N-terminal regions of Src-family kinases (SFK) appear to contribute to the varied functions of different family members (36). As in Abl, the SH3 and SH2 domains of Src recognize poly-proline motifs, bind to appropriate sequencing containing phosphotyrosine residues and contribute to the formation of a cap over the active site. However, the stabilization of the Src SH3/SH2 cap is distinct from Abl. The C-terminus of Src can interact with the SH2 domain and serve to stabilize the SH3/SH2 cap. This stands in contrast to c-Abl, which utilizes the N-terminus to stabilize the SH3/SH2 cap. Moreover, this distinction may account for the divergent manner in which Src and Abl can act as oncogenes. Interestingly v-Src contains retains all the domains and general structure found in c-Src. Studies suggest that the dysregulation of v-Src likely results from a series of mutations found within the various regulatory components. These mutations likely destabilize the inactive conformation of c-Src and enhance its activity. On going investigations from Kuriyan and others, are working to identify mutations in v-Src critical to the regulation of c-Src(1). The mutations within v-Src that confer transformational activity may be of particular interest to cancer biologists. Particularly to inform models of kinase regulation

and as a means to help identify second site mutations that enhance the activity of BCR-Abl in CML patients.

The translocation that produces the BCR-Abl gene removes the N-terminus and destabilizes the inhibitory ability of SH3-SH2 cap. Thus the BCR-Abl protein is decreased in its ability to maintain an inactive conformation and becomes hyperactive. The deregulation of c-Abl engenders the appearance of additional secondary mutations within the regulatory domains, further increasing aberrant activity. Indeed, in some patients both the SH3 domain and N-terminus entirely absent from BCR-Abl (78). It has been observed that the additional deletion of the SH3 domain accounts for more severe disease in some patients(49, 63). However, not all patients lacking SH3 does exhibit more severe disease, illustrating the complex nature of Abl auto-regulation (78). Nevertheless, either deletion or mutation of the N-terminus, SH3, and SH2 removes the auto-regulatory capacity of BCR-Abl, leading to unchecked stimulation of cell division and eventually CML.

Small Molecule Inhibition of Tyrosine Kinases

In 1960 Nowell and Hungerford described the translocation ultimately responsible for CML (60). Subsequent work identified the BCR-Abl gene, demonstrated the dysregulated activity of the BCR-Abl protein, and confirmed its oncogenic role in CML (19, 26, 31, 46). While rare, CML proved exceedingly difficult to successfully treat with conventional cancer therapies. Structural studies of tyrosine kinases demonstrated diversity in the conformation of their ATP-binding pockets(35). Further work illustrated the varied activities and specificities among tyrosine kinases were largely determine by their components (35). Together these observations highlighted the possibility of a pharmaceutical approach to treating CML. Researchers at Novartis created a library of 400 compounds based upon phenylaminopyrimidines, which they found could inhibit tyrosine kinases (9). Inherent to the design of this library was the knowledge that the structure of kinase ATP-binding pockets exhibit significant variation, thus creating the possibility that a molecule may preferentially bind to a particular kinase (or group). In 1996, Drucker and colleagues screened the Novartis library of small-molecules for their ability to limit the growth of CML cells in tissue culture and identified STI-571 (20). STI-571 competitively inhibits the active form of BCR-Abl. By occluding the ATP- binding pocket, STI-571 reduces aberrant signaling and mitigates the progression of CML. In 2001, the FDA approved STI-571 (Imatinib, Gleevec) for the treatment of patients with CML.

Even prior to FDA approval, resistance to STI-571 had been observed (48). As a competitive inhibitor of ATP binding, STI-571 likely engenders resistance due to its preferential binding of activated BCR-Abl. When the kinase becomes inactive, the ATP-pocket conformation changes and STI-571 can no longer bind. Soon however, in the case of BCR-Abl, the kinase regains an active conformation, and the competition between ATP and STI-571 for the binding pocket renews. Each instance where ATP gains access over STI-571 facilitates the selection of alleles less sensitive to STI-571. A variety of point mutations both within the ATP-binding pocket and throughout the protein can allosterically inhibit the binding of STI-571, while still allowing ATP access (65). It is estimated that 20-30% patients develop some degree of resistance to STI-571 (65).

A second generation of compounds has been developed to address STI-571 resistance. One such compound, BMS-354825 (Dasatinib, Sprycel) gained FDA approval in 2006. Though BMS-354825 was originally developed as an inhibitor of Src-family tyrosine kinases, additional activity against BCR-Abl was observed. When tested, BMS-354825 is 325 fold more potent than STI-571 against BCR-Abl and is effective against most alleles resistant to STI-571 (56, 72).

Although BMS-354825 demonstrates its “off-target” inhibition of Src-family and other proteins, it is used clinically to treat patients insensitive to STI-571 (68). However one particular mutation, T315I, remains insensitive to current therapies. Numerous “third generation” molecules are currently under development and demonstrate potential utility against this allele, though none have received FDA

approval(64).

Like BMS-354825, “off target” activity has been described for STI-571. Early in Druker’s testing of STI-571 he observed additional activity against PDGF-R (9). Indeed, STI-571 demonstrates activity against not only Abl, but also its paralog Abl-2, PDGF-R and c-Kit (8). Despite lacking complete specificity, STI-571 exhibits relatively few side effects in patients. Notably however, there have been reports of myocardial toxicity in some patients receiving STI-571 (41). There is a benefit to the promiscuity of STI-571 inhibition. Dysregulation of c-Kit can lead to the development of gastrointestinal stromal tumors (GIST). STI-571 can inhibit c-Kit and can be used to treat GIST patients (30). STI-571 and the lessons derived from its development now serve a template for the numerous efforts are underway seeking to identify additional molecules to limit aberrant signaling and the resulting pathology.

Research Objectives

A feature central to these studies is ability of microbes to usurp host proteins and signaling cascades towards their own ends. Specifically, we sought to explore the means by which a viral pathogen, vaccinia virus, can induce rearrangement of the actin cytoskeleton to facilitate its dissemination. In the course of these investigations we uncovered the previously undescribed role for Abl-family kinases in the release of virus from the cell.

Previous work from Kalman and others observed that phosphorylation of the EPEC protein Tir lead to the recruitment of WASP and Arp2/3 leading to the formation of actin pedestals (38, 40). However, the kinase responsible for Tir phosphorylation remained unknown at the time.

Building upon these observations, Way and colleagues demonstrated that vaccinia virus utilizes a highly analogous mechanism to polymerize actin beneath the virion and form actin tails. The study from Way and colleagues also proposed that the host tyrosine kinase Src alone was responsible for the phosphorylation of the viral protein A36R, an ortholog of Tir.

However, work ongoing in our lab at the time suggested that several kinases were sufficient for the phosphorylation of Tir. Our data demonstrated that Abl-family and another unidentified kinase were sufficient for actin pedestal formation. Thus, we were confronted with an interesting divergence. A single kinase, Src, was proposed to be necessary and sufficient for vaccinia actin polymerization. However, our work with EPEC suggested that several kinases were simultaneously sufficient for the phosophorylation of Tir. This raised two possibilities. First, EPEC and vaccinia differed in their requirements for phosphorylation, while recruiting a virtually identical set of actin polymerizing proteins. Alternatively, several kinases were sufficient in both systems and the experimental design of the vaccinia work had inadvertently obscured this possibility.

Protein sequence alignment of the Tir and A36R phosphorylation sites showed a single amino acid change. In addition there were several caveats within the vaccinia data. Together, these observations further raised the likelihood that several kinases were sufficient to phosphorylate A36R and induce actin tail formation. At the time, the identity of all the kinases sufficient for EPEC pedestals were unknown, only the Abl-kinases were confirmed. Thus, the prospect of another system where we might define all the kinases sufficient and explore the various mechanisms of redundancy was especially interesting.

The impetus for these studies was to explore the means by which vaccinia utilizes the host machinery as part of its pathogenic program. We hypothesized that investigation into the mechanism of poxvirus actin motility would address questions regarding host protein recruitment and potential kinase redundancy and potentially generate novel drug targets. Later efforts sought to characterize the role of various host kinases in viral dissemination and the utility of drugs targeting host proteins in limiting viral pathogenesis. Ultimately, these investigations provide a comprehensive view of the process basic virology and cell biology experiments informing the development of a novel method of drug development.In particular we made use of immunofluorescent deconvolution microscopy, in concert with traditional biochemical and virological methods as a means to test and inform our hypostheses. The following chapters describe these efforts.

References

1. **Azam, M., M. A. Seeliger, N. S. Gray, J. Kuriyan, and G. Q. Daley.** 2008. Activation of tyrosine kinases by mutation of the gatekeeper threonine. Nat Struct Mol Biol **15:**1109-18.
2. **Baxby, D.** 1979. Edward Jenner, William Woodville, and the origins of vaccinia virus. J Hist Med Allied Sci **34:**134-62.
3. **Baxby, D.** 1996. Should smallpox virus be destroyed? The relevance of the origins of vaccinia virus. Soc Hist Med **9:**117-9.
4. **Baxby, D.** 1977. The origins of vaccinia virus. J Infect Dis **136:**453-5.
5. **Blasco, R., and B. Moss.** 1992. Role of cell-associated enveloped vaccinia virus in cell-to-cell spread. J Virol **66:**4170-9.
6. **Bommarius, B., D. Maxwell, A. Swimm, S. Leung, A. Corbett, W. Bornmann, and D. Kalman.** 2007. Enteropathogenic Escherichia coli Tir is an SH2/3 ligand that recruits and activates tyrosine kinases required for pedestal formation. Mol Microbiol **63:**1748-68.
7. **Breman, J. G., and D. A. Henderson.** 2002. Diagnosis and management of smallpox. N Engl J Med **346:**1300-8.
8. **Buchdunger, E., C. L. Cioffi, N. Law, D. Stover, S. Ohno-Jones, B. J. Druker, and N. B. Lydon.** 2000. Abl protein-tyrosine kinase inhibitor STI571 inhibits in vitro signal transduction mediated by c-kit and platelet-derived growth factor receptors. J Pharmacol Exp Ther **295:**139-45.
9. **Buchdunger, E., J. Zimmermann, H. Mett, T. Meyer, M. Muller, B. J. Druker, and N. B. Lydon.** 1996. Inhibition of the Abl protein-tyrosine

kinase in vitro and in vivo by a 2-phenylaminopyrimidine derivative. Cancer Res **56:**100-4.

10. **CDC.** 2003. Basic Information about Monkeypox, p. 2. *In* D. o. H. a. H. Services (ed.). CDC, Atlanta.
11. **CDC.** 2008. Frequently Asked Question: For Everyone, Molluscum Contagiousum, p. 2. *In* D. o. H. a. H. Services (ed.).
12. **CDC.** 2003. Multistate Outbreak of Monkeypox --- Illinois, Indiana, and Wisconsin, 2003. MMWR **52:**537-540.
13. **CDC.** 2004. Smallpox Fact Sheet, p. 2. *In* D. o. H. a. H. Services (ed.).
14. **CDC.** 2003. Smallpox Vaccination and Adverse Reactions Guidance for Clinicians 52(RR04). CDC.
15. **Cossart, P.** 2000. Actin-based motility of pathogens: the Arp2/3 complex is a central player. Cell Microbiol **2:**195-205.
16. **Cossart, P., and M. Lecuit.** 1998. Interactions of Listeria monocytogenes with mammalian cells during entry and actin-based movement: bacterial factors, cellular ligands and signaling. EMBO J **17:**3797-806.
17. **Coyne, C. B., and J. M. Bergelson.** 2006. Virus-induced Abl and Fyn kinase signals permit coxsackievirus entry through epithelial tight junctions. Cell **124:**119-31.
18. **Dai, E., K. Viswanathan, Y. M. Sun, X. Li, L. Y. Liu, B. Togonu-Bickersteth, J. Richardson, C. Macaulay, P. Nash, P. Turner, S. H. Nazarian, R. Moyer, G. McFadden, and A. R. Lucas.** 2006. Identification

of myxomaviral serpin reactive site loop sequences that regulate innate immune responses. J Biol Chem **281:**8041-50.

19. **Daley, G. Q., R. A. Van Etten, and D. Baltimore.** 1990. Induction of chronic myelogenous leukemia in mice by the P210bcr/abl gene of the Philadelphia chromosome. Science **247:**824-30.

20. **Druker, B. J., S. Tamura, E. Buchdunger, S. Ohno, G. M. Segal, S. Fanning, J. Zimmermann, and N. B. Lydon.** 1996. Effects of a selective inhibitor of the Abl tyrosine kinase on the growth of Bcr-Abl positive cells. Nat Med **2:**561-6.

21. **Esposito, J., and Fenner, F.** 1999. Poxviruses, p. 2 v. (xix, 2336). *In* B. N. Fields and D. M. Knipe (ed.), Fields Virology, 2nd ed. Raven Press, New York.

22. **Fenner.** 1994. Poxviral Zoonoses, p. 485-503. *In* S. J. Viral. Beran GW (ed.), Handbook of Zoonoses, Second ed. CRC Press, Inc.

23. **Frischknecht, F., V. Moreau, S. Rottger, S. Gonfloni, I. Reckmann, G. Superti-Furga, and M. Way.** 1999. Actin-based motility of vaccinia virus mimics receptor tyrosine kinase signalling. Nature **401:**926-9.

24. **Goldberg, M. B., and J. A. Theriot.** 1995. Shigella flexneri surface protein IcsA is sufficient to direct actin-based motility. Proc Natl Acad Sci U S A **92:**6572-6.

25. **Gouin, E., M. D. Welch, and P. Cossart.** 2005. Actin-based motility of intracellular pathogens. Curr Opin Microbiol **8:**35-45.

26. **Groffen, J., J. R. Stephenson, N. Heisterkamp, A. de Klein, C. R. Bartram, and G. Grosveld.** 1984. Philadelphia chromosomal breakpoints are clustered within a limited region, bcr, on chromosome 22. Cell **36:**93-9.

27. **Gubser, C., and G. L. Smith.** 2002. The sequence of camelpox virus shows it is most closely related to variola virus, the cause of smallpox. J Gen Virol **83:**855-72.

28. **Haglund, K., T. E. Rusten, and H. Stenmark.** 2007. Aberrant receptor signaling and trafficking as mechanisms in oncogenesis. Crit Rev Oncog **13:**39-74.

29. **Hantschel, O., and G. Superti-Furga.** 2004. Regulation of the c-Abl and Bcr-Abl tyrosine kinases. Nat Rev Mol Cell Biol **5:**33-44.

30. **Heinrich, M. C., D. J. Griffith, B. J. Druker, C. L. Wait, K. A. Ott, and A. J. Zigler.** 2000. Inhibition of c-kit receptor tyrosine kinase activity by STI 571, a selective tyrosine kinase inhibitor. Blood **96:**925-32.

31. **Heisterkamp, N., J. R. Stephenson, J. Groffen, P. F. Hansen, A. de Klein, C. R. Bartram, and G. Grosveld.** 1983. Localization of the c-ab1 oncogene adjacent to a translocation break point in chronic myelocytic leukaemia. Nature **306:**239-42.

32. **Henderson, D. A., T. V. Inglesby, J. G. Bartlett, M. S. Ascher, E. Eitzen, P. B. Jahrling, J. Hauer, M. Layton, J. McDade, M. T. Osterholm, T. O'Toole, G. Parker, T. Perl, P. K. Russell, and K. Tonat.**

1999. Smallpox as a biological weapon: medical and public health management. Working Group on Civilian Biodefense. JAMA **281:**2127-37.

33. **Heymann, D. L., M. Szczeniowski, and K. Esteves.** 1998. Re-emergence of monkeypox in Africa: a review of the past six years. Br Med Bull **54:**693-702.

34. **Hooper, J. W., D. M. Custer, and E. Thompson.** 2003. Four-gene-combination DNA vaccine protects mice against a lethal vaccinia virus challenge and elicits appropriate antibody responses in nonhuman primates. Virology **306:**181-95.

35. **Hubbard, S. R., and J. H. Till.** 2000. Protein tyrosine kinase structure and function. Annu Rev Biochem **69:**373-98.

36. **Ingley, E.** 2008. Src family kinases: regulation of their activities, levels and identification of new pathways. Biochim Biophys Acta **1784:**56-65.

37. **Insall, R., A. Muller-Taubenberger, L. Machesky, J. Kohler, E. Simmeth, S. J. Atkinson, I. Weber, and G. Gerisch.** 2001. Dynamics of the Dictyostelium Arp2/3 complex in endocytosis, cytokinesis, and chemotaxis. Cell Motil Cytoskeleton **50:**115-28.

38. **Kalman, D., O. D. Weiner, D. L. Goosney, J. W. Sedat, B. B. Finlay, A. Abo, and J. M. Bishop.** 1999. Enteropathogenic E. coli acts through WASP and Arp2/3 complex to form actin pedestals. Nat Cell Biol **1:**389-91.

39. **Kenny, B.** 1999. Phosphorylation of tyrosine 474 of the enteropathogenic Escherichia coli (EPEC) Tir receptor molecule is essential for actin

nucleating activity and is preceded by additional host modifications. Mol Microbiol **31:**1229-41.

40. **Kenny, B., A. Abe, M. Stein, and B. B. Finlay.** 1997. Enteropathogenic Escherichia coli protein secretion is induced in response to conditions similar to those in the gastrointestinal tract. Infection and Immunity **65:**2606-2612.

41. **Kerkela, R., L. Grazette, R. Yacobi, C. Iliescu, R. Patten, C. Beahm, B. Walters, S. Shevtsov, S. Pesant, F. J. Clubb, A. Rosenzweig, R. N. Salomon, R. A. Van Etten, J. Alroy, J. B. Durand, and T. Force.** 2006. Cardiotoxicity of the cancer therapeutic agent imatinib mesylate. Nat Med **12:**908-16.

42. **Koch, C. A., D. Anderson, M. F. Moran, C. Ellis, and T. Pawson.** 1991. SH2 and SH3 domains: elements that control interactions of cytoplasmic signaling proteins. Science **252:**668-74.

43. **Laliberte, J. P., and B. Moss.** 2009. Appraising the apoptotic mimicry model and the role of phospholipids for poxvirus entry. Proc Natl Acad Sci U S A.

44. **Laneuville, P.** 1995. Abl tyrosine protein kinase. Semin Immunol **7:**255-66.

45. **Law, M., and G. L. Smith.** 2001. Antibody neutralization of the extracellular enveloped form of vaccinia virus. Virology **280:**132-42.

46. **Lugo, T. G., A. M. Pendergast, A. J. Muller, and O. N. Witte.** 1990. Tyrosine kinase activity and transformation potency of bcr-abl oncogene products. Science **247:**1079-82.

47. **Machesky, L. M., and R. H. Insall.** 1998. Scar1 and the related Wiskott-Aldrich syndrome protein, WASP, regulate the actin cytoskeleton through the Arp2/3 complex. Curr Biol **8:**1347-56.

48. **Mahon, F. X., M. W. Deininger, B. Schultheis, J. Chabrol, J. Reiffers, J. M. Goldman, and J. V. Melo.** 2000. Selection and characterization of BCR-ABL positive cell lines with differential sensitivity to the tyrosine kinase inhibitor STI571: diverse mechanisms of resistance. Blood **96:**1070-9.

49. **Martinelli, G., M. Amabile, C. Terragna, N. Testoni, E. Ottaviani, V. Montefusco, A. de Vivo, M. Baccarani, P. Ricci, G. Saglio, and S. Tura.** 1999. Concomitant expression of the rare E1/A3 and B2/A3 types of BCR/ABL transcript in a chronic myeloid leukemia (CML) patient. Leukemia **13:**1463-4.

50. **May, R. C., E. Caron, A. Hall, and L. M. Machesky.** 2000. Involvement of the Arp2/3 complex in phagocytosis mediated by FcgammaR or CR3. Nat Cell Biol **2:**246-8.

51. **Mayr, A., H. Stickl, H. K. Muller, K. Danner, and H. Singer.** 1978. [The smallpox vaccination strain MVA: marker, genetic structure, experience gained with the parenteral vaccination and behavior in organisms with a

debilitated defence mechanism (author's transl)]. Zentralbl Bakteriol B **167:**375-90.

52. **McFadden, G.** 2005. Poxvirus tropism. Nat Rev Microbiol **3:**201-13.

53. **Meyer, H., G. Sutter, and A. Mayr.** 1991. Mapping of deletions in the genome of the highly attenuated vaccinia virus MVA and their influence on virulence. J Gen Virol **72 (Pt 5):**1031-8.

54. **Moss, B.** 1999. Poxviridae: The Viruses and Their Replication, p. 2 v. (xix, 2336). *In* B. N. Fields and D. M. Knipe (ed.), Fields Virology, 2nd ed. Raven Press, New York.

55. **Mukinda, V. B., G. Mwema, M. Kilundu, D. L. Heymann, A. S. Khan, and J. J. Esposito.** 1997. Re-emergence of human monkeypox in Zaire in 1996. Monkeypox Epidemiologic Working Group. Lancet **349:**1449-50.

56. **Muller, M. C., J. E. Cortes, D. W. Kim, B. J. Druker, P. Erben, R. Pasquini, S. Branford, T. P. Hughes, J. P. Radich, L. Ploughman, J. Mukhopadhyay, and A. Hochhaus.** 2009. Dasatinib treatment of chronic phase chronic myeloid leukemia: analysis of responses according to preexisting BCR-ABL mutations. Blood.

57. **Musacchio, A., M. Saraste, and M. Wilmanns.** 1994. High-resolution crystal structures of tyrosine kinase SH3 domains complexed with proline-rich peptides. Nat Struct Biol **1:**546-51.

58. **Nagar, B., W. G. Bornmann, P. Pellicena, T. Schindler, D. R. Veach, W. T. Miller, B. Clarkson, and J. Kuriyan.** 2002. Crystal structures of the

kinase domain of c-Abl in complex with the small molecule inhibitors PD173955 and imatinib (STI-571). Cancer Res **62:**4236-43.

59. **Nhieu, G. T., and P. J. Sansonetti.** 1999. Mechanism of Shigella entry into epithelial cells. Curr Opin Microbiol **2:**51-5.

60. **Nowell, P. C.** 1962. The minute chromosome (Phl) in chronic granulocytic leukemia. Blut **8:**65-6.

61. **Nowell, P. C., and D. A. Hungerford.** 1961. Chromosome studies in human leukemia. II. Chronic granulocytic leukemia. J Natl Cancer Inst **27:**1013-35.

62. **Pluk, H., K. Dorey, and G. Superti-Furga.** 2002. Autoinhibition of c-Abl. Cell **108:**247-59.

63. **Polak, J., Z. Zemanova, K. Michalova, H. Klamova, J. Cermak, and C. Haskovec.** 1998. A new case of chronic myeloid leukemia (CML) in myeloid blast crisis with an atypical (b3/a3) junction of the BCR/ABL gene. Leukemia **12:**250.

64. **Quintas-Cardama, A., and J. Cortes.** 2008. Therapeutic options against BCR-ABL1 T315I-positive chronic myelogenous leukemia. Clin Cancer Res **14:**4392-9.

65. **Quintas-Cardama, A., H. M. Kantarjian, and J. E. Cortes.** 2009. Mechanisms of primary and secondary resistance to imatinib in chronic myeloid leukemia. Cancer Control **16:**122-31.

66. **Razzell, P.** 1999. The origins of vaccinia virus - a brief comment. Soc Hist Med **12:**141.

67. **Reeves, P. M., B. Bommarius, S. Lebeis, S. McNulty, J. Christensen, A. Swimm, A. Chahroudi, R. Chavan, M. B. Feinberg, D. Veach, W. Bornmann, M. Sherman, and D. Kalman.** 2005. Disabling poxvirus pathogenesis by inhibition of Abl-family tyrosine kinases. Nat Med **11:**731-9.

68. **Rix, U., O. Hantschel, G. Durnberger, L. L. Remsing Rix, M. Planyavsky, N. V. Fernbach, I. Kaupe, K. L. Bennett, P. Valent, J. Colinge, T. Kocher, and G. Superti-Furga.** 2007. Chemical proteomic profiles of the BCR-ABL inhibitors imatinib, nilotinib, and dasatinib reveal novel kinase and nonkinase targets. Blood **110:**4055-63.

69. **Roberts, K. L., and G. L. Smith.** 2008. Vaccinia virus morphogenesis and dissemination. Trends Microbiol **16:**472-9.

70. **Rowley, J. D.** 1973. Letter: A new consistent chromosomal abnormality in chronic myelogenous leukaemia identified by quinacrine fluorescence and Giemsa staining. Nature **243:**290-3.

71. **Scaplehorn, N., A. Holmstrom, V. Moreau, F. Frischknecht, I. Reckmann, and M. Way.** 2002. Grb2 and Nck act cooperatively to promote actin-based motility of vaccinia virus. Curr Biol **12:**740-5.

72. **Shah, N. P., C. Tran, F. Y. Lee, P. Chen, D. Norris, and C. L. Sawyers.** 2004. Overriding imatinib resistance with a novel ABL kinase inhibitor. Science **305:**399-401.

73. **Shtivelman, E., B. Lifshitz, R. P. Gale, and E. Canaani.** 1985. Fused transcript of abl and bcr genes in chronic myelogenous leukaemia. Nature **315:**550-4.

74. **Sicheri, F., and J. Kuriyan.** 1997. Structures of Src-family tyrosine kinases. Curr Opin Struct Biol **7:**777-85.

75. **Smith, G. L.** 2007. Genus Yatapoxvirus, p. 113-125, Poxviruses, vol. 1. Birkhause Basel.

76. **Smith, G. L., A. Vanderplasschen, and M. Law.** 2002. The formation and function of extracellular enveloped vaccinia virus. J Gen Virol **83:**2915-31.

77. **Swimm, A., B. Bommarius, Y. Li, D. Cheng, P. Reeves, M. Sherman, D. Veach, W. Bornmann, and D. Kalman.** 2004. Enteropathogenic Escherichia coli use redundant tyrosine kinases to form actin pedestals. Mol Biol Cell **15:**3520-9.

78. **Tiribelli, M., A. Tonso, D. Ferrro, A. Parzilae, G. R. Cambrin, P. Scaravaglio, D. Cilloni, E. Gottardi, and G. Saglio.** 2000. Lack of SH3 domain does not imply a more severe clinical course in Ph+ chronic myeloid leukemia patients. Blood **95:**4019-20.

79. **Tulman, E. R., G. Delhon, C. L. Afonso, Z. Lu, L. Zsak, N. T. Sandybaev, U. Z. Kerembekova, V. L. Zaitsev, G. F. Kutish, and D. L. Rock.** 2006. Genome of horsepox virus. J Virol **80:**9244-58.

80. **Van Etten, R. A.** 1999. Cycling, stressed-out and nervous: cellular functions of c-Abl. Trends Cell Biol **9:**179-86.

81. **Vanderplasschen, A., E. Mathew, M. Hollinshead, R. B. Sim, and G. L. Smith.** 1998. Extracellular enveloped vaccinia virus is resistant to complement because of incorporation of host complement control proteins into its envelope. Proc Natl Acad Sci U S A **95:**7544-9.

82. **Wehrle, P. F., J. Posch, K. H. Richter, and D. A. Henderson.** 1970. An airborne outbreak of smallpox in a German hospital and its significance with respect to other recent outbreaks in Europe. Bull World Health Organ **43:**669-79.

83. **Welch, M. D., A. Iwamatsu, and T. J. Mitchison.** 1997. Actin polymerization is induced by Arp2/3 protein complex at the surface of Listeria monocytogenes. Nature **385:**265-9.

84. **Wolffe, E. J., A. S. Weisberg, and B. Moss.** 1998. Role for the vaccinia virus A36R outer envelope protein in the formation of virus-tipped actin-containing microvilli and cell-to-cell virus spread. Virology **244:**20-6.

85. **Zhou, H. X.** 2003. How often does the myristoylated N-terminal latch of c-Abl come off? FEBS Lett **552:**160-2.

Figure Legends

Figure 1 Cartoon of the orthopoxvirus lifecycle.

Following infection and replication intracellular Mature Virions (IMV) move on microtubules (MT) to a trans-golgi network (TGN) or early endosomal compartment. There IMV acquire additional membranes to form intracellular enveloped virions (IEV) which then transport to the plasma membrane on MT. Upon arrival, IEV merge their outermost layer with the plasma membrane to form cell-associated eveloped virions (CEV). There, CEV can either induce actin tails or release directly to become extracellular enveloped virions (EEV).

Figure 2 Actin polymerization cascade.

Arrows indicate junctions where microbes, interact with host proteins. The name of microbe and the associated protein are indicated for each interaction.

Figure 3 Kinase domain organization

Schematic representation of the domain architecture of the c-Src, c-Abl and BCR-Abl proteins.

Figure 1

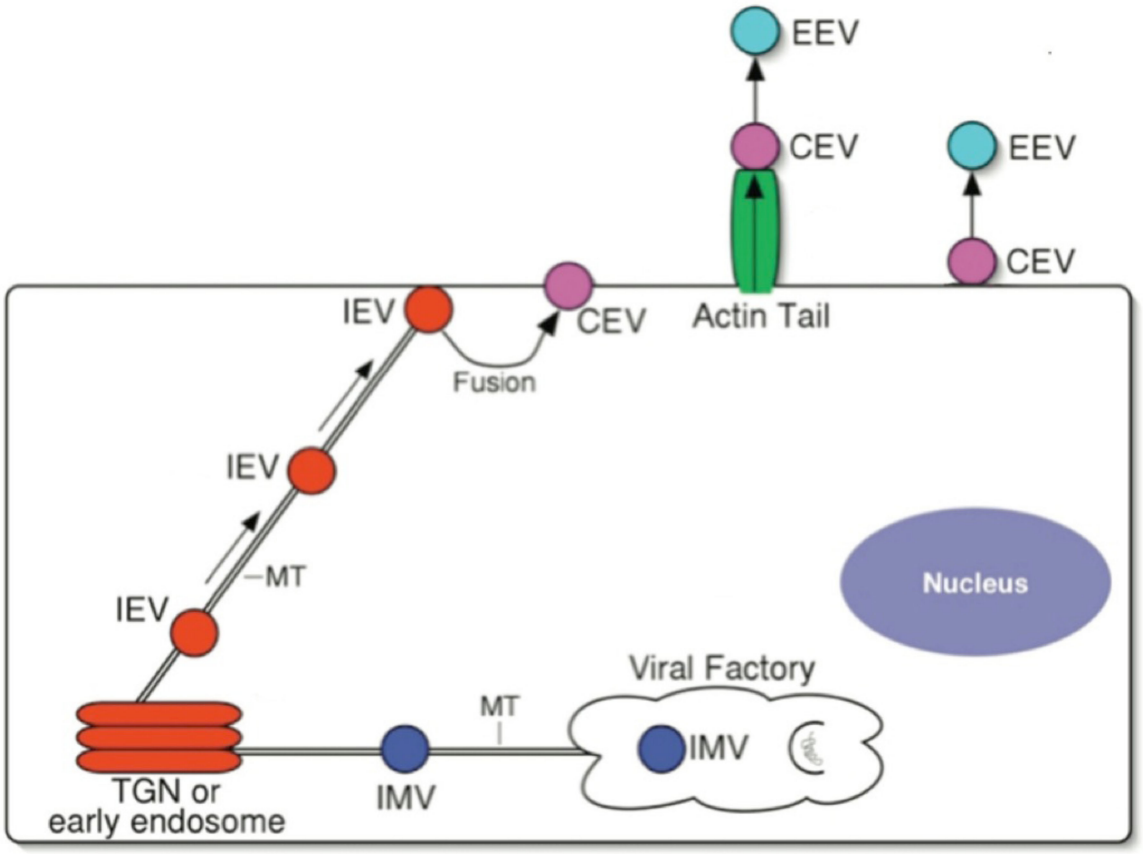
EEV
CEV
EEV
CEV
IEV
CEV
Actin Tail
Fusion
IEV
MT
IEV
Nucleus
Viral Factory
MT
IMV
TGN or
early endosome
IMV

Figure 2

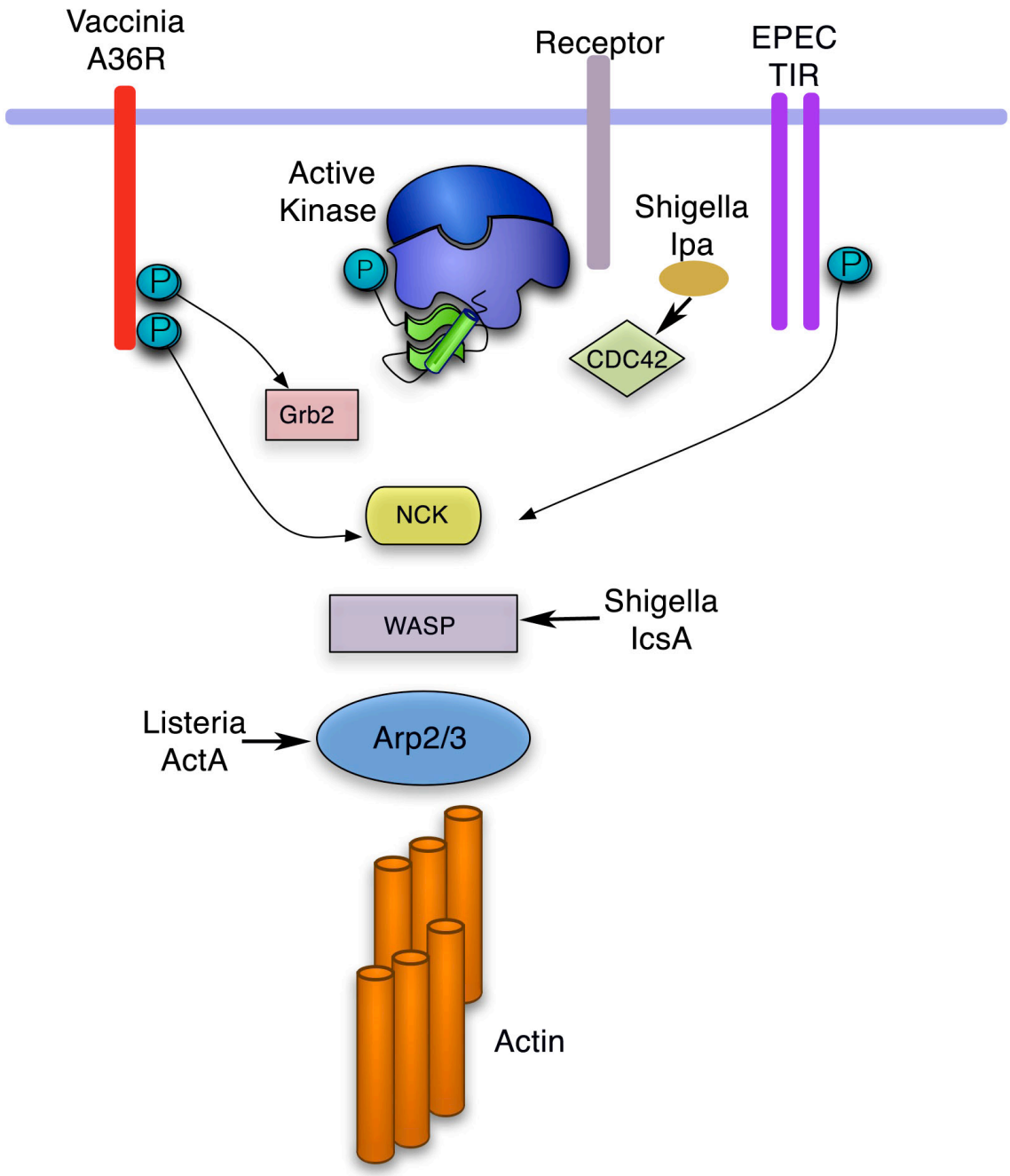
Vaccinia
A36R
Receptor
EPEC
TIR
Active
Kinase
Shigella
Ipa
P
P
P
P
CDC42
Grb2
NCK
WASP
Shigella
IcsA
Listeria
ActA
Arp2/3
Actin

Figure 3

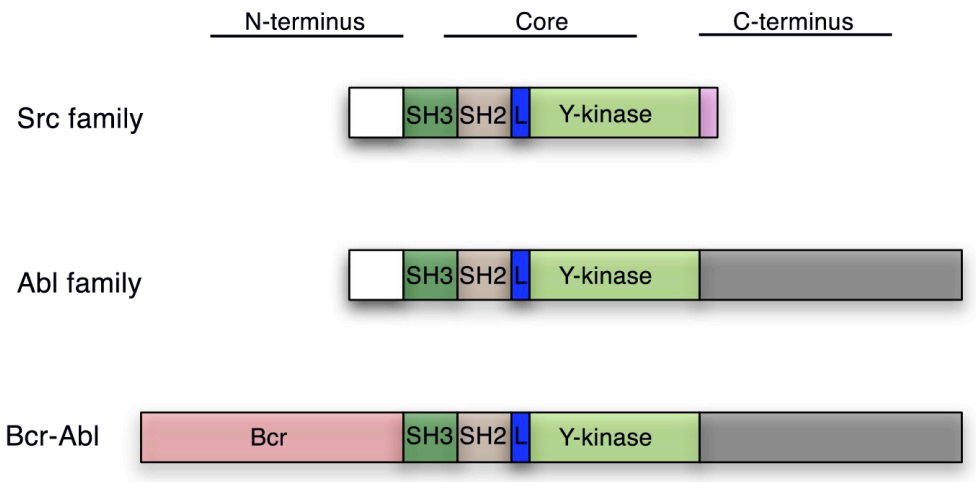
N-terminus
Core
C-terminus
Src family
SH3
SH2
L
Y-kinase
Abl family
SH3
SH2
L
Y-kinase
Bcr-Abl
Bcr
SH3
SH2
L
Y-kinase

Chapter 2

Disabling poxvirus pathogenesis by inhibition of Abl-family tyrosines

Published in Nature Medicine

July 2005 Volume11, No. 7 p.731-9

This manuscript was written by Patrick M. Reeves and Daniel Kalman

Patrick M. Reeves was intellectually involved in the concept, experimental design, and implementation of this project from its conception as well as the analysis and interpretation of the results. Patrick was involved in the preparation of all versions of the manuscript and was responsible for incorporating necessary revisions.

Disabling poxvirus pathogenesis by inhibition of Abl-family tyrosines

Patrick M. Reeves[$*], Bettina Bommarius[*], Sarah Lebeis[$*] , Shannon McNulty[$*], Jens Christensen[*], Ann Charoudi[%], Rahul Chavan[%], Mark B. Feinberg[%], Darren Veach[!], William Bornmann[^], Melanie Sherman[*], and Daniel Kalman[*+]

[*]Departments of Pathology and Laboratory Medicine, [%]The Emory Vaccine Center, and the [$]Microbiology and Molecular Genetics Graduate Program, Emory University School of Medicine, Atlanta, Georgia 30322

[!]Memorial Sloan Kettering Cancer Center, New York, New York

[^]Organic Chemistry Section, M.D. Anderson Cancer Center, University of Texas, Houston, Texas

Abbreviations used in this paper: PD, pyrido[2,3-d]pyrimidine; HA, haemagglutinin A; mAb, monoclonal antibody; CML, chronic myelogenous leukemia; pAb, polyclonal antiserum; P-Tyr, phosphotyrosine; α, anti.

Abstract

The *Poxviridae* family members Vaccinia and variola enter mammalian cells, replicate extranuclearly, and produce virions that travel to the cell surface along microtubules, fuse with the plasma membrane, and egress away from infected cells towards apposing cells on actin-filled membranous protrusions. We show that cell-associated enveloped virions (CEV) utilize Abl- and Src-family tyrosine kinases for actin motility, and that these kinases act in a redundant fashion, perhaps permitting motility in a greater range of cell types. Additionally, release of CEV from the cell requires Abl- but not Src-family tyrosine kinases, and is blocked by STI-571 (Gleevec), an Abl-family kinase inhibitor used to treat chronic myelogenous leukemia in humans. Finally, we demonstrate that STI-571 reduces viral dissemination by five orders of magnitude and promotes survival in infected mice, suggesting a possible utility of this drug in treating smallpox or complications associated with vaccination. This therapeutic approach may prove generally efficacious in treating microbial infections that rely on host tyrosine kinases, and because the drug targets host but not viral molecules, this strategy is much less likely to engender resistance compared to conventional anti-microbial therapies.

Introduction

Vaccinia virus (VV) and variola major are members of the *Poxviridae* family [1, 2]. VV serves as the vaccinating agent for variola major, the cause of smallpox. In 1980, the WHO declared smallpox eradicated. Routine vaccinations for smallpox ceased in 1972, and though immunity in vaccinated individuals does not appear to have abated [3, 4], a large proportion of the general population is still considered extremely susceptible to variola or other poxviruses [4, 5]. Moreover, vaccination itself is known to produce serious side effects in immunosuppressed individuals [6-8], raising the possibility that vaccination may no longer prove completely effective as a means to control an outbreak [6].

Upon entry, pox virions move to juxtanuclear locations where they replicate up to 10^4 concatameric genomes [2]. The concatamers resolve into unit genomes which are packaged in individual enveloped particles (called intracellular mature virions (IMV; [9], some of which are wrapped in additional membranes to form IEVs (intracellular enveloped virions (IEV); [10]). Cytolysis releases IMV from the cell. Prior to cytolysis, some IEV travel towards the host cell periphery via a kinesin/microtubule transport system [11-14]. To exit the cell, the IEV particle fuses with the plasma membrane of the host cell to form a cell-associated enveloped virus (CEV), leaving behind one of its two outer membranes [10, 15]. CEV either detach directly, or initiate actin polymerization to propel the particle on an actin-filled membrane protuberance towards an apposing cell and then detach [10]. Once detached, CEV form extracellular enveloped virus (EEV; [10]. It has

been proposed that IMV are readily detected and inactivated by the host immune system *in vivo*, but CEV and EEV evade immune detection and mediate spread of the infection [15].

The protein encoded by the VV A36R gene, located in the membrane surrounding the CEV, is required for actin polymerization [16] and virulence [17]. Previous reports suggest the mammalian tyrosine kinase c-Src localizes to virions and phosphorylates A36R [18]. Once phosphorylated, A36R facilitates detachment of kinesin [19], and, following virion fusion with the plasma membrane, recruitment and activation of host cell proteins, including Nck, Grb2, N-WASP, and Arp2/3, which initiate actin polymerization beneath the particle [20-22]. The mechanism by which CEV detach from the cell or from the actin protuberance (thereby generating EEV) and enter apposing cells is less well understood, and no role for tyrosine kinases in this process has been established.

Investigations of the mechanism of actin polymerization by the bacterial pathogen enteropathogenic E. coli (EPEC; [23]) have demonstrated that phosphorylation of the virulence factor Tir [24] and subsequent recruitment of actin polymerizing factors [25] is mediated by several redundant tyrosine kinases [26]. The similarity of the phosphorylation sites in the bacterial Tir protein and VV A36R (Supplementary Figure 1; [20] led us to consider whether the role of tyrosine kinases in VV actin polymerization might be similarly complex.

Here we show that redundant Src- and Abl-family kinases mediate actin motility, that Abl-family kinases mediate efficient release of infectious EEV, and that inhibitors of Abl-family kinases such as the 2-phenylpyrimidine STI-571 [27]; also called imatinib mesylate or Gleevec) block infectious EEV release, and limits spread of infection *in vivo* and promotes survival. STI-571 has proven clinically useful in treating chronic myelogenous leukemia (CML) in humans, a disease resulting from dysregulation of c-Abl [28, 29]. Our results raise the possibility of using STI-571 to treat variola infections or complications associated with vaccination.

Results

c-Src, c-Fyn, c-Yes, c-Abl and c-Arg localize in VV actin tails

To test whether Src- and Abl-family tyrosine kinases participate in VV actin motility, we first determined whether endogenous proteins resembling kinases in these families localized on the virion at the tip of the actin tail. 3T3 cells were exposed to VV, and then stained with antibodies against c-Src, c-Fyn, c-Yes, c-Abl, and the Abl-related kinase c-Arg. Infected cells were identified by staining with DAPI to label extranuclear replication centers ("RC", Supplementary Figure 2a), or by staining with α-TW2.3, an antibody that recognizes a vaccinia protein expressed early in infection (Supplementary Figure 2a; [30]). Virions on actin tails were recognized by DAPI staining or by fluorescence of a VV with GFP-B5R fusion protein (GFP-VV; [31]) localized in the membrane of the virion (Figure 1a; Supplementary Figure 2b). Actin tails are seen as intense phalloidin staining directly apposed to the virion (Figure 1a).

An endogenous protein recognized by α-Arg pAb was enriched at the tips of the actin tails relative to the cytoplasm (Figure 1a). Proteins recognized by the α-Abl mAb 8E9 (Figures 1b, 1bi or AB3 (not shown)), α-Src pAb (Figure 1d), α-Fyn mAb (Figure 1e), and α-Yes mAb (Figure 1f) were also enriched at the tips of the actin tails relative to the cytoplasm. The antibodies were specific and did not recognize epitopes in cells lacking these kinases (Figure 2e,f), and showed no cross-reactivity with other family members as judged by transfection experiments in cells lacking the kinases [26]. Notably, each kinase was detectable in only a

fraction of actin tails. For example, c-Abl was detectable in some tails (Figure 1bi) but not in others (Figure 1bii) within the same cell (Figure 1b). Staining with combinations of antibodies (e.g. α-Abl mAb together with α-Arg pAb) indicated that tails containing one kinase did not generally contain detectable levels of another kinase type (~95%; e.g. Figure 1c). Similar results were obtained with combinations of other anti-kinase antibodies (not shown), though because many were of similar isotype, testing all combinations was not feasible. Of the five Src- and Abl-family kinases, proteins resembling c-Fyn were the most frequently observed in actin tails (Figure 1e,g). PDGFR, FGFR, Lck, FAK, Ntk, Lyn, Jak1, Csk, Tyk2, and Pyk2 did not appear localized (not shown), suggesting that localization is specific for Src- and Abl-family kinases. Finally, staining with antibody recognizing phosphorylated Y412 (α-PY412) in the activation domain of Abl and Arg [32] indicated that these kinases were active in tails (Figure 1h). Staining with α-PY412 was specific for c-Abl or c-Arg, and was not evident in tails formed in cells lacking c-Abl and c-Arg [26].

Localization and distribution of exogenously expressed and endogenous kinases were similar. For example, YFP-c-Arg was present in only a fraction of actin tails in transfected cells (Supplementary Figure 2c,d), and even in cells expressing high levels of YFP-c-Arg, some tails contained no YFP-c-Arg, suggesting that localization of overexpressed kinase was specific (Supplementary Figure 2d). Co-localization with virions was not observed for other overexpressed proteins including GFP, YFP, or the kinase Hck (not

shown). The possibility exists that kinases sequentially associate with tails, or that one kinase begets recruitment of another, or that different virion types recruit different kinases. Together, these data suggest that Abl-and Src-family kinases localize in VV actin tails, though other kinases may localize as well.

Abl and Src-family kinases are not necessary for VV actin motility

To determine whether Src and/or Abl family tyrosine kinases were necessary for actin tail formation, we infected 3T3 cells derived from mice lacking lacking c-Src ($Src^{-/-}$; Figure 2a), c-Src and Yes ($Src^{-/-}/Yes^{-/-}$; not shown), c-Fyn and c-Yes ($Fyn^{-/-}/Yes^{-/-}$; not shown) or c-Src, c-Fyn, and c-Yes ($Src^{-/-}/Fyn^{-/-}/Yes^{-/-}$; Figure 2b), or from mice lacking c-Abl alone ($Abl^{-/-}$; not shown), c-Arg alone ($Arg^{-/-}$; not shown), or both c-Abl and c-Arg ($Abl^{-/-}/Arg^{-/-}$; Figure 2c). No differences were apparent in the capacity to form actin tails in these cell lines compared to wild-type cells (Figure 2a-c), though the proportion of tails occupied by particular kinases differed depending on the cell line and kinase (Supplementary Figure 2e,f). Despite the differences in distribution of kinases, neither c-Abl, c-Arg, c-Src, c-Fyn, nor c-Yes alone appear necessary for VV actin motility.

A role for Abl and Src-family kinases in actin motility.

To determine whether Abl- or Src-family kinases are sufficient for actin motility, we first identified inhibitors of tyrosine kinases that block actin motility, and then determined whether mutant kinases resistant to such inhibitors could support actin motility with the inhibitor present. To identify inhibitors of actin motility, we assessed the effects of pyrido[2,3-d]-pyrimidine (PD) compounds

(Supplementary Figure 3a), which competitively inhibit binding of ATP to Abl-family kinases and Src-family kinases [33-35]. With 10μM PD-166326 treatment, the number of infected cells with actin tails was reduced by 50 fold compared to the carrier control (0.1% DMSO; Figure 2d,f). Concentrations of PD-166326 less than 1μM were without effect (not shown). Staining with α-TW2.3 was evident in cells treated with 10μM PD-166326, suggesting that the drug did not block viral entry (not shown). Staining with DAPI or α-phosphotyrosine pAb (Figure 2c) revealed the presence of extranuclear replication centers in the presence of 10μM PD-166326. In a one-step growth curve (m.o.i.=5), viral yield was unaffected by PD-166326 except at the initial time point where it was reduced by one order of magnitude (Figure 3h). Consistent with an effect on cell-to-cell spread, PD-166326 reduced plaque diameter (Supplementary Figure 5a,b), and viral yield in a one-step growth curve at low m.o.i (0.1) indicated a reduction in viral yield by three orders of magnitude (Supplementary Figure 5f). Addition of 10μM PD-166326 eight hours after infection for as little as 20 minutes also resulted in loss of actin motility (Figure 2e). Compounds structurally related to PD-166326 (e.g. SKI-DV-1-10, 10 μM) were as effective as PD-166326 in blocking actin tails (not shown), and PP1 and PP2, which similarly inhibit activity of Src- and Abl-family kinases [36, 37], also blocked actin tails at concentrations of 25μM or greater as reported (Figure 3f; [18]). The effects of PD-166326 were not due to non-specific block of actin polymerization, as PD-166326 had no effect on actin tails induced by *Listeria monocytogenes* or *Shigella flexneri* [26]. PD-

166326 also blocked localization on the virion of factors critical for actin polymerization. Colocalization with the virion of phosphotyrosine, Nck, N-WASP, Grb-2, and Arp2/3 [21, 22] was not evident in GFP-VV-infected cells treated with 10μM PD-166326 (e.g. Figure 2g; Supplementary Figure 4e,f). Together, these results suggest that PD-166326 blocks tyrosine kinase activity essential for actin motility.

Abl- and Src-family kinases are sufficient for VV actin motility

To determine whether Abl, Arg, or Yes was sufficient for VV actin motility, we assessed whether each kinase could support VV actin motilty in the absence of activity from other Src- or Abl-family kinases. Specifically, we tested whether expression of PD-resistant alleles of c-Abl or c-Arg allowed actin motility to persist in the presence of PD-166326. Mutations within the ATP binding pocket disrupt Van der Waals interaction between PD-166326 and the kinases (Abl-T315I and Arg-T314I), and increase the K_i of PD-166326 from 10 nM to 1 μM as measured by *in vitro* kinase assay [26]. As seen in Figure 3a, actin tails were evident in PD-treated cells expressing YFP-c-Arg-T314I (Figure 3a upper cell), but not in cells expressing endogenous c-Arg (Figure 3a, lower cell), or in cells overexpressing c-Arg-WT (Supplementary Figure 4a) or in cells expressing c-Abl-T315I (Figure 3b). Tails were also evident in PD-treated cells expressing c-Yes-T348I (Figure 4c), but not c-Yes (Supplementary Figure 4b). These data indicate that c-Arg and c-Yes, but not c-Abl, are sufficient among tyrosine kinases for VV actin motility.

To determine whether other Src-family kinases were sufficient for VV actin motility, we treated $Src^{-/-}/Fyn^{-/-}/Yes^{-/-}$ cells or cell lines lacking subsets of Src-family kinases with 10μM STI-571 (Supplementary Figure 3b), a 2-phenylpyrimidine compound which inhibits Abl-family kinases but not Src-family kinases [27]. STI-571 did not block actin motility in wild-type 3T3 cells (Figure 3d), even at concentrations as high as 25μM, and did not reduce viral yield (Figure 2h) or the appearance of viral replication centers (Figure 3d), and had no effect on transit of GFP-labeled virions to the cell periphery (Figure 3e). Addition of 10 μM STI-571 severely limited VV actin motility in $Src^{-/-}/Fyn^{-/-}/Yes^{-/-}$ cells, reducing the average number of actin tails per cell by 16 fold to ~3 per cell (Supplementary Figure 4d) with 30% of cells having none (e.g. Figure 3e). The carrier for STI-571, DMSO, was without effect (Figure 3f). To determine whether c-Fyn or c-Src were sufficient for VV actin motility, we tested the effects of 10μM STI-571 on VV actin motility in $Src^{-/-}/Yes^{-/-}$ cells (Figure 3g; Supplementary Figure 4c) and $Fyn^{-/-}/Yes^{-/-}$ cells (Figure 3h). Treatment with STI-571 also had no detectable effects on the number of actin tails per cell in either line (Supplementary Figure 4d). Together, these results suggest that c-Arg, c-Yes, c-Src and c-Fyn are all sufficient for VV actin motility.

To determine whether redundant tyrosine kinases mediate plaque formation, monolayers of 3T3 cells or cells lacking various kinases were infected with VV (Figure 4). In accordance with a requirement of actin tails for cell-to-cell spread [15, 38], plaques formed on all these cell lines with equal efficacy. Treatment of

3T3 or BSC-40 cells with 10μM PD-166326 reduced plaques to "pinpoints" (Figure 4d; Supplementary Figure 5a,b). STI-571 did not produce significant changes in plaque number in BSC-40 cells, though this compound did reduce plaque size (Figure 4c,e; Supplementary Figure 5c,d). Single step growth assays indicated that in BSC-40 cells 10μM STI-571 had little effect on viral yield (m.o.i =0.1 or 5; Figure 2h) or in $Src^{-/-}/Fyn^{-/-}/Yes^{-/-}$ cells (m.o.i= 5; Supplementary Figure 5e). These data suggest that redundant Abl- and Src-family kinases mediate actin motility and cell-to-cell spread, but have little effect on viral replication.

Abl-family kinases mediate release of infectious EEV.

We next determined whether tyrosine kinases mediated long-range spread of VV by facilitating release of infectious EEV from the plasma membrane. To do this, wild-type 3T3 cells or 3T3 cells lacking various tyrosine kinases were infected with VV. Supernatants containing EEV were collected from cells 24 hrs after infection. At this time point, the supernatant contains plaque-forming units (PFU) composed of EEV and to a lesser extent IMV released from lysed cells [39]. The supernatant was then used to assess plaque formation in BSC-40 cells. In some experiments, supernatants were incubated with 2D5 mAb to neutralize contaminating IMV [39, 40] (Figure 5h; Supplementary Figure 7a,b). Analysis of plaques indicated that supernatants from wild-type 3T3 cells (Figure 5a), $Src^{-/-}/Fyn^{-/-}/Yes^{-/-}$ cells (Figure 5b), $Abl^{-/-}$ cells (Figure 5c), and $Arg^{-/-}$ cells (Figure 5d) all contained approximately the same PFU, but supernatants from $Abl^{-/-}/Arg^{-/-}$ cells (Figure 5e,h center) contained ~4-fold fewer PFU. Such a decrease could not be

accounted for by lower infectivity of $Abl^{-/-}/Arg^{-/-}$ cells compared to wild type cells because the same number of plaques formed on both cell types (Figure 4a,b). In accordance with these data, treatment of wild-type cells (BSC-40 or 3T3) with 10 μM STI-571 caused a ~3-fold reduction in EEV (Figure 5f-h), without significantly affecting viral yield (Figure 2h; Supplementary Figure 5f and 6d,e). Treatment with 10μM STI-571 also blocked the formation of "comets" apposed to plaques in BSC-40 cells (Supplementary Figure 5c,d), a phenomena associated with EEV [41]. The decrease in EEV observed with STI-571 may also account for the reduction in plaque size in BSC-40 cells treated with this compound (Figure 4c,e; Supplementary Figure 5c,d). The effect of STI-571 on EEV release was not restricted to VV strain WR. Release of EEV by VV strain IHD-J, which releases 40-fold more EEV than WR [42], was similarly inhibited (Figure 5h). Treatment of 3T3 cells with 10μM PD-166326 likewise reduced the number of EEV (not shown). However, because PD-166326 blocks actin tails (Figure 2), we could not distinguish whether the drug caused a decrease in the number of virions reaching the cell surface or blocked EEV release or both. Taken together, these observations suggest that c-Abl and c-Arg, but not Src-family kinases, are each sufficient for release of infectious EEV *in vitro,* and together they are necessary.

STI-571 promotes survival in VV-infected mice.

EEV are less immunogenic than other forms of the virus [43], and have been proposed to mediate spread of infection and virulence *in vivo* [17, 44, 45]. The involvement of Abl-family kinases in release of infectious EEV *in vitro* suggested

that STI-571 might control VV infection *in vivo*. STI-571 at 100mg/kg/day or the saline carrier was delivered to mice via Alzet osmotic pumps placed subcutaneously. This drug concentration has been used in mouse leukemia models for a period of months without significant side effects, and was equivalent to doses used in humans with CML [46]. Four days post-infection, the number of viral genomes in ovaries was measured by quantitative PCR [47]. In untreated animals or animals with pumps containing carrier, $\sim 10^7$ copies/250ng DNA was detected (Figure 6a). The detection limit of the assay, determined by serial dilution, was 10 viral genomes. Treatment with STI-571 reduced viral genome copies in ovaries by five orders of magnitude (Figure 6a). These differences were judged statistically significant by a two-sided Fisher's exact test ($P<10^{-6}$; see Methods). In accordance with an inhibition of EEV release (Figure 5g), these results suggest that STI-571 inhibits spread of VV *in vivo*.

We next assessed whether STI-571 promotes survival in response to a lethal challenge. Mice were inoculated intranasally with 10^4 PFU VV IHD-J, and sacrificed upon loss of 30% of their body weight. With this innoculum, only 30% of carrier-treated mice survived, compared to 100% of STI-571-treated mice (Figure 6b; $P<10^{-6}$, Fisher's test). These data suggest that STI-571 prevents lethality likely by preventing dissemination of virus without interfering with immune clearance.

Discussion

Previous reports concluded that Src or Src-family kinases mediate release of virions from microtubules [19] and actin motility [18]. However, these studies were based on localization of c-Src to the virion, and block of virion detachment from microtubules or actin motility with kinase-dead alleles of Src and with PP1, an inhibitor of Src-family kinases [36]. Our data showing actin motility in $Src^{-/-}/Fyn^{-/-}/Yes^{-/-}$ cells suggests that kinase requirements are more complex. In this regard, PP1 and PP2 have been recently found to additionally inhibit Abl-family kinases [37], and kinase-dead Src may have competed with not only c-Src but also other Src- or Abl-family kinases. Results presented here suggest that c-Arg, c-Src, c-Fyn, and c-Yes all likely mediate release of virions from microtubules and actin motility, though the possibility exists that additional functionally redundant tyrosine kinases, defined by their sensitivity to STI-571 and PD-166326, also suffice. This possibility is supported by our observation that only ~80% of the tails in $Src^{-/-}/Fyn^{-/-}/Yes^{-/-}$ cells contain both c-Abl and c-Arg (Supplementary Figure 2e). Our results additionally indicate a role for Abl and Arg, but not Src-family kinases, in release of infectious EEV. A model summarizing the dependence of actin tails and EEV release on tyrosine kinases, and the effects of the various inhibitors, is presented in Figure 6c.

Why might VV utilize multiple kinases in infected cells? One possibility is that multiple kinases ensure phosphorylation of targets crucial for pathogenesis and broaden the range of cell types susceptible to infection. Such mechanisms are

not unprecedented among viral or even bacterial pathogens. For example, polyoma virus middle T protein dysregulates Src-family kinases to facilitate transformation [48]. Likewise, Enteropathogenic E. coli (EPEC) take advantage of redundancy in both tyrosine kinases and downstream adaptors to form actin-filled membranous pedestals [26, 49]. Notably, EPEC utilizes c-Abl, Arg and other tyrosine kinases to phosphorylate the virulence factor Tir, a molecule that shares striking homology to VV A36R [20]. Finally, retroviruses such as Rous sarcoma virus and Ableson leukemia virus have long been recognized to harbor oncogenes which activate mammalian signaling pathways regulating cell division, as a means of indirectly facilitating viral replication [50]. Given the widespread utilization of cellular signaling molecules by microbial pathogens, the possibility exists that inhibitors developed against host signaling molecules dysregulated in cancer may prove effective as anti-microbial agents against a wide variety of pathogens.

The identification of the Src- and Abl-family kinases as participants in dissemination of VV has important implications for treating poxvirus infections. Variola infections or severe adverse reactions associated with vaccination against smallpox are primarily treated with vaccinia immune globulin (VIG) and the nucleotide analog cidofovir [7, 51]. VIG has only limited efficacy in controlling symptoms associated with severe adverse reactions [5, 7]. Cidofovir is effective against poxviruses but is extremely toxic [5, 7]. Moreover, protocols used in the 1970s to control smallpox outbreaks [5, 7] may not be valid today because

vaccination may prove lethal in individuals with acquired or congenital immunocompromising conditions, and rapid identification of such individuals may be impractical [6].

STI-571 is a well-established therapy for chronic myelogenous leukemia and stromal tumors, and has relatively few serious side effects [29]. In the event of a poxvirus outbreak, administration of STI-571 in either a therapeutic or prophylactic capacity may prove effective alternative. The use of STI-571 to treat poxvirus infections still requires that the infection be cleared by an effective immune response, and more experimental work will be required to determine whether the drug can protect immunocompromised individuals from side effects associated with vaccination, and whether STI-571 affects immune responses required for clearance of poxviruses or for the acquisition of memory. In this regard, however, no serious immunosuppressive effects have been reported with long-term (months) treatment of CML patients with STI-571 [29], and lethally infected mice treated with STI-571 fully recover (Figure 6b). Our data showing that STI-571 limits EEV production (Figure 5) and reduces spread of VV to adjacent organs (Figure 6a) is in accordance with reports suggesting that EEV mediate virulence *in vivo*. Antibodies against EEV and CEV protect against virus challenge *in vivo* and *in vitro* [44, 45], and viral strains with deletions in A36R form fewer CEV and EEV and exhibit attenuated virulence in mice [17]. Finally, EEV are less immunogenic than IMV [43].

Smallpox infections commence with respiratory inoculation by small numbers of variola particles (~10; [4]), which then disseminate in two stages of viremia. Data presented here suggest that STI-571 will likely prove effective both as a prophylactic and when administered prior to systemic dissemination. Consistent with this idea, STI-571 prevented dissemination to ovaries following IP infection (Figure 7A), and promoted survival in a lethal challenge (Figure 7B). Drugs such as PD-166326 may prove useful once the virus has disseminated, a prospect we are currently testing. Finally, use of STI-571 in conjunction with cidofovir may permit use of the latter at less toxic doses.

The strategy of using STI-571 to treat a poxvirus infection suggests an important general solution to the capacity of infectious microbes to develop drug resistance. Resistance to drugs directed against microbial targets occurs by mutation of binding sites for the drug [52], or by drug inactivation or removal [53]. However, STI-571 disables *host* proteins essential for the virus life cycle. To develop resistance, a microbe would have to significantly alter its pathogenic strategy without strong growth selection, making the likelihood of engendering resistance much lower than with conventional antibiotics or antimicrobials [54]. That STI-571 inhibits release of IHD-J EEV suggests that mutations in viral proteins cannot easily overcome an inhibitor of EEV release directed at a host target.

In summary, we propose the use of STI-571, a drug developed to treat cancer without significant side effects, as a therapeutic for infections caused by

poxviruses. Our approach of interfering with host targets may have general utility in developing novel drugs, or novel uses for existing drugs, to combat a variety of microbial pathogens that acquire drug resistance.

Methods

Cell culture. BSC-40 cells from ATCC, 3T3 cells and 3T3 cells derived from $Abl^{-/-}$/$Arg^{-/-}$ mice [55], or 3T3 cells derived from $Src^{-/-}$/$Fyn^{-/-}$/$Yes^{-/-}$ mice (ATCC CRL-2459) were maintained in DMEM supplemented with 10% fetal bovine serum (FBS), penicillin, and streptomycin as described [26]. For microscopy cells were grown on glass coverslips in DMEM containing serum and incubated for sixteen hours at 37 °C with VV (strain WR) or VV-GFP-B5R [31] with ~10^4 PFU. For some experiments, cells were transfected one to two days prior to infection with plasmid vectors using Fugene-6 (Roche). Abl-T315I and Arg-T314I were constructed using Quik-Change site directed mutagenesis technology (Stratagene) as described [26]. PD compounds (e.g. PD-166326 and SKI-DV1-10; Supplementary Figure 3), were synthesized as described [33, 56], and were indistinguishable in their effects in all assays. PD-166326 and the mesylate salt of STI-571 was synthesized as described [33, 56]. PD compounds, and PP2 (Calbiochem) were dissolved in 100% DMSO. STI-571 was dissolved in water. For most experiments, PD-166326, PP2, or DMSO was added to cells immediately prior to infection. For post-infection treatment experiments, compound or DMSO was added to cells fourteen hours after addition of VV, and the cells fixed fifteen minutes to two hours subsequently. Although the K_i of PD-166326 for Abl is about 5-10 nM as measured by *in vitro* kinase assay, micromolar concentrations of PD-166326 are required to block actin tails or plaques in cells. We surmise that this discrepancy arose because the drug when

applied to the medium may not achieve the same concentration in the cell. In this regard, we have now synthesized more soluble derivatives of PD-166326, which have the same K_i for WT Abl but which block actin tails at slightly lower concentrations (i.e. 1 μM; not shown). Additionally, the ATP concentration within the cell may increase the effective K_i. In vitro kinase assays are carried out at nM-μM ATP concentrations whereas the free ATP concentration inside the cell has been estimated to be around 2 to 5 mM. Because ATP and PD-166326 compete for the same binding site it is not at all unreasonable to expect that the effective K_i increases. *In vitro* kinase assays with high concentrations of ATP appear consistent with this prediction. Moreover, in systems where Src family kinases have been implicated, PP1 concentrations in the μM range are routinely used despite a measured K_i in vitro of 5-50 nM depending on the kinase.

Immunofluorescence staining. For immunofluorescence analysis, cells were fixed in 2% formaldehyde and permeablized in Triton-X-100 as described [25, 57]. VV was recognized by staining with 4,6-diamidino-2-phenylindole (DAPI; 1 μg/ml; Sigma), and actin by staining with 488-phalloidin, 566-phalloidin, or 594-phalloidin (1 μg/ml; Molecular Probes). The primary antibodies and concentrations used in this study were as follows: α-WASP pAb (affinity purified, 1:200 dilution), α-HA mAb (3F10; .01 μg/ml, Roche), α-Nck mAb (1 μg/ml; Oncogene Research), α-Abl mAb (AB3; 0.5 μg/ml for overexpressed Abl proteins; 50 μg/ml for endogenous Abl proteins; 8E9; 0.05 μg/ml; Pharmingen), α-Src pAb (0.1 μg/ml; Santa Cruz), α-Fyn mAb (0.1 μg/ml; ABCAM), α-Yes pAb

(0.1 μg/ml; Cell Signalling), α-Arg pAb (1:200; UBI), α-pY412 (0.1 μg/ml; Cell signaling), and α-TW2.3 mAb (ascites, 1:2000 for microscopy; [30]). The specificity of anti-kinase antibodies was determined by staining of cell lines lacking particular kinases [26]. Cells expressing exogenous c-Abl-WT were distinguished by relatively high fluorescence intensity with lower α-Abl mAb concentrations. Thus images were acquired with much shorter exposures than those used to detect endogenous c-Abl-like protein. Secondary antibodies were obtained from Jackson Immunochemicals.

Microscopy. Images were acquired with a scientific-grade cooled charge-coupled device (Cool-Snap HQ with ORCA-ER chip) on a multi-wavelength wide-field three-dimensional microscopy system (Intelligent Imaging Innovations) based on a Zeiss 200M inverted microscope using a 63x N.A.1.4 lens (Zeiss). Immunofluorescent samples were imaged at room temperature using a standard Sedat filter set (Chroma) in successive 0.20 μm focal planes through the samples, and out-of-focus light was removed with a constrained iterative deconvolution algorithm [58]. Actin tails were recognized by intense phalloidin staining associated with DAPI or GFP fluorescence objects measuring ~200 nm in diameter. Localization of fluorescence at the end of actin tails and colocalized with GFP florescence in cells infected with GFP-VV was used to indicate localization. Colocalization was assessed by coincidence of fluorescent staining of kinases in the Cy5 and Cy3 channels. The microscope filters were calibrated with multicolored fluorescent beads to insure coincidence of fluorescent signals in

all channels to within a pixel (100nm for the 63x N.A. 1.4 lens). For quantitative measurements of kinase localization, approximately 500 tails in at least seven cells were assessed for each kinase.

Plaque assays For plaque assays, cells were seeded in 6-well dishes, grown to confluence, and incubated with serial dilutions of VV strain WR or IHD-J. After one hour the cells were washed to remove excess virus, and DMEM was replaced the cells were incubated for an additional 3-4 days. Cells were then fixed and stained with 15% ethanol and 1% crystal violet to visualize plaques. For measurements of secreted EEV, cells were incubated in 2% FBS DMEM, media was removed 24 hours after infection centrifuged for 15 minutes at 400 x g, dilutions made and added to uninfected BSC-40 cell monolayers, and the number of plaques assessed 2-4 days subsequently. For some experiments, the supernatant collected from infected cells was incubated with α-IMV mAb (2D5; at various dilutions of ascites ranging from 1:100 to 1:1000; Supplementary Figure 7a,b; [40]), which has been shown to inactivate IMV but not EEV. Plaque assays were used to determine if different cell lines were infected with equal efficacy. Single step growth curves were used to determine yield of virus in different cell lines. To do this, cell monolayers were infected at an m.o.i. of 0.1 or 5. Monolayers were harvested one, two, or three days post-infection, frozen and thawed three times to release viral particles in the cell, and centrifuged to remove cellular debris. The supernatant was then serially diluted and added to

monolayers of uninfected BSC-40 cells, and the number of plaques assessed after two days.

Mouse assays For mouse experiments the mesylate salt of STI-571 was dissolved in saline and loaded into Alzet pumps (1007D or 2002) capable of dispensing continuous flow of drug 100mg/kg/day. The pumps were inserted subcutaneously into anaesthetized six-week old female C57/Bl6 mice (Jackson laboratories). The level of STI-571 in the blood was not determined. At these drug concentrations, we observed no loss in weight or other adverse effects in uninfected animals, and such concentrations have been used to treat cancer in mice over prolonged periods (up to 3 months; [46]. Thus the drug appeared non-toxic. Twenty-four hours after insertion of the pump, some of the mice were infected by intraperitoneal inoculation with 10^4 PFU VV (see also [59]). After four days, the mice were sacrificed and their ovaries extracted for analysis of viral load by real-time PCR. For survival experiments mice were inoculated intranasally with 10^4 PFU one day after implantation of pumps containing drug or carrier. Weight was monitored daily and mice were sacrificed if their weight declined by more than 30%.

Viral copy number measurements. The probe and primers for real-time PCR were designed by the use of Primer Express software (Applied Biosystems) within the conserved region of the VV UDG gene. The TaqMan Probe: 5'-CGAGACGAGACGTCGCCTATTCCTG-3' (Applied Biosystems) was labeled at 5' end with the reporter dye FAM (6-carboxyfluorescein) and at the 3' end with

the quencher dye TAMRA (6-carboxytetramethyl-rhodamine) with a melting temperature (Tm) of 68°C. The primer sequences were as follows: 5'-GGTAGAGTTTTATAACGAAGTAGCCAGTT-3'(sense; length, 29 bases, Tm = 58°C) and 5'-CTCGTTTATTTCTAAGCGGTTGTTT- 3' (antisense; length, 25 bases, Tm = 58°C). Real-time PCR was performed using the ABI Prism 7900HT sequence detection system (Applied Biosystems) with TaqMan Gold kit under the following conditions: the 50 μl reactions contained 5 μl of 10X TaqMan buffer A; 4 mM $MgCl_2$; 200 mM dNTPs; 200 nM of each primer, 125 nM fluorogenic probe, and 1.25 units of AmpliTaq Gold DNA polymerase. Universal thermal cycling conditions consisted of 10 min at 95°C, followed by 45 cycles of 15 sec at 95°C and 1 min at 60°C. 250 nanograms of DNA isolated from ovaries using DNAeasy Kit (Qiagen) were analyzed as template for amplification and results were expressed in VV copies per 250 ng of DNA. Each reaction was carried out in duplicate. For statistical analysis, mice with a viral copy number of greater than 10^4 were scored as clinically ill. By this criterion, all of the mice in the carrier group, and one of the twelve mice in the group treated with STI-571 were ranked clinically ill. This difference was judged statistically significant by a two-sided Fisher's exact test ($P<10^{-6}$).

Online supplemental material

Supplementary Figures 1-7 referred to throughout are available for viewing online at www.naturemedicine.com.

Acknowledgements

The authors thank David Kalman, David Steinhauer, Orion Weiner, Jack Taunton and Karl Saxe for helpful discussions; Afrooz Family, Silvia Staprans, Natalia Kozyr, and Ronald Griffith, for assistance and advice; Bruce Meyer and Jean Wang for Abl cDNAs; Tony Koleske for $Abl^{-/-}/Arg^{-/-}$ cells, $Abl^{-/-}$ cells, and $Arg^{-/-}$ cells, and c-Arg-YFP cDNA; Bernie Moss and John Yudell for α-TW2.3 mAb; Raphael Blasco for GFP-VV; Cliff Lowell for $Src^{-/-}$ cells, $Src^{-/-}/Fyn^{-/-}$ cells, and $Src^{-/-}/Yes^{-/-}$ cells; Geoff Smith for α-IMV mAb; and Laura Burleigh, David Steinhauer, and Charlie Moran for commenting on the manuscript. The work was supported by NIH grant PO1 AI 46007 (to M.B.F.), and by grants from the University Research Council, Emory University, the Southeastern Regional Center for Excellence in Bioterrorism (SERCEB) Pilot Project Feasibility Award, grant R01-AI056067-01 from the N.I.A.I.D., and an award from the Emtech Biotechnology Foundation (all to D.K.).

References

1. Esposito, J., and Fenner, F, *Poxviruses*, in *Fields Virology*, B.N. Fields and D.M. Knipe, Editors. 1999, Raven Press: New York. p. 2 v. (xix, 2336).

2. Moss, B., *Poxviridae: The Viruses and Their Replication*, in *Fields Virology*, B.N. Fields and D.M. Knipe, Editors. 1999, Raven Press: New York. p. 2 v. (xix, 2336).

3. Crotty, S., et al., *Cutting edge: long-term B cell memory in humans after smallpox vaccination.* J Immunol, 2003. **171**(10): p. 4969-73.

4. National Research Council, I.o.M., *Assessment of Future Scientific Needs for Live Variola Virus*. 1999, Washington, D.C.: National Academy Press. 126.

5. Harrison, S.C., et al., *Discovery of antivirals against smallpox.* Proc Natl Acad Sci U S A, 2004. **101**(31): p. 11178-92.

6. Amorosa, V.K. and S.N. Isaacs, *Separate worlds set to collide: smallpox, vaccinia virus vaccination, and human immunodeficiency virus and acquired immunodeficiency syndrome.* Clin Infect Dis, 2003. **37**(3): p. 426-32.

7. CDC, *Vaccinia (Smallpox) Vaccine Recommendations of the Advisory Committee on Immunization Practices (ACIP), 2001*. 2001, CDC: Atlanta. p. 1-25.

8. CDC, *Smallpox Vaccination and Adverse Reactions Guidance for Clinicians*. 2003, CDC: Atlanta. p. 1-28.

9. Smith, J.N. and B.M. Ahmer, *Detection of other microbial species by Salmonella: expression of the SdiA regulon.* J Bacteriol, 2003. **185**(4): p. 1357-66.

10. Smith, G.L., B.J. Murphy, and M. Law, *Vaccinia virus motility.* Annu Rev Microbiol, 2003. **57**: p. 323-42.

11. Carter, G.C., et al., *Vaccinia virus cores are transported on microtubules.* J Gen Virol, 2003. **84**(Pt 9): p. 2443-58.

12. Hollinshead, M., et al., *Vaccinia virus utilizes microtubules for movement to the cell surface.* J Cell Biol, 2001. **154**(2): p. 389-402.

13. Rietdorf, J., et al., *Kinesin-dependent movement on microtubules precedes actin-based motility of vaccinia virus.* Nat Cell Biol, 2001. **3**(11): p. 992-1000.

14. Ward, B.M. and B. Moss, *Vaccinia virus intracellular movement is associated with microtubules and independent of actin tails.* J Virol, 2001. **75**(23): p. 11651-63.

15. Smith, G.L., A. Vanderplasschen, and M. Law, *The formation and function of extracellular enveloped vaccinia virus.* J Gen Virol, 2002. **83**(Pt 12): p. 2915-31.

16. Wolffe, E.J., A.S. Weisberg, and B. Moss, *Role for the vaccinia virus A36R outer envelope protein in the formation of virus-tipped actin-containing microvilli and cell-to-cell virus spread.* Virology, 1998. **244**(1): p. 20-6.

17.Parkinson, J.E. and G.L. Smith, *Vaccinia virus gene A36R encodes a M(r) 43-50 K protein on the surface of extracellular enveloped virus.* Virology, 1994. **204**(1): p. 376-90.

18.Frischknecht, F., et al., *Actin-based motility of vaccinia virus mimics receptor tyrosine kinase signalling.* Nature, 1999. **401**(6756): p. 926-9.

19. Newsome, T.P., N. Scaplehorn, and M. Way, *SRC mediates a switch from microtubule- to actin-based motility of vaccinia virus.* Science, 2004. **306**(5693): p. 124-9.

20.Frischknecht, F. and M. Way, *Surfing pathogens and the lessons learned for actin polymerization.* Trends Cell Biol, 2001. **11**(1): p. 30-38.

21. Moreau, V., et al., *A complex of N-WASP and WIP integrates signalling cascades that lead to actin polymerization.* Nat Cell Biol, 2000. **2**(7): p. 441-8.

22.Scaplehorn, N., et al., *Grb2 and Nck act cooperatively to promote actin-based motility of vaccinia virus.* Curr Biol, 2002. **12**(9): p. 740-5.

23. Nataro, J.P. and J.B. Kaper, *Diarrheagenic Escherichia coli.* Clin Microbiol Rev, 1998. **11**(1): p. 142-201.

24. Kenny, B., et al., *Enteropathogenic E. coli (EPEC) transfers its receptor for intimate adherence into mammalian cells.* Cell, 1999. **91**(4): p. 511-520.

25.Kalman, D., et al., *Enteropathogenic E. coli acts through WASP and Arp2/3 complex to form actin pedestals.* Nat Cell Biol, 1999. **1**(6): p. 389-91.

26.Swimm, A., et al., *Enteropathogenic Escherichia coli use redundant tyrosine kinases to form actin pedestals.* Mol Biol Cell, 2004. **15**(8): p. 3520-9.

27. Schindler, T., et al., *Structural mechanism for STI-571 inhibition of abelson tyrosine kinase.* Science, 2000. **289**(5486): p. 1938-42.

28. Druker, B.J., et al., *Chronic myelogenous leukemia.* Hematology (Am Soc Hematol Educ Program), 2001: p. 87-112.

29.Goldman, J.M. and B.J. Druker, *Chronic myeloid leukemia: current treatment options.* Blood, 2001. **98**(7): p. 2039-42.

30. Yuwen, H., et al., *Nuclear localization of a double-stranded RNA-binding protein encoded by the vaccinia virus E3L gene.* Virology, 1993. **195**(2): p. 732-44.

31.Ward, B.M. and B. Moss, *Visualization of intracellular movement of vaccinia virus virions containing a green fluorescent protein-B5R membrane protein chimera.* J Virol, 2001. **75**(10): p. 4802-13.

32.Pluk, H., K. Dorey, and G. Superti-Furga, *Autoinhibition of c-Abl.* Cell, 2002. **108**(2): p. 247-59.

33.Kraker, A.J., et al., *Biochemical and cellular effects of c-Src kinase-selective pyrido[2, 3- d]pyrimidine tyrosine kinase inhibitors.* Biochem Pharmacol, 2000. **60**(7): p. 885-98.

34.Dorsey, J.F., et al., *The pyrido[2,3-d]pyrimidine derivative PD180970 inhibits p210Bcr-Abl tyrosine kinase and induces apoptosis of K562 leukemic cells.* Cancer Res, 2000. **60**(12): p. 3127-31.

35.Wisniewski, D., et al., *Characterization of potent inhibitors of the Bcr-Abl and the c-kit receptor tyrosine kinases.* Cancer Res, 2002. **62**(15): p. 4244-55.

36.Liu, Y., et al., *Structural basis for selective inhibition of Src family kinases by PP1.* Chem Biol, 1999. **6**(9): p. 671-8.

37.Tatton, L., et al., *The Src-selective kinase inhibitor PP1 also inhibits Kit and Bcr-Abl tyrosine kinases.* J Biol Chem, 2003. **278**(7): p. 4847-53.

38.Ward, B.M., A.S. Weisberg, and B. Moss, *Mapping and functional analysis of interaction sites within the cytoplasmic domains of the vaccinia virus A33R and A36R envelope proteins.* J Virol, 2003. **77**(7): p. 4113-26.

39.Law, M. and G.L. Smith, *Antibody neutralization of the extracellular enveloped form of vaccinia virus.* Virology, 2001. **280**(1): p. 132-42.

40. Ichihashi, Y. and M. Oie, *Neutralizing epitope on penetration protein of vaccinia virus.* Virology, 1996. **220**(2): p. 491-4.

41. Law, M., R. Hollinshead, and G.L. Smith, *Antibody-sensitive and antibody-resistant cell-to-cell spread by vaccinia virus: role of the A33R protein in antibody-resistant spread.* J Gen Virol, 2002. **83**(Pt 1): p. 209-22.

42. Blasco, R., J.R. Sisler, and B. Moss, *Dissociation of progeny vaccinia virus from the cell membrane is regulated by a viral envelope glycoprotein: effect of a point mutation in the lectin homology domain of the A34R gene.* J Virol, 1993. **67**(6): p. 3319-25.

43. Vanderplasschen, A., et al., *Extracellular enveloped vaccinia virus is resistant to complement because of incorporation of host complement control proteins into its envelope.* Proc Natl Acad Sci U S A, 1998. **95**(13): p. 7544-9.

44. Boulter, E.A. and G. Appleyard, *Differences between extracellular and intracellular forms of poxvirus and their implications.* Prog Med Virol, 1973. **16**: p. 86-108.

45. Appleyard, G., A.J. Hapel, and E.A. Boulter, *An antigenic difference between intracellular and extracellular rabbitpox virus.* J Gen Virol, 1971. **13**(1): p. 9-17.

46. Wolff, N.C. and R.L. Ilaria, Jr., *Establishment of a murine model for therapy-treated chronic myelogenous leukemia using the tyrosine kinase inhibitor STI571.* Blood, 2001. **98**(9): p. 2808-16.

47.Chahroudi, A., Chavan, R., Kozyr, N., Silvestri, G., Feinberg, M.B., *"Vaccinia virus tropism for primary hematolymphoid cells is determined by restricted expression of a unique virus receptor".* The Journal of Virology, 2005. **In Press**.

48.Ichaso, N. and S.M. Dilworth, *Cell transformation by the middle T-antigen of polyoma virus.* Oncogene, 2001. **20**(54): p. 7908-16.

49. Gruenheid, S., et al., *Enteropathogenic E. coli Tir binds Nck to initiate actin pedestal formation in host cells.* Nat Cell Biol, 2001. **3**(9): p. 856-9.

50.Bishop, J.M., *Molecular themes in oncogenesis.* Cell, 1991. **64**(2): p. 235-48.

51. Baker, R.O., M. Bray, and J.W. Huggins, *Potential antiviral therapeutics for smallpox, monkeypox and other orthopoxvirus infections.* Antiviral Res, 2003. **57**(1-2): p. 13-23.

52.Idemyor, V., *Bacterial resistance to antimicrobial agents--the time for concern.* Ann Pharmacother, 1993. **27**(10): p. 1285.

53. Li, X.Z. and H. Nikaido, *Efflux-mediated drug resistance in bacteria.* Drugs, 2004. **64**(2): p. 159-204.

54.Gould, I.M., *Antibiotic policies and control of resistance.* Curr Opin Infect Dis, 2002. **15**(4): p. 395-400.

55. Koleske, A.J., et al., *Essential roles for the Abl and Arg tyrosine kinases in neurulation.* Neuron, 1998. **21**(6): p. 1259-72.

56.Nagar, B., et al., *Crystal Structures of the Kinase Domain of c-Abl in Complex with the Small Molecule Inhibitors PD173955 and Imatinib (STI-571).* Cancer Res, 2002. **62**(15): p. 4236-43.

57.Kalman, D., et al., *Ras family GTPases control growth of astrocyte processes.* Mol Biol Cell, 1999. **10**(5): p. 1665-83.

58. Swedlow, J.R., J.W. Sedat, and D.A. Agard, *Deconvolution in Optical Microscopy*, in *Deconvolution of Images and Spectra*, P.A. Jansson, Editor. 1997, Academic Press, Inc.: San Diego. p. 284-307.

59.Ramirez, J.C., et al., *Tissue distribution of the Ankara strain of vaccinia virus (MVA) after mucosal or systemic administration.* Arch Virol, 2003. **148**(5): p. 827-39.

60. Kenny, B., *Phosphorylation of tyrosine 474 of the enteropathogenic Escherichia coli (EPEC) Tir receptor molecule is essential for actin nucleating activity and is preceded by additional host modifications.* Mol Microbiol, 1999. **31**(4): p. 1229-41.

Figure 1. Abl and Src-family tyrosine kinases localize in VV actin tails. a-d. **a.** 3T3 cell infected with GFP-VV infected 3T3 cell stained with Cy3-phalloidin to visualize actin and α-Arg-Cy5 pAb. In the merged image, GFP-VV are pseudocolored blue, Arg red, and actin green. Note the colocalization of c-Arg and the virion.

b. Merged images of 3T3 cells exposed to VV and stained with α-phosphotyrosine pAb to recognize extranuclear replication centers (pseudocolored blue), FITC-phalloidin to recognize actin (pseudocolored green), and α-Abl 8E9 mAb (pseudocolored red). The upper white box in **b**, is shown in expanded scale in **bi**, and the lower white box in **bii**.

c. ci-ciii. Merged images of 3T3 cell exposed to VV and stained with FITC-phalloidin to recognize actin (pseudocolored green), together with α-Abl-Cy3 (pseudocolored blue) and α-Arg-Cy5 (pseducolored red). Images are from different locations within the same cell. Note that c-Abl but not c-Arg is evident at the tip of the actin tail in **ci**, and c-Arg but not c-Abl in **cii**. In **ciii**, both kinases are evident in the same tail. **civ**. Quantitation of the percentage of tails in 3T3 cells containing Abl, Arg, both Abl and Arg, or neither Abl nor Arg. Note most tails contain one or the other kinase, but few contain both.

d-f. Merged image of 3T3 cell exposed to VV and stained with FITC-phalloidin to recognize actin (pseudocolored green), together with α-Src pAb (**d**), or α-Fyn mAb (**e**), or α-Yes mAb (**f**; all pseudocolored red).

g. Quantitation of distribution of Src-family kinases in VV actin tails.

h. Merged image of 3T3 cell exposed to VV and stained with FITC-phalloidin to recognize actin (pseudocolored green), together with α-phosphotyrosine (pY)-412 pAb (pseudocolored blue) which recognizes activated Abl or activated Arg. Note that pY-412 staining is evident in one tail in this image but not in others, consistent with the lack of Abl or Arg staining in all tails. Scale bars represent 5 μm.

Figure 2. VV actin motility persists in cell lines lacking Abl and Src family kinases. Cell lines derived from mice with homozygous deletions of c-Src ($Src^{-/-}$; **a**), or c-Src, c-Fyn, and c-Yes ($Src^{-/-}/Fyn^{-/-}/Yes^{-/-}$) **b**), or c-Abl and c-Arg ($Abl^{-/-}/Arg^{-/-}$; **c**), were exposed to VV (**a**) or GFP-VV (**b,c**) and stained with Cy3-phalloidin. Scale bars represent 5 μm.

d,e Images of 3T3 cells infected with VV for 8 hrs and treated with the Abl and Src family kinase inhibitor PD-166326 (10μM) either for the duration of the infection (**d**) or for 10 minutes prior to fixation (**e**). Cells were stained with DAPI

and α-pY pAb to recognize infected cells, and FITC-phalloidin to recognize actin. In merged images, DAPI is pseudocolored blue, actin green and pY red.

f Quantitation of percentage of cells with actin tails after 8 hours of infection with VV. 3T3 cells were exposed to 0.1% DMSO, 25 μm PP2, 10 μm PD-166326.

g Merged images of cells exposed to DMSO or 10μM PD-166236. (Upper) DMSO treated cell infected with GFP-VV (pseudocolored green) and stained with α-pY mAb 4G10 (pseudocolored blue) and Alexa 546-phalloidin (pseudocolored red). The α-pY 4G10 mAb recognizes residues in the tip of the actin tail. (lower) PD-166326-treated cell infected with GFP-VV for 8 hrs, and stained as above. α-pY 4G10 mAb staining is not evident upon PD-166326 treatment (see also Supplementary Figure 4e,f). Note that the effect of PD-166326 on phosphotyrosine was selective because targets in the replication centers recognized by α-phosphotyrosine pAb were unaffected (d,e).

h. Measurement of viral yield by single step growth curves in BSC-40 cells infected with VV at an m.o.i. of 5, and treated with 10 μM PD-166326, or DMSO (the carrier for PD-166326), or 10 μM STI-571. Note that PD-166326 has no effect on viral yield except at the initial time point. STI-571 does not reduce viral yield. Scale bars represent 5 μm.

Figure 3. Redundant Abl and Src-family tyrosine kinases are sufficient for VV actin tail formation. Pseudocolors in parenthesis refer to merged images.

a, Images of 3T3 cells transfected with YFP-c-Arg-T314I (green), treated with 10 μM PD-166326 and exposed to VV for 8 hrs, and then stained with 594-phalloidin (red) to recognize actin, and DAPI (blue). Note the presence of actin tails in the cell expressing YFP-c-Arg-T314I (upper), but not in the nonexpressing cell (lower).

b, Images of 3T3 cells transfected with c-Abl-T315I, treated with 10 μM PD-166326 and exposed to VV for 8 hrs, and then stained with FITC-phalloidin (green), DAPI (blue), and α-Abl mAb 8E9 (red). Note the absence of actin tails in the cell expressing c-Abl-T315I.

c, Images of $Src^{-/-}/Fyn^{-/-}/Yes^{-/-}$ cells transfected with c-Yes-T348I, treated with 10 μM PD-166326 and exposed to VV for 8 hrs, and then stained with FITC-phalloidin (green), DAPI (blue), and α-Yes mAb (red). Note the presence of actin tails in the cell.

d, Images of 3T3 cells treated with Abl family kinase inhibitor 10 μM STI-571 and exposed to VV for 8 hrs. Cells were stained with DAPI and α-pY pAb (red) to recognize infected cells, FITC-phalloidin (green). Note the presence of actin tails.

e, Images of $Src^{-/-}/Fyn^{-/-}/Yes^{-/-}$ cells treated with 10 μM STI-571 and exposed to GFP-VV (green) for 8 hrs, and stained with 546-phalloidin (red). Note the absence of actin tails in **e** despite the presence of GFP-VV at the cell periphery.

f, Images of $Src^{-/-}/Fyn^{-/-}/Yes^{-/-}$ cells treated with DMSO (0.1%) and exposed to GFP-VV for 8 hrs, and stained as in **e**. In the merged image, note the presence of GFP-VV at the tip of the actin tails.

g,h Images of $Src^{-/-}/Yes^{-/-}$ cells (**g**) or $Fyn^{-/-}/Yes^{-/-}$ cells (**h**) treated with 10 μM STI-571, exposed to VV for 8 hours, and stained with FITC-phalloidin (green), and DAPI (blue). Note the presence of actin tails in these cells. Scale bars, 5 μm.

Figure 4. Redundant Abl and Src-family tyrosine kinases are required for cell-to-cell spread.

a-g, Plaque assays of VV-WR on BSC-40 cells (**c-e**) or 3T3 cells derived from wild-type animals (**a**) or from animals lacking c-Abl and c-Arg (**b**), or c-Src, c-Fyn and cYes (**f,g**). Cells were fixed three (**c-e**) or four (**a,b,f,g**) days after infection. No VV was added to the wells depicted in the first column. VV was added to wells depicted in the other columns at the dilutions indicated. The titre of undiluted VV added to all wells was 10^4 PFU/ml, as measured on BSC-40 cells. 10 μM PD-166326 was added 1 hour after infection to the well depicted in **d**, and 10 μM STI571 to the wells depicted in **e** and **g**. Note that PD-166326 blocked plaque formation in BSC-40 cells and 3T3 cells (see Supplementary Figure 5a,b),

whereas STI-571 only blocked plaque formation in the absence of c-Src, c-Fyn, and c-Yes.

Figure 5. Redundant Abl-family kinases are required for EEV release.

a-e, Plaque assays of BSC-40 cells infected with supernatants derived from uninfected cells (first column) or VV-WR infected wild-type 3T3 cells (**a**) or 3T3 cells derived from animals lacking c-Src, c-Fyn and c-Yes (**b**), c-Abl (**c**), c-Arg (**d**), or c-Abl and c-Arg (**e**).

f,g, Plaque assays of BSC-40 cells infected with supernatants derived from uninfected BSC-40 cells (first column) or VV-infected BSC-40 cells. For a-g, supernatant was added neat (second column) or diluted 1:10 (third column). For f and g, initial infections, but not plaque assays, were carried out in the absence of drug (**f**), or in the presence of 10 μM STI-571 (**g**). Note that plaques are present except when both c-Abl and c-Arg are absent (**e**), or when their activity is blocked with drug (**g**).

h. (left) Quantitation of EEV from supernatants of VV-infected BSC-40 cells or BSC-40 cells treated with 10 μM STI-571. Supernatants were treated with 2D5 mAb to reduce contamination from IMV. **(middle)** Quantitation of EEV from supernatants of VV-WR-infected 3T3 cells, or 3T3 cells treated with 10 μM STI-571, or $Abl^{-/-}/Arg^{-/-}$ cells. Supernatants were treated with 2D5 mAb to reduce contamination from IMV. **(right)** Effects of STI-571 on VV-IHD-J EEV. Quantitation of EEV from supernatants of VV-IHD-J-infected 3T3 cells or 3T3

cells treated with 5 μM STI-571. Supernatants were treated with 2D5 mAb to reduce contamination from IMV. Note that as with VV-WR EEV, STI-571 reduced VV-IHDJ EEV production.

Figure 6. STI-571 reduces number of viral genomes and promotes survival in VV-infected mice.

a. STI-571 reduces VV dissemination. Six week-old C57/B6 mice were left uninfected (no virus), or infected with 10^4 PFU VV-WR intraperitoneally. One day prior to infection, continuous release osmotic pumps containing PBS (carrier) or STI-571 (100mg/kg/day) were surgically implanted subcutaneously (see Methods). Four days after infection ovaries were harvested and the number of viral genomes quantitated by real-time PCR. Note that numbers of viral genomes in ovaries from mice receiving STI-571 was 5 orders of magnitude less than mice receiving carrier. Combined data from three separate experiments is shown (n=12 mice per condition). The line in each data set represents the median number of viral genomes. The background of the PCR assay is ~10 viral genomes.

b. STI-571 promotes survival in VV-infected mice. Six week-old C57/B6 mice were left uninfected (no virus), or infected with $2x10^4$ PFU VV-IHD-J intranasally. One day prior to infection, osmotic pumps containing PBS or STI-571 (100mg/kg/day) were implanted. The percentage of mice surviving after infection is plotted as a function of the time after infection (n=12 mice for each condition).

Note that all STI-571-treated mice survive after 15 days compared to 30% of carrier or untreated mice.

c. Summary of effects of tyrosine kinases on VV motility and formation of EEV. (**1**) VV is produced in juxta-nuclear replication centers or "factories" forming intracellular mature virions (IMV; blue). (**2**) Some of the virions are then wrapped in additional membranes within a trans-golgi compartment (intracellular enveloped virions, IEVs; red). (**3**) IEVs then travel towards the cell surface on microtubules where they fuse with the plasma membrane (**4**) and emerge outside the cell (CEV). (**5**) Some CEV initiate actin polymerization using c-Src, c-Fyn, c-Yes, or c-Arg in a redundant fashion. These CEV egress towards an adjacent cell on an actin-filled membranous protrusion or "tail". Actin tails are blocked by PD-166326, but not by STI-571. CEV associated with the plasma membrane or at the tip of actin tails then detach to form EEV (**6**). Formation of infectious EEV requires the Abl family kinases c-Abl and c-Arg, and is inhibited by STI-571 and PD-166326. EEV have been proposed to mediate virulence *in vivo*.

Supplementary Figure Legends

Supplementary Figure 1. Protein sequences surrounding phosphorylation sites in VV A36R and enteropathogenic E. coli Tir. Note that although the sequences in Tir comprise a consensus Src phosphorylation site [60], Abl but not Src family kinases localize to pedestals [26].

Supplementary Figure 2. Identification of VV-infected cells.

a, Images of 3T3 cells exposed to VV and stained with DAPI to visualize extranuclear replication centers ("RC"), Cy3-phalloidin to recognize actin tails, and α-TW2.3 to recognize a VV protein expressed early in infection. In the merged image, DAPI is pseudocolored blue, actin red, and TW2.3 green. Note that replication centers could also be identified by staining with an α-phosphotyrosine pAb (e.g. see Figure 2d). Insets show identical staining in an uninfected cell. Note that TW2.3 staining is not evident in uninfected cells.

b, Images of 3T3 cells exposed to GFP-VV, and stained with DAPI to visualize extranuclear replication centers, and Cy3-phalloidin to recognize actin tails. In the merged image, DAPI is pseudocolored blue, actin red, and GFP-VV green. Inset in **b** shows expanded scale of actin tails in lower left corner.

c,d, Merged images of 3T3 cells transfected with YFP-c-Arg and exposed to VV and stained with Alexa 594-phalloidin to recognize actin (pseudocolored red). Fluorescence in the YFP channel indicates the presence of transfected YFP-c-Arg. Note that YFP-c-Arg localizes at the tip of some actin tails (c) but not others (d), even when YFP-c-Arg is expressed at high levels.

e,f, Quantitation of distribution of Abl- and Src-family kinases in VV actin tails in $Src^{-/-}/Fyn^{-/-}/Yes^{-/-}$ cells (**e**), or $Abl^{-/-}/Arg^{-/-}$ cells (**f**). Note that although the

distribution of kinases on VV actin tails is somewhat different in these cell lines compared to wild type 3T3 cells, neither Src- nor Abl family kinases alone appear necessary for actin tail formation. Scale bars, 5 μm.

Supplementary Figure 3. Structures of PD-166326 and STI-571.

Supplementary Figure 4. Characterization of kinases sufficient for VV actin motility.

a, Images of 3T3 cells transfected with YFP-c-Arg, treated with 10 μM PD-166326 and exposed to VV for 8 hrs, and then stained with DAPI and 594 phalloidin. In the merged image, YFP-c-Arg is pseudocolored green, actin red, and DAPI blue. The cell is infected as evidenced by the presence of replication centers (extranuclear staining in DAPI). However, the absence of actin tails in the cell expressing YFP-c-Arg indicates that a wild-type allele of c-Arg is unable to confer resistance to PD-166326.

b, Images of 3T3 cells transfected with c-Yes, treated with 10 μM PD-166326 and exposed to VV for 8 hrs, and then stained with DAPI, α-Yes mAb and 594-phalloidin. In the merged image, Yes is pseudocolored red, actin green, and DAPI blue. Wild-type Yes, like Arg is unable to support actin tails in PD-166326.

c, Actin tails in a $Src^{-/-}/Yes^{-/-}$ cell treated with 10 μM STI-571 and infected with GFP-VV. Note that actin tails are abundant in this representative cell. Actin is pseudocolored red, and GFP-VV green.

d, Quantitation of number of actin tails in $Src^{-/-}/Yes^{-/-}$ cells and $Src^{-/-}/Fyn^{-/-}/Yes^{-/-}$ cells left untreated or treated with 10 μM STI-571. Note that $Src^{-/-}/Yes^{-/-}$ cells have on average ~30 tails per cell, suggesting that Fyn present in these cells is sufficient for actin tail formation. In $Src^{-/-}/Fyn^{-/-}/Yes^{-/-}$ cells, number of tails per cells isreduced from 60 to 3, suggesting that Src-family kinases and STI-571-sensitive kinases are the only ones required for VV actin motility.

e,f 3T3 cells infected with GFP-VV (green in merged image), and treated with DMSO (e) or 10 μM PD-166326 (f), and then fixed and stained with phalloidin (red in merged image), and α-phosphotyrosine mAB 4G10 (blue in merged image). Note absence of phosphotyrosine staining colocalized with virion in the presence of PD. Images shown are the individual channels of Figure 2g.

Supplementary Figure 5. Effects of tyrosine kinase inhibitors on VV plaque formation.

a-b. PD-166326 blocks plaque formation in 3T3 cells. Plaque assays of VV 3T3 cells derived from wild-type animals. VV was added to both wells at a 1:10 dilution. The titre of the undiluted VV was 10^4 PFU/ml, as measured on BSC-40

cells. 10 μM PD-166326 was added 1 hour after infection to the well depicted in b. Note that PD-166326 blocked plaque formation in 3T3 cells.

c,d. Effects of STI-571 on formation of "comets" associated with plaques. BSC-40 cells were infected with VV and left untreated (c) or were treated with 10 μM STI-571 throughout. Note that while treatment with STI-571 does not block plaque formation per se, it does reduce formation of "comets," consistent with an effect of the drug on production of infectious EEV.

e. Measurement of viral yield in $Src^{-/-}/Fyn^{-/-}/Yes^{-/-}$ cells or 3T3 cells infected with VV at an m.o.i. of 5 and treated with 10 μM STI-571, or Saline, the carrier for STI-571. STI-571 did not significantly affect viral yield in wild-type or $Src^{-/-}/Fyn^{-/-}/Yes^{-/-}$ cells at this m.o.i.

f. Measurement of viral yield by single step growth curves in BSC-40 cells infected with VV at an m.o.i. of 0.1, and treated with 10 μM PD-166326, or DMSO, the carrier for PD-166326, or 10 μM STI-571, or saline. Note that PD-166326 reduced viral yield by three orders of magnitude whereas STI-571 did not.

Supplementary Figure 6. **a-e**. Viral yield assays of VV on 3T3 cells (a,b), $Abl^{-/-}/Arg^{-/-}$ cells (c), and BSC-40 cells (d,e). Cells were infected for one day with VV at 10^4 PFU/ml (as measured on BSC-40 cells). The supernatent was removed, the

cells lysed and the supernatant added neat or in the dilutions indicated to monolayers of naïve BSC-40 cells. After three days the cells were fixed, stained, and imaged. The presence of equivalent PFU in the lysates from 3T3 cells (a) and $Abl^{-/-}/Arg^{-/-}$ cells (c) indicates that Abl-family kinases did not affect viral replication. Cells in c and e were treated with 10 μM STI-571 throughout. The presence of equivalent numbers of PFU in the lysates from STI-571-treated and untreated cells indicates that the drug did not affect viral replication in 3T3 or BSC-40 cells.

Supplementary Figure 7. Distinguishing the effects of Abl and Arg on EEV and IMV.

a, EEV assays were carried out as described in Figure 5. Supernatants were incubated with or without 2D5 mAb. Treatment with antibody reduced the number of plaques in supernatants, but the effects of STI-571 were apparent in both conditions, indicating that the drug likely affected release of infectious EEV but not IMV.

b, Effects of 2D5 antibody dilution on EEV. 2D5 ascites was incubated with supernatant from 3T3 cells prior to addition of supernatants to monolayers. Note that dilutions greater than 1:1000 had little effect.

Figure 1.

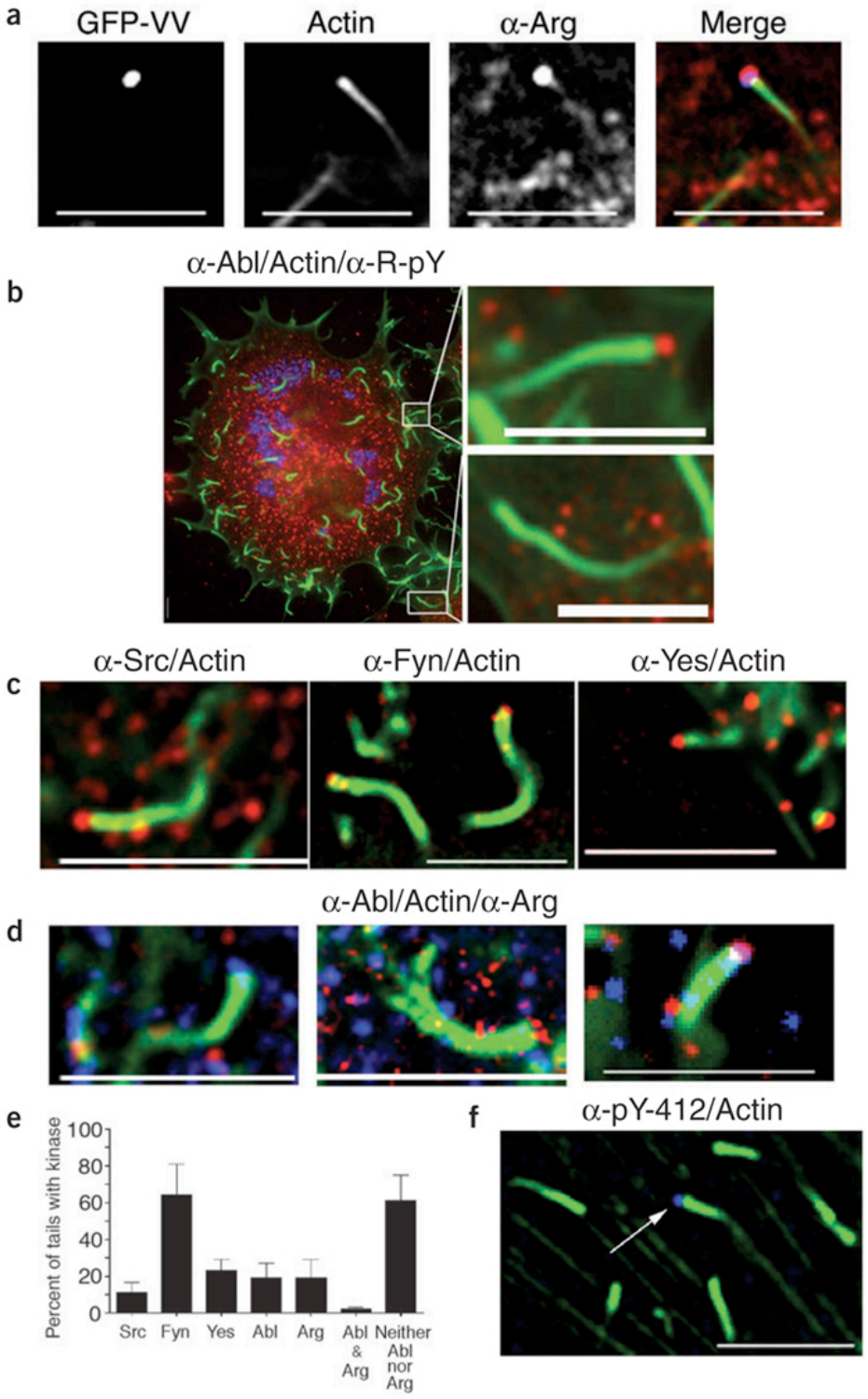
a
GFP-VV
Actin
α-Arg
Merge
b
α-Abl/Actin/α-R-pY
c
α-Src/Actin
α-Fyn/Actin
α-Yes/Actin
d
α-Abl/Actin/α-Arg
e
Percent of tails with kinase
100
80
60
40
20
0
Src
Fyn
Yes
Abl
Arg
Abl & Arg
Neither Abl nor Arg
f
α-pY-412/Actin

Figure 2.

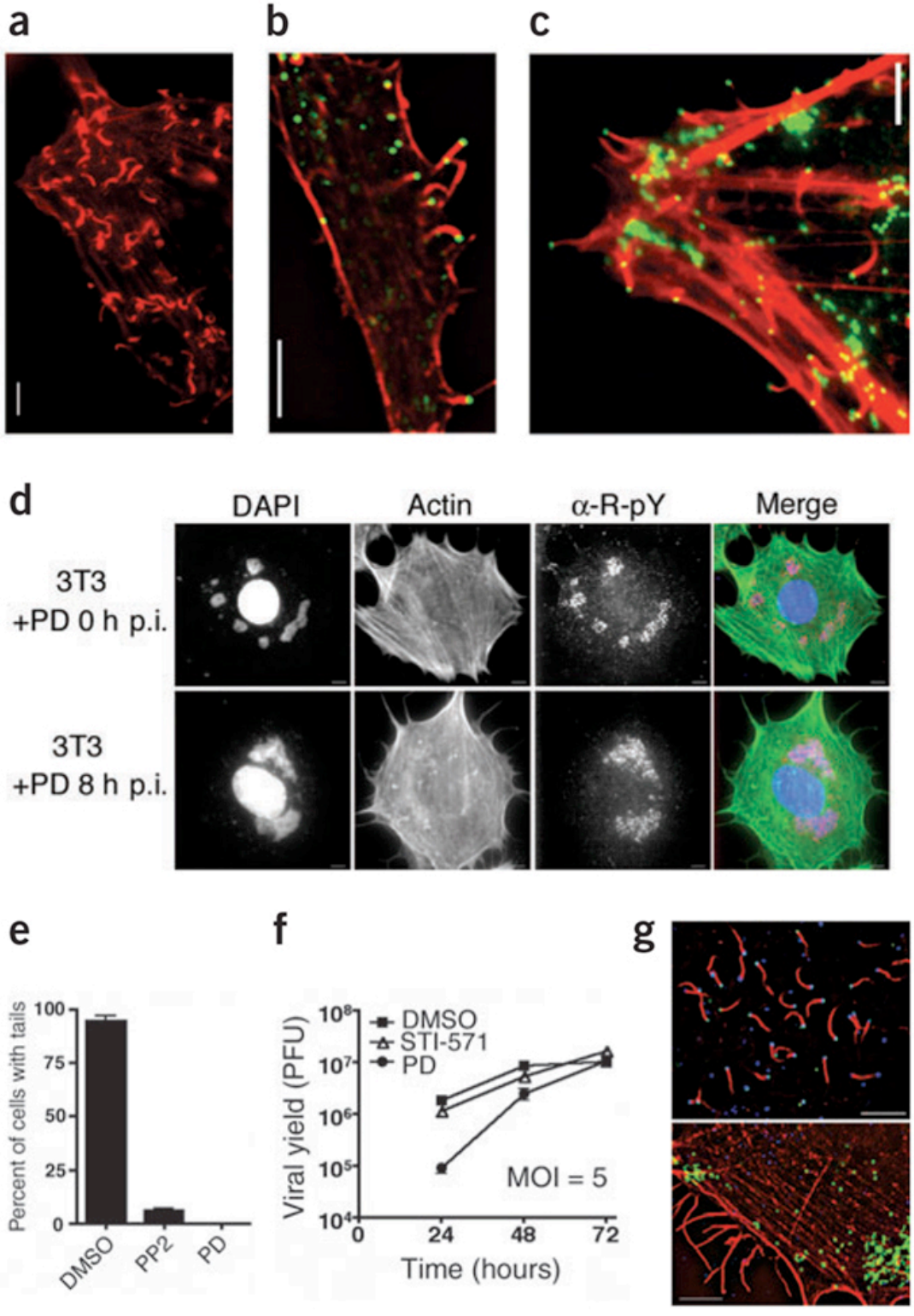
a
b
c
d
DAPI
Actin
α-R-pY
Merge
3T3
+PD 0 h p.i.
3T3
+PD 8 h p.i.
e
Percent of cells with tails
100
75
50
25
0
DMSO
PP2
PD
f
Viral yield (PFU)
10⁸
10⁷
10⁶
10⁵
10⁴
DMSO
STI-571
PD
MOI = 5
0
24
48
72
Time (hours)
g

Figure 3.

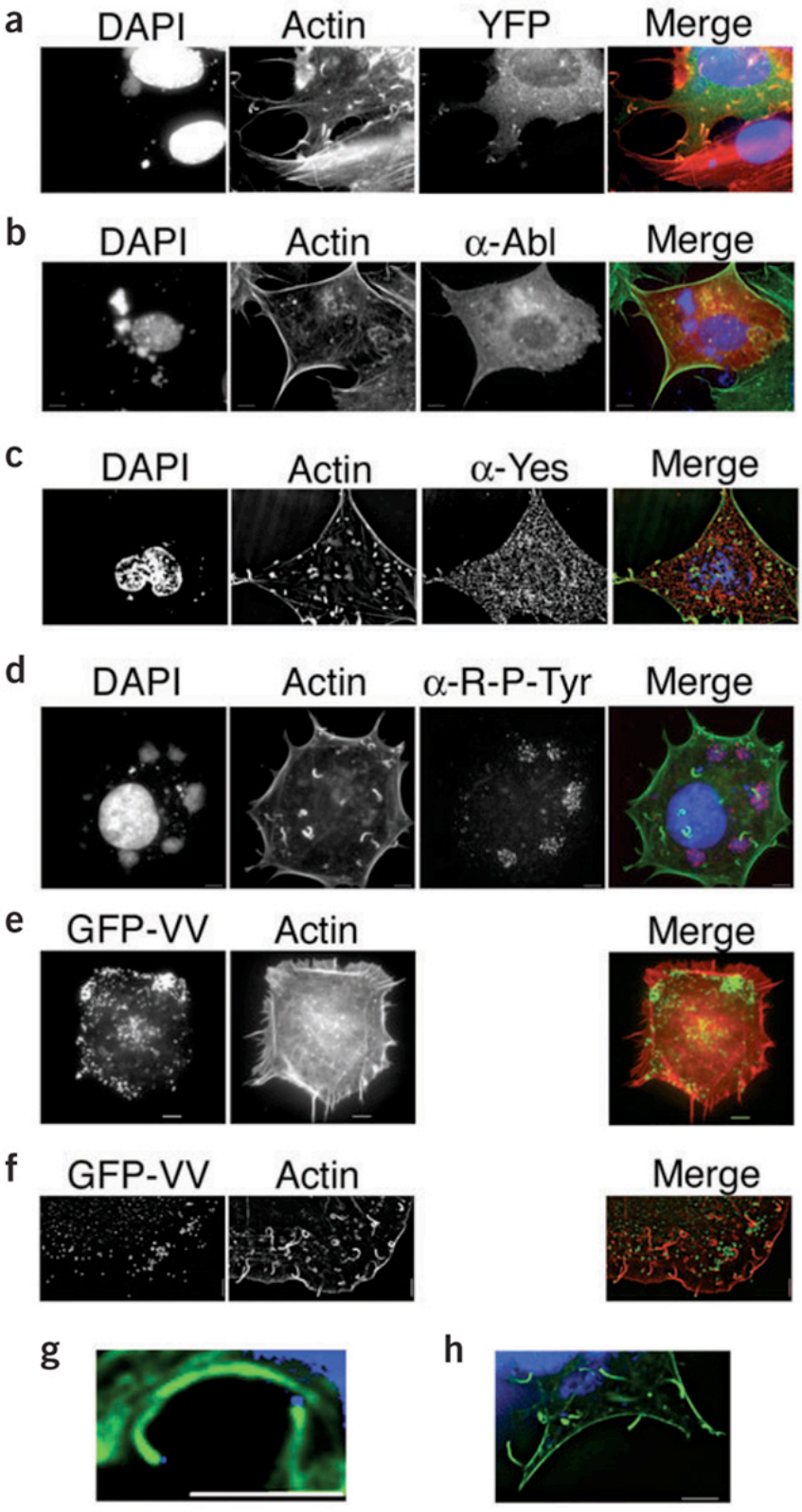
a
DAPI
Actin
YFP
Merge
b
DAPI
Actin
α-Abl
Merge
c
DAPI
Actin
α-Yes
Merge
d
DAPI
Actin
α-R-P-Tyr
Merge
e
GFP-VV
Actin
Merge
f
GFP-VV
Actin
Merge
g
h

Figure 4.

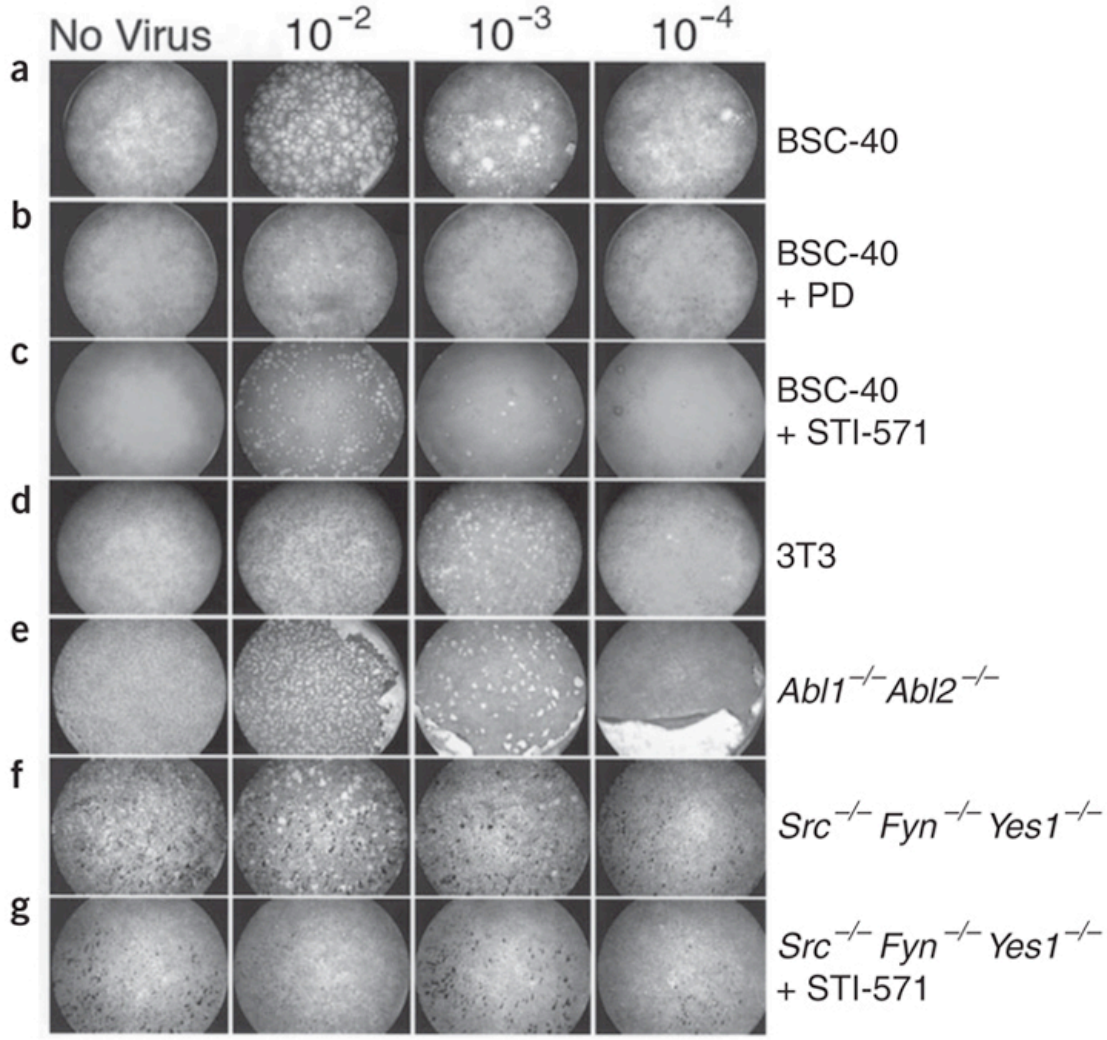
No Virus
10^-2
10^-3
10^-4
a
BSC-40
b
BSC-40
+ PD
c
BSC-40
+ STI-571
d
3T3
e
Abl1−/−Abl2−/−
f
Src−/− Fyn−/− Yes1−/−
g
Src−/− Fyn−/− Yes1−/−
+ STI-571

Figure 5.

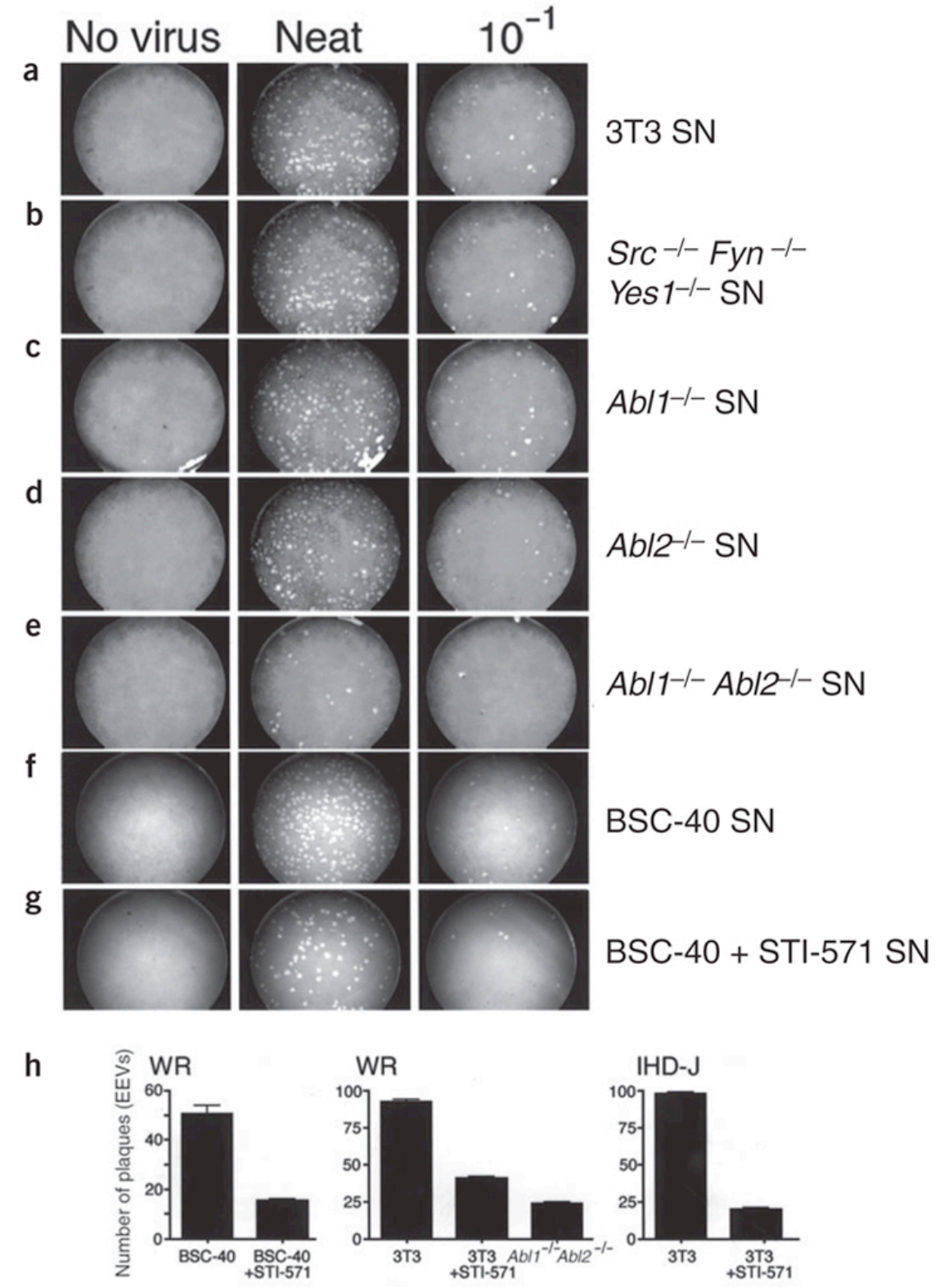
No virus
Neat
10^{-1}
a
3T3 SN
b
Src $^{-/-}$ *Fyn* $^{-/-}$ *Yes1* $^{-/-}$ SN
c
Abl1 $^{-/-}$ SN
d
Abl2 $^{-/-}$ SN
e
Abl1 $^{-/-}$ *Abl2* $^{-/-}$ SN
f
BSC-40 SN
g
BSC-40 + STI-571 SN
h
Number of plaques (EEVs)
WR
60
40
20
0
BSC-40
BSC-40 +STI-571
WR
100
75
50
25
0
3T3
3T3 +STI-571
Abl1 $^{-/-}$ *Abl2* $^{-/-}$
IHD-J
100
75
50
25
0
3T3
3T3 +STI-571

Figure 6.

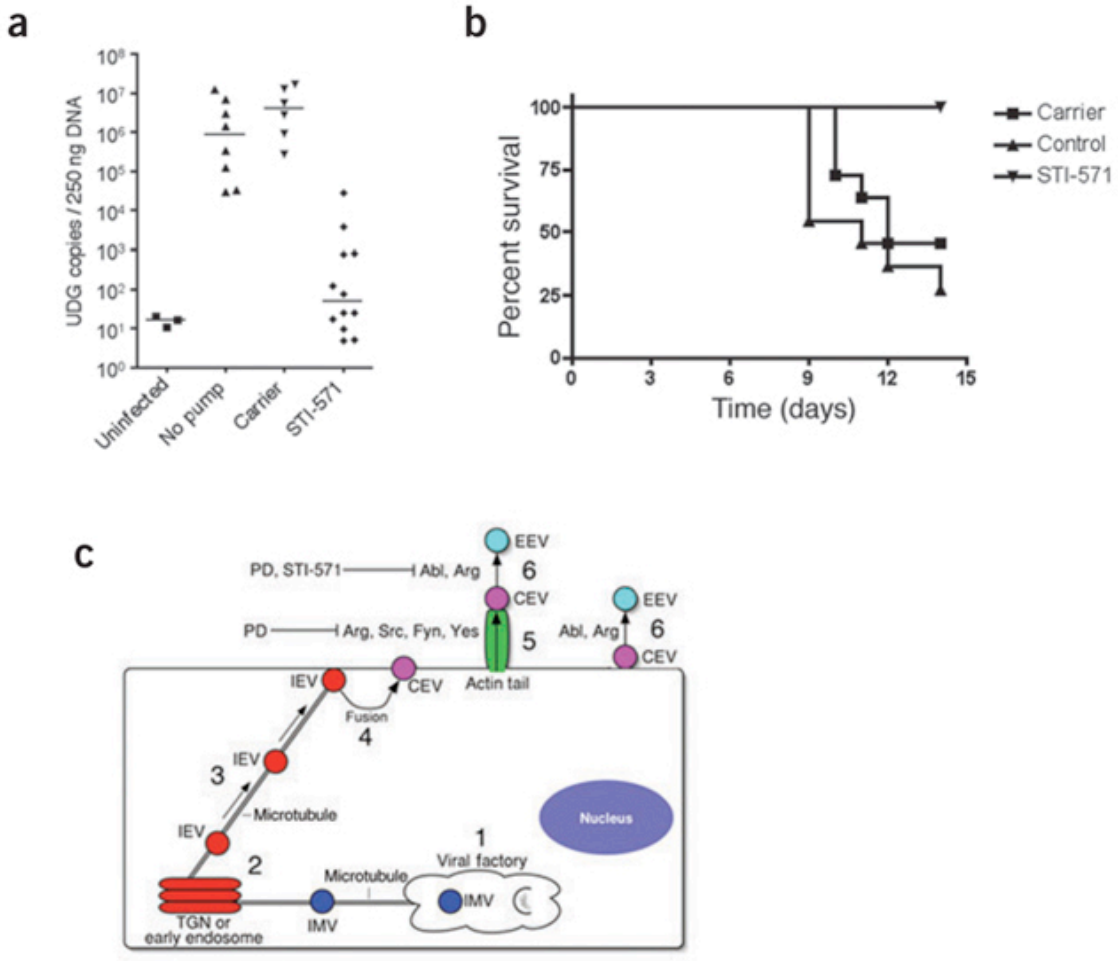
a
UDG copies / 250 ng DNA
Uninfected
No pump
Carrier
STI-571
b
Percent survival
Time (days)
Carrier
Control
STI-571
c
EEV
PD, STI-571
Abl, Arg
6
CEV
PD
Arg, Src, Fyn, Yes
5
Actin tail
IEV
CEV
Fusion
4
3
Microtubule
Nucleus
1
Viral factory
2
TGN or
early endosome
IMV

Supplementary Figure 1.

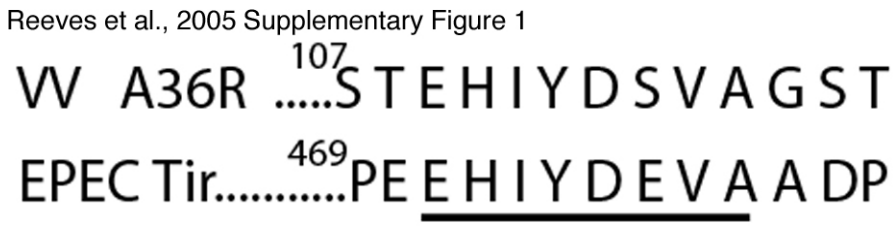

Supplementary Figure 2.

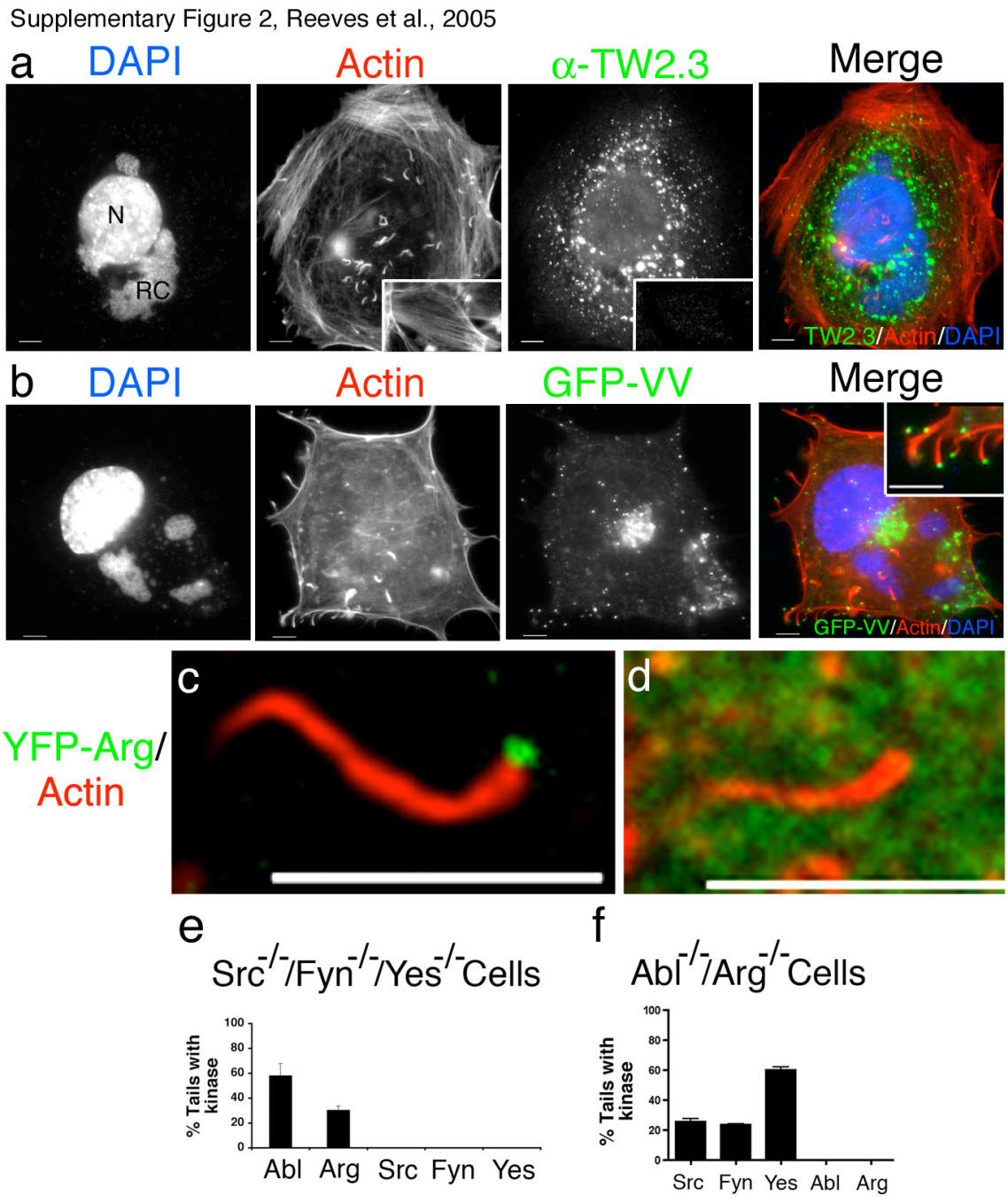

Supplementary Figure 3.

a. PD-166326

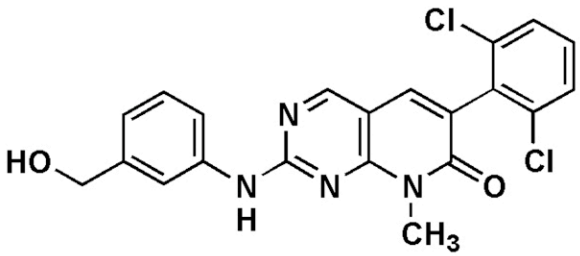

b. STI-571 (Gleevec)

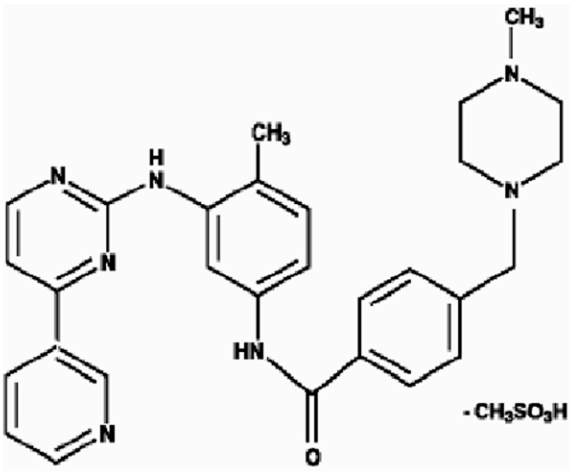

Supplementary Figure 3, Reeves et al., 2005

Supplementary Figure 4.

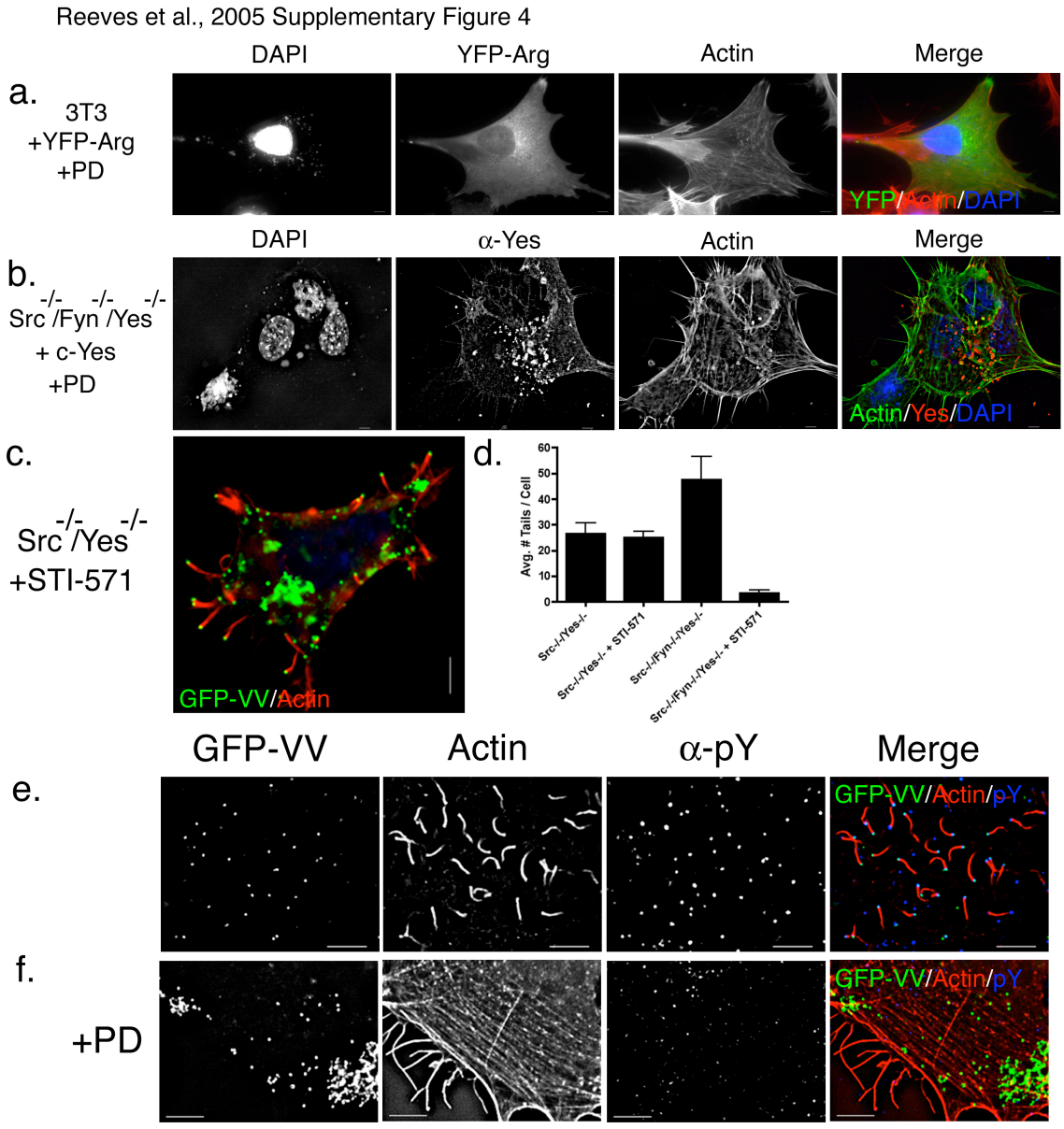

Supplementary Figure 5.

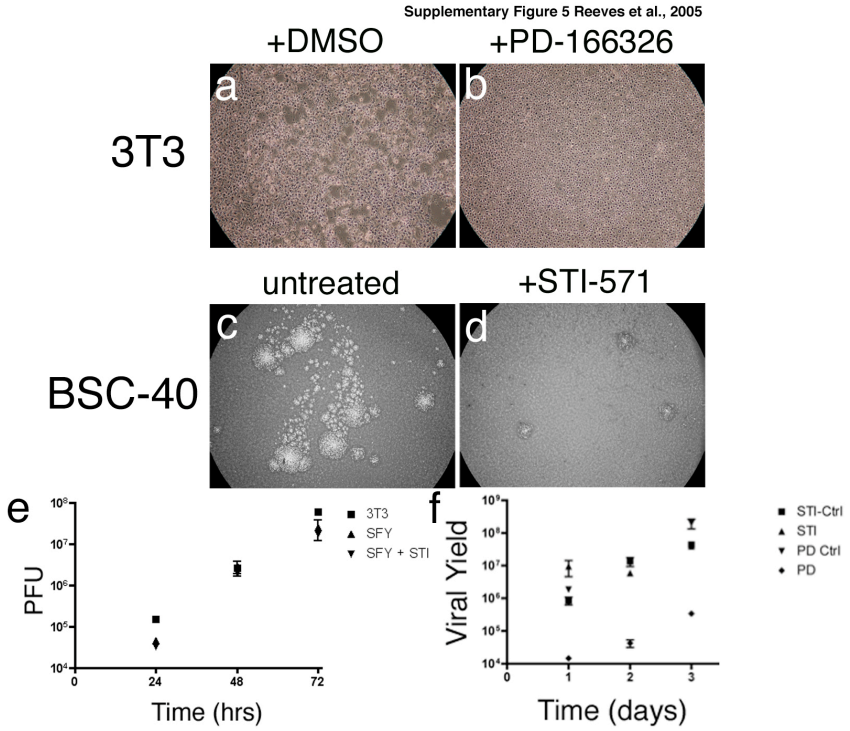

Supplementary Figure 6.

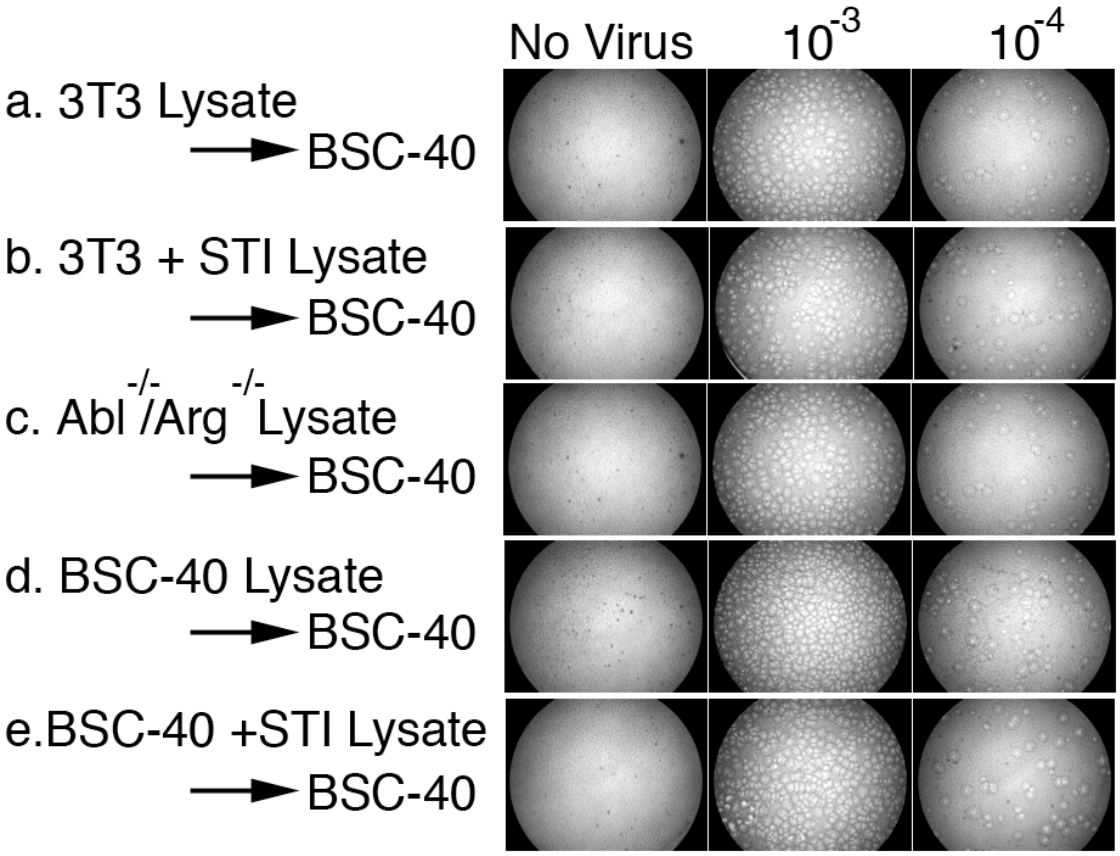

Supplementary Figure 6. Reeves et al., 2005

Supplementary Figure 7.

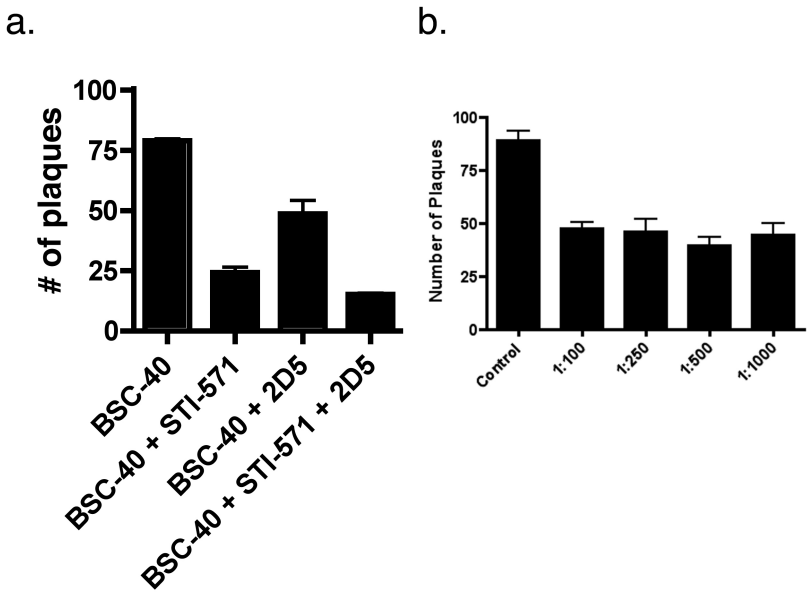

Reeves et al. 2005, Supplementary Figure 7

Chapter 3

Variola and monkeypox utilize conserved mechanisms of virion motility and release that depend on Abl- and Src-family tyrosine kinases

Submitted to Journal of Virology November, 2009

This manuscript was written by Patrick M. Reeves and Daniel Kalman

Patrick M. Reeves was intellectually involved in the concept, experimental design, and implementation of this project from its conception as well as the analysis and interpretation of the results. Patrick was involved in the preparation of all versions of the manuscript and was responsible for incorporating necessary revisions.

Variola and monkeypox utilize conserved mechanisms of virion motility and release that depend on Abl- and Src-family tyrosine kinases

Patrick M. Reeves[1], Scott K. Smith[3], Victoria A. Olson[3], William Bornmann[2], Inger K. Damon[3], and Daniel Kalman[1,4]

[1] Microbiology and Molecular Genetics Graduate Program, Emory University School of Medicine, 615 Michael Street, Whitehead Research Building #155, Atlanta, Georgia 30322, USA.

[2] MD Anderson Cancer Center, University of Texas, Houston, TX, USA.

[3] Poxvirus Team, Poxvirus and Rabies Branch, Division of Viral and Rickettsial Diseases, National Center for Zoonotic, Viral and Enteric Diseases, Centers for Disease Control and Prevention, Atlanta, GA 30333, USA.

[4] Department of Pathology and Laboratory Medicine, Emory University School of Medicine, 615 Michael Street, Whitehead Research Building #144, Atlanta, Georgia 30322, USA.

[4]Corresponding Author
Department of Pathology and Laboratory Medicine
Emory University
Whitehead Research Bldg. 144
165 Michael St.
Atlanta GA 30322
404 712-2326 (office)
404 712-8538 (facsimile)
dkalman@emory.edu

Running Title: Src- and Abl-family kinases in poxvirus pathogenesis
Key Words: Src, Abl, tyrosine kinase, tyrosine kinase inhibitor, STI-571, Gleevec, poxvirus, Vaccinia, Variola, monkeypox, smallpox.
Illustrations: 6 Figures + 5 Supplementary Figures.

Abbreviations used in this paper: PD, pyrido[2,3-d]pyrimidine; mAb, monoclonal antibody; CML, chronic myelogenous leukemia; pAb, polyclonal antiserum; P-Tyr, phosphotyrosine; α, anti; MOI, multiplicity of infection; IN, intranasal; IP, intraperitoneal; LD_{100}, Lethal Dose for 100% of animals.

Abstract

Orthopoxviruses enter mammalian cells, replicate extranuclearly, and produce virions that move to the cell surface along microtubules, fuse with the plasma membrane, and move from infected cells towards apposing cells on actin-filled membranous protrusions or actin tails. To form actin tails, cell-associated enveloped virions (CEV) require Abl- and Src-family tyrosine kinases. Further, release of CEV from the cell requires Abl- but not Src-family tyrosine kinases, and is blocked by STI-571 (Gleevec), an Abl-family kinase inhibitor used to treat chronic myelogenous leukemia in humans. Here we demonstrate that the *Poxviridae* family members Monkeypox (MPX) and Variola (VarV) used conserved mechanisms for actin motility and EEV release. Furthermore, we show that STI-571 is effective in a mouse model of infection with vaccinia, whether delivered prophylactically or post-infection. While inhibitors of both Src- and Abl-family kinases, such as BMS-354825 (Sprycel), are effective in limiting dissemination *in vitro*, members of this class of drugs appear to have immunosuppressive effects *in vivo* that preclude their use as anti-infectives for orthopoxviruses. Together, these data suggest a possible utility for Gleevec in treating smallpox or monkeypox infections, or complications associated with vaccination.

Introduction

Vaccinia virus (VacV) monkeypox virus (MPX), and variola (VarV) virus are members of the *Poxviridae* orthopox family (9, 16). Vaccination with VacV provides protection against MPX and VarV, the cause of smallpox. Routine vaccinations for smallpox ceased in 1977, and smallpox was declared eradicated by the World Health Organization (WHO) in 1980. Estimates indicate that about half the individuals in the general population are not vaccinated (18). As such, the general population is considered extremely susceptible to a smallpox outbreak resulting from release of the virus. Moreover, recent outbreaks of MPX in the United States and in the Democratic Republic of Congo have raised the prospect that emergent poxviruses may also pose a significant threat (20, 22).

Vaccination, even post exposure, is still considered the method of choice for treatment of orthopoxvirus infections. However, the window for efficacious post-exposure vaccination is small (~4-7 days) (15). Moreover, individuals with acquired or congenital immunocompromising conditions appear to be at high risk for developing complications upon vaccination (5, 6) which include encephalitis, fetal vaccinia, progressive vaccinia, and eczema vaccinatum, a localized or systemic dissemination of the virus (6, 18, 34).

The mechanisms of poxvirus entry into host cells, replication, and exit have been extensively studied (16). Upon entry, the virion moves to a juxtanuclear location where it replicates up to 10^4 concatameric genomes, which resolve into individual unit genomes, and then are packaged into virions (called intracellular

mature virions) (IMV). Some IMV are packaged in additional membranes to form IEV (intracellular enveloped virions (IEV)), which travel toward the host cell periphery via a kinesin/microtubule transport system (4, 10, 21, 25) and fuse with the plasma membrane of the host cell to form a cell-associated enveloped virions (CEV), leaving behind one of its two outer membranes (16, 27, 28). CEV can initiate actin polymerization, which propels the particle on an actin-filled membrane protuberance (called a “tail”) towards an adjacent cell. CEV can detach from the tip of a tail or directly from the membrane (27) to form an extracellular enveloped virions (EEV; (28)). EEV are assessed *in vitro* as “comets”, consisting of an archipelago of secondary satellite plaques appose to a larger plaque (28). EEV have been proposed to mediate long-range spread of the virus *in vivo* (28). Experiments with VacV demonstrate that Src- and Abl-family kinase activity modulate intracellular spread and release. In particular, phosphorylation of tyrosine residues of A36R, a viral protein in the outer membrane of IEV, by Abl-or Src-family kinases is required for recruitment of Nck, Grb2 and the Arp2/3 complex, molecules that stimulate actin polymerization and tail formation (26). Abl-family kinases, but not Src-family kinases, also mediate release of CEV to form EEV (24).

The proposed dependence of poxvirus dissemination *in vivo* upon release of EEV (28), and the requirement for Abl-family tyrosine kinases in EEV release (24) raised the possibility that tyrosine kinase inhibitors originally developed for treating cancers may also have utility as therapeutics for infections caused by

poxviruses. STI-571 (Gleevec) and AMN-107 (nilotinib) and the related small-molecule inhibitor BMS-354285 (Sprycel) are all approved for treating human cancers including chronic myelogenous leukemia (CML) and gastrointestinal stromal tumors (32, 35). STI-571 and AMN-107 inhibit Abl-family kinases, whereas BMS-354285 and another structurally related compound, PD-166236, inhibit both Src- and Abl-family kinases. Notably, STI-571 reduces VacV dissemination *in vivo*, and provides protection from a lethal infection when delivered prophylactically (24).

Although VarV, MPX, and VacV genomes have been sequenced and are 95% identical (9), there is no evidence that MPX and VarV form actin tails and release EEV using the same host molecules as VacV. Our data suggest that these mechanisms are highly conserved amongst poxviruses. We also test the hypothesis that tyrosine kinase inhibitors approved for use in humans, such as Gleevec and Sprycel, may have utility against poxvirus infections *in vivo*. We report here that Gleevec is effective in both a prophylyactic and therapeutic capacty against VacV infections in mice. Moreover, Gleevec does not interfere with the acquisition of protective immunity. By contrast, while Sprycel has strong efficacy *in vitro* against all poxviruses, immunosuppressive effects *in vivo* appear to preclude its use as a therapeutic agent. Together, these data provide an experimental basis for the development of small molecule tyrosine kinase inhibitors for poxvirus infections.

Methods

Cells and viruses. African green monkey kidney cells (BSC-40) or murine fibroblasts cells (3T3, $Src^{-/-}/Fyn^{-/-}/Yes1^{-/-}$ and $Abl1^{-/-}/Abl2^{-/-}$) were cultured as described previously (31). For VacV experiments, cells were maintained in DMEM supplemented with 10% FBS, penicillin and streptomycin (complete media) as described (31). For MPX and VarV experiments, BSC-40 cells were cultured as described previously (29). Viruses were obtained from crude lysate preparations of infected BSC-40 cells as described (29). For these experiments, we used VacV strains WR and IHD-J, MPX strain MPXV-1979-ZAI-005 and VarV strains BSH74-sol (BSH; Bangladesh) or SLN68-258 (SLN; Sierra Leone). VacV and MPX experiments were conducted under appropriate biosafety conditions. Assays with VarV were performed in a maximum-containment laboratory under biosafety level 4 conditions. For microscopy, murine fibroblast 3T3, $Src^{-/-}/Fyn^{-/-}/Yes1^{-/-}$ or $Abl1^{-/-}/Abl2^{-/-}$ cells were cultured on glass coverslips in complete media, and then incubated with virus at an MOI of 5 for 1 hour in DMEM lacking serum. The cells were then washed, and incubated in complete media. After 18-24 hours, cells were fixed and prepared for immunofluorescence as described below.

Immunofluorescencence analysis. Cells previously infected with VacV, MPX, or VarV were fixed in 2% formaldehyde and permeablized in Triton-X-100 as described (12). Viral DNA was recognized by staining with DAPI (1 mg/ml; Sigma), and actin by staining with 488-phalloidin (1μg/ml; Molecular Probes). The

primary antibodies and concentrations used in this study were as follows: Nck monoclonal antibody (mAb; 1 μg/ml; Oncogene Research), Abl1 mAb (8E9; 0.05 μg/ml; Pharmingen), Src polyclonal antibody (pAb; 0.1 μg/ml; Santa Cruz), Fyn mAb (0.1 μg/ml; ABCAM), Yes pAb (0.1 μg/ml; Cell Signaling), Abl2 pAb (1:200; UBI), Grb2 mAb (3F2, 1:200), and phosphotyrosine mAb (4g10; 1:200; We determined the specificity of kinase-specific antibodies using the staining of cell lines lacking particular kinases (24). Secondary antibodies were obtained from Jackson Immunochemicals. Following fixation VarV samples were stained with DAPI (1 μg/ml; Sigma) and 488-phalloidin (10 μg/ml; Molecular Probes). The samples were then incubated with 3% Amphyll for 30min in accordance with Center for Disease Control and Prevention's (CDC) Office of Health and Safety (OHS) guidelines for removing inactivated samples from the BSL4 facility. Following incubation with Amphyll, VarV slips were washed three times with PBS and stained as described above.

Microscopy. Images were acquired with a scientific-grade cooled charge-coupled device (Cool-Snap HQ with ORCA-ER chip) on a multi-wavelength wide-field three-dimensional microscopy system (Intelligent Imaging Innovations) based on a Zeiss 200M inverted microscope using a 63x N.A.1.4 or 100x N.A.1.4 lens (Zeiss). Imaging of immunofluorescent samples was done at room temperature (22–25 °C) using a standard Sedat filter set (Chroma) in successive 0.20 μm focal planes through the samples, and out-of-focus light was removed with a constrained iterative deconvolution algorithm (30). Actin tails were

recognized by intense phalloidin staining associated with DAPI or GFP fluorescence objects measuring approximately 200nm in diameter. Fluorescence at the end of actin tails which colocalized with DAPI staining or with GFP fluorescence in cells infected with GFP-labeled VacV was used to indicate localization of kinases or other cellular molecules to virions. Co-localization was assessed by coincidence of fluorescent staining of kinases in the Cy5 and Cy3 channels. We calibrated the microscope filters with multicolored fluorescent beads to insure coincidence of fluorescent signals in all channels to within a pixel (100 nm for the 63x N.A.1.4 lens).

Mouse assays. Gleevec (STI-571) delivery was achieved as described previously (24). Briefly, we delivered 200 mg/kg via Alzet osmotic pumps inserted subcuatenously into anesthetized 6 week-old female C57/Bl6 mice. Sprycel (BMS-354825) was suspended in 50% DMSO/H20 at various concentrations (noted in figure legends) and delivered into animals as described above. Mice were infected either intraperitoneally or intranasally with 10^4 pfu VacV IHD-J as previously reported (24). To measure viral copy number, organs were harvested four days post infection and prepared as previously described (24). For survival studies, mice were sacrificed at 70% of original weight or as directed by veterinary staff. Mice were monitored daily, and all experiments were carried out in accordance with Institutional Animal Care and Use Committee regulations (Emory University protocol number AD07-1156-03R04).

Viral copy number measurements. Viral genome copy number measurements were carried out as described previously (24). Probes and primers were obtained from Operon Biotechnologies. Taqman probe analysis was conducted on a Roche Lightcycler 480, utilizing a standard curve for absolute quantification.

Plaque assays and immunohistochemistry. Assays were conducted as described previously with minor modifications (36). BSC-40 cells were seeded in six-well plates and grown to confluence. VacV, MPX or VarV were diluted in RPMI containing 2% FBS, and ~25 PFU were added to each well. Following 1 hour incubation with virus, Gleevec (STI-571), Spyrcel (BMS-354285), or PD-166326 was added to final concentrations of 10-0.05 μM. Immunohistochemistry (IHC) was performed as described previously (7) (36). Briefly, the cells were incubated with polyclonal rabbit anti-variola virus antibody and goat anti-rabbit immunoglobulin G-horseradish peroxidase conjugate (KPL 074-1506; Kirkegaard & Perry Laboratories). The plaques were visualized by development with TrueBlue peroxidase substrate (KPL 71-00-64; Kirkegaard & Perry Laboratories). Assays with VarV were performed in a maximum-containment laboratory under biosafety level 4 conditions. Six-well plates containing VarV were double sealed in Kapak/Scotchpak pouches and gamma irradiated at the kill dose of 4.4×10^6 rads prior to IHC staining (18).

Comet assays. Confluent monolayers of BSC-40 wells in 6-well dishes were infected with ~25 pfu of VacV-WR, MPX, or VarV-BSH diluted in 2%FBS RPMI. The comet assay was performed as described previously (24) (7) with some

modifications. The cells, viral dilutions, infection procedures, and drug concentrations, gamma irradiation for VARV, and IHC were as described above for the plaque size evaluation assay. During the two, three, or four day incubation period for VacV, MPX, or VarV, respectively, the plates were placed at a fixed angle of approximately 5 degrees, and then fixed and stained with antibody as described (7, 36).

EEV quantification assays. Methods for quantification of EEV have been described previously (24). Briefly, 6-well dishes were seeded with BSC-40 cells, which were allowed to grow to ~90% confluence. Cells were then incubated with VacV, MPX, or VarV at an MOI of either 5 or 0.1. The supernatants were harvested at 18-24 hours post infection and were incubated with IMV neutralizing antibody for 1h. To quantify the remaining infectious particles, serial dilutions of the neutralized supernatant were incubated with naive BSC-40 monolayers. After one hour, media was exchanged and two, three, or four days later for VacV, MPX, or VarV, respectively, cells were stained with 1% crystal violet and plaques enumerated. To enumerate CAV, cells were plated andthe infected as cells described above. After 24h, cells were scraped and lysed by freeze thaw. Serial dilutions of the supernatant were incubated with BSC-40 monolayers for one hour, the media exchanged, and two, three, or four days later for VacV, MPX, or VarV, respectively, cells were stained with 1% crystal violet and plaques enumerated.

Results

Actin motility in VarV and MPX. To determine whether the orthopoxviruses VacV, MPX and VarV use common mechanisms of actin motility, we assessed the capacity of these viruses to induce actin tail formation in infected cells. 3T3 mouse fibroblast cells were infected with either VarV or MPX, and then fixed and stained with FITC-phalloidin to recognize actin, and DAPI to recognize DNA. Both MPX and VarV formed actin filled membranous protrusions ("tails") in infected cells (Figure 1a; Supplementary Figure 1a). VarV and MPX actin tails appeared generally similar to those of VacV (Supplementary Figure 2a), though some subtle morphological differences were evident. Thus, occasionally induced formation of a "doublet" tails consisting of two fused tails with two virions at the tip (Supplementary Figure 2b), and variola induced "horseshoe" tails (Figure 2a,e), morphologies that were not apparent in cells infected with VacV (e.g. Supplementary Figure 2a).

The complement of proteins at the tips of VarV and MPX actin tails was identical to those seen in VacV. Thus, phosphotyrosine (pY) staining and the virus specific antigen B5R were evident at the tips of tails (Figure 1a,b; Supplementary Figure 1a,b). Likewise, the tyrosine kinases Src, Fyn, Yes1, Abl1, and Abl2, and the accessory proteins Nck and Grb2, which are required for actin motility in VacV, all localized to the tips of VarV and MPX actin tails (Figure 1c-i, Supplementary Figure 1c-i). In some samples, DAPI staining at the tips of actin tails co-localized with Grb2, Nck, and Abl2 (Figure 1j-l). Together, these data

indicate that VarV and MPX recruit cellular proteins in a manner analogous to VacV.

Redundant Abl- and Src-family Tyrosine Kinases mediate VarV and MPX actin motility. To determine whether Src- and Abl-family kinase activity were required by VarV and MPX to form actin tails, we first assessed the capacity of MPX and VarV to form actin tails in 3T3 cells derived from animals lacking Src, Fyn, and Yes1 ($Src^{-/-}/Fyn^{-/-}/Yes1^{-/-}$), or from animals lacking Abl1 and Abl2 ($Abl1^{-/-}/Abl2^{-/-}$). VarV and MPX induced comparable actin tails in 3T3 cells (Figure 2a,b), $Src^{-/-}/Fyn^{-/-}/Yes1^{-/-}$ cells (Figure 2c,d) or in $Abl1^{-/-}/Abl2^{-/-}$ cells (Figure 2e,f), in accordance with previous observations with VacV (24). We next tested the effects of two classes of tyrosine kinase inhibitors on actin tails formed by VarV or MPX. STI-571 is an inhibitor of Abl-family kinases (also called imatinib mesylate or Gleevec), whereas PD-166326 and BMS-354825 (Sprycel) inhibit both Abl- and Src-family kinases. As with VacV, treatment of 3T3 cells with STI-571 (10 μM) did not prevent actin tail formation by VarV, MPX (Figure 3a,b) (24). However, no actin tails were evident in cells treated with either PD-166326 or BMS-354825 (Figure 3,c-f; Supplementary Figure 2b; see also (24)). Notably, neither MPX nor VarV induced actin tails in $Src^{-/-}/Fyn^{-/-}/Yes1^{-/-}$ cells treated with STI-571 (Figure 3g,h). Collectively, these data indicate that VarV and MPX can utilize Abl- or Src-family tyrosine kinase activity to form actin tails. Moreover, like VacV, usage of these kinases by VarV or MPX appears to be functionally redundant; that is, any one kinase can suffice in the absence of others.

Effects of tyrosine kinase inhibitors on CAV and EEV. We next tested the effect of tyrosine kinase inhibitors on formation of plaques and associated "comets," which are indicators of released EEV. Following adsorption with VacV, MPX, or VarV, BSC-40 cells were treated with Src- and Abl-family inhibitors PD-166326 or BMS-354825, or the Abl-family inhibitors STI-571 or AMN-107, at various concentrations. Cells were fixed after 48, 72, or 96 hours for VacV, MPX, and VarV, respectively, and stained with a poxvirus pAb to identify infected cells. PD-166326 or BMS-354825 at concentrations of 1 to 10 μM reduced plaque size in cells infected with VarV-BSH, MPX, or VacV strain IHD-J (Figure 4; Supplementary Figure 3; see also (24)), and no "comets" were evident. By contrast, the Abl-family kinase inhibitors STI-571 or AMN-107 at a concentration of 10μM had no effect on plaque size, but reduced "comets" (Figure 4; Supplementary Figure 3).

To more carefully assess the effects of drugs on actin motility and plaque size, and to reduce the contribution of EEV to plaque size, we next carried out carboxy methyl-cellulose (CMC) overlay experiments. The CMC media restricts the movement of released particles, thereby eliminating comets. Following the initial incubation with virus, inoculum media was replaced with CMC media containing either PD-166326, or BMS-354825, or STI-571, or AMN-107 at various concentrations. Under these conditions, PD-166326 and BMS-354825 reduced plaque size, whereas STI-571 and AMN-107 were without effect compared to

untreated controls, in accordance with the microscopy and comet assays (Supplementary Figure 4).

To quantify the effect of BMS-354825, PD-166326 and STI-571 on EEV, we enumerated the number of virions released from BSC-40 cells infected at an MOI of 5 into the supernatant, as well as the total CAV produced. Cell supernatants were harvested at 18-24 hours post infection, the time at which EEV release is maximal. Supernatants were then treated with IMV mAb (2D5 or L1R), and the released virus titred on naïve cells. STI-571 reduced EEV by 22%, 88%, 53%, and 6%, for VarV-BSH, VarV-SLN, MPX and VacV-WR, respectively (Figure 5a,b,c). BMS-354825 and PD-166326 produced similar effects on EEV produced by VacV, MPX, and VarV-SLN (Figure 5a,b,c), though BMS-354825 appeared without effect on VarV-BSH. To measure viral replication in the presence of the tyrosine kinase inhibitors, the infected cells were harvested and lysed, and the titres assessed on naïve cells (Figure 5d,e,f). None of the compounds affected production of CAV, with the exception of PD-166326, which caused a slight dimunition, in accordance with previous findings (24). Collectively, these data suggest that inhibition of Abl kinase activity reduced EEV, but not CAV, produced by VarV, MPX and VacV.

Effects of tyrosine kinase inhibitors on VacV infections *in vivo*. Based on the capacity of BMS-354825 to prevent the formation of actin tails and reduce EEV, we tested whether administration of the drug could afford protection in mice challenged with an otherwise lethal inoculum of VacV. Beginning 24h prior to

infection, BMS-354825 was administered either by twice-daily injections or by osmotic pump implanted subcutaneously to deliver drug at a constant rate for the duration of the experiment. Mice were then challenged intranasally (IN) with $2x10^4$ pfu of VacV strain IHD-J, the LD_{100} (lethal dose for 100% of mice). No dose of BMS-354825 or delivery condition tested provided any survival benefit to the mice compared to PBS controls (Figure 6a).

To investigate the capacity of BMS-354825 to limit dissemination, mice were implanted with osmotic pumps to deliver drugs and then challenged with sub-lethal inocula of VacV IHD-J ($2x10^4$ pfu, IP). Concentrations tested ranged between 0.05 and 240 mg/kg/d. After four days, the ovaries were removed, and viral genome copies quantified by Q-PCR. The data indicated that none of the doses of BMS-354825 within the range tested significantly reduce viral load in mice (Supplementary Figure 5a). During post-mortem analysis, spleens of mice treated with this drug appeared significantly reduced in weight relative to infected controls ($p = 0.001$; Supplementary Figure 5b). Taken together, these data suggested that BMS-354825 may negatively impact the immune response. To test this possibility directly, viral loads were assessed in ovaries of mice infected with a sub-lethal inoculum of VacV IHD-J ($2x10^4$ pfu intraperitoneally (IP)), treated with STI-571 (200 mg/kg/d) together with BMS-354825 at either 0.5 or 0.05 mg/kg/d. As controls, we tested the effects of PBS, STI-571 alone (200 mg/kg/d), or BMS-354825 alone at either 0.05 or 0.5 mg/kg/d. In accordance with previous work, STI-571 reduced viral genome copies by ~4 logs (Figure 6b; (24)).

By contrast, BMS-354825 alone at either 0.5 mg/kg/d or 0.05 mg/kg/d reduced viral genome copies by ~1 log. When BMS-354825 at 0.5 mg/kg/d was delivered together with STI-571, the viral load was nearly identical to that seen with BMS-354825 at 0.5 mg/kg/d alone. These data suggest that BMS-354825 at 0.5 mg/kg/day itself had little impact on viral load, but that at this dose the drug could abrogate the protective effects of STI-571. Notably, when 0.05 mg/kg/d BMS-354825 was delivered together with STI-571, the beneficial effects of STI-571 were apparent though diminished by ~1 log. Taken together, these data indicate that BMS-354825 treatment is unlikely to afford protection to lethally infected mice, and indeed may have an immunosuppressive activity, likely due to inhibition of Src-family kinases.

Previous work demonstrated that STI-571 was capable of protecting mice from a lethal-challenge when administered prophylactically. We next sought to extend this observation and test the therapeutic potential of STI-571. To do this, mice were challenged with $2x10^4$ pfu IN VacV IHD-J, the LD_{100}. Mice were implanted with osmotic pumps to deliver STI-571 (200 mg/kg/d) 24 hours prior to infection, at the time of infection, or 24 or 48 hours post infection. In accordance with previous reports (24), all mice treated with drug prior to infection survived (Figure 6c). Administration of drug at the time of, or following infection, resulted in significant survival, though the percentage was lower than that seen with pretreatment, and decreased as the time following inoculation was extended.

Together, these data suggest that STI-571 has protective effect whether delivered prophylactically or in a therapeutic context.

We next tested whether STI-571 interfered with the acquisition of protective immune memory. To do this, mice previously challenged with the LD_{100} and treated with STI-571 were allowed to rest for 10-12 weeks ("STI-571 survivors"). The mice were then challenged with $1x10^8$ pfu of IHD-J IP. As controls, mice were inoculated IP with $2x10^4$ pfu IHDJ, a non-lethal inoculum, and allowed to rest for 10-12 weeks before being rechallenged with $1x10^8$ pfu of IHD-J IP ("immunized"). A control group of naïve age-matched mice was also challenged with IP $1x10^8$ pfu of IHD-J ("naïve"). As shown in Figure 6d, naïve mice all succumbed within 4-9 days, whereas all STI-571 survivors and immunized mice remained viable. Together, these data indicate that administration of STI-571 does not interfere with the acquisition of protective immune memory.

Discussion

Studies using VacV have led to a comprehensive understanding of orthopoxvirus replication, dissemination and pathogenesis. Additionally, VacV, VarV and MPX share 98% sequence homology. However, there is some variance among poxviruses in the precise mechanisms of dissemination *in vivo* and *in vitro*. For example, different strains of VarV exhibit distinct plaque phenotypes *in vitro* and and mortality profiles *in vivo* (19). Given the potential clinical significance of VarV and MPX, we set out to assess whether the mode of dissemination was conserved between these viruses and VacV. Our data

demonstrate VarV and MPX are capable of inducing actin tails in a manner analogous to VacV. Thus, to form actin tails, MPX, VarV, and VacV, localize host factors known to regulate actin polymerization such as Grb-2 and Nck. Like VacV, VarV and MPX appear to utilize Src- and Abl-family tyrosine kinases in a redundant fashion (24).

Of importance from a clinical perspective, actin tails formed by VacV, MPX and VarV are similarly sensitive to Src- and Abl-family tyrosine kinase inhibitors. In plaque assays BMS-354825 or PD-166326 reduced the size of plaques and comets, whereas STI-571 reduced the appearance of comets without diminishing plaque size. The findings of EEV assays were generally consistent with the comet assay, with one exception. Although BMS-354825 reduced plaque size and inhibited comets formed by VarV strain BSH, as well as by MPX, VarV-SLN, and VacV, the drug had no effect on EEV produced by VarV-BSH. Because PD-166326 was effective in both the comet and EEV assays on this strain, we attribute this inconsistency to variance in the EEV assay. The comet assay directly measures viral spread, whereas the EEV assay measures the fraction of infectious particle that remain infectious after treatment with the IMV mAb. Harvesting, antibody treatment, and serial dilution however introduce variability, as does the difficulty of carrying out complex experimental manipulations under BSL4 conditions. As such, our confidence in the comet assays remains high. In any case, given the lack of efficacy of BMS-354825 *in vivo*, we could not justify further investigation of this variance.

Drugs that affect poxvirus replication or spread are important to mollify symptoms associated with vaccination, or for smallpox or monkeypox infections in individuals for whom vaccination poses a significant risk or would prove ineffective. The therapies currently approved for poxvirus infections are Vaccinia Immune Globulin (VIG; (5, 6)) and cidofovir, a DNA polymerase inhibitor (3). However, the efficacy of VIG in late stage infections is limited and while effective, cidofovir causes severe renal toxicity at the doses required and must be administered with IV hydration and in conjunction with probenecid, a renal tubular blocker that is also not without complications (13). It is unlikely that this regimen could be implemented to successfully treat a significant number of infected individuals. Another drug, ST-246, blocks formation of CEV and EEV, and has shown efficacy in mouse and non-human primate models of poxvirus infection (11)(23). ST-246 is currently in human trials.

Would tyrosine kinase inhibitors such as BMS-354825 or STI-571 prove efficacious *in vivo*? The *in vivo* shortcomings of BMS-354825 stand in stark contrast to its apparent promise based on *in vitro* assays. Despite the robust *in vitro* effects on plaque size and comets, BMS-354825 neither reduces load nor protects mice from lethal challenge. During the course of our experiments, the European Medicines Agency (EMEA) reported immunotoxicity for BMS-354825 (8). Specifically, treatment with 25 mg/kg, but not 15 mg/kg, delivered once daily prevents graft rejection in a murine cardiac transplant model. Further, BMS-354825 inhibits murine splenic T-cell proliferation and induces lymphoid depletion

of the thymus and spleen. These data are in accordance with our observation that BMS-354825 induces splenopenia and suppresses the effects of STI-571 on dissemination of VacV. Taken together, these data indicate that immunotoxicity of BMS-354825 likely accounts for the failure to provide benefit for poxvirus infections. Unfortunately, we were unable to define a concentration or dosing regimen that would minimize immunosuppressive effects, yet still abrogate viral dissemination.

The most likely explanation for the immunosuppressive effects of BMS-354825 is the inhibition of Src-family kinases rather than Abl-family kinases. In particular, Fyn and other Src-family tyrosine kinases have been implicated in various aspects of immune response including innate and antigen signaling, phagocytosis, and T- and B-cell development (14), (17, 33). BMS-354825 also more potently inhibits Abl-family kinases than STI-571. However, our data with STI-571 suggests that inhibition of Abl-family kinases per se likely does not contribute to immunosuppression; STI-571 does not prevent acquisition of protective immunity to poxviruses, and the drug is well tolerated in human patients who show little increased incidence of infection (35). Together these data suggest that dual-Src/Abl inhibitors provide little *in vivo* benefit against microbial infections, despite their apparent efficacy *in vitro*.

In contrast to BMS-354825, data presented here suggest that STI-571 can provide significant protection when administered post-infection, in addition to prophylactic effects reported previously (24). Nevertheless, the benefits of STI-

571 decrease in a time-dependent manner following inoculation. The absence of STI-571 during the period following inoculation may permit virus to establish the infection and spread to distal tissues. Once established in distal tissues, viral replication and actin tails may contribute to further expansion of virus, despite the addition of the drug. A similar argument may account for our observation that increasing the inoculum to $2x10^5$ pfu, 10 times the LD_{100}, overcomes the protective benefit of STI-571 (data not shown). Another factor contributing to efficacy of STI-571 following inoculation may be that drug delivered via osmotic pump reaches therapeutic levels only after 16-18 hours. Despite these caveats on the precise timing of its delivery, STI-571 provides a significant level of protection pre- or post-infection, perhaps by allowing time for an effective immune response to develop. Moreover, STI-571 does not interfere with acquisition of protective immune memory. Collectively, these data lead us to suggest the potential utility of STI-571 for treatment of poxvirus infections should be evaluated further.

In this regard, prairie dogs may offer means to assess the therapeutic value of STI-571 for MPX infections. Similar to the murine model, an inoculum of $5x10^4$ IN is used. However, this model is distinguished by the appearance of disseminated lesions or “pox” 9-12 days post-infection, a phenotype previously observed only in primate models. In humans, pox lesions generally appear 7-19 days following infection and have been attributed to migration of EEV through the lymphatic system to the skin. Thus, presentation of pox in the prairie dog model

recapitulates an important aspect of disease progression seen in humans, but not other small animal models. Our data demonstrating the capacity of STI-571 to limit EEV *in vitro* and dissemination *in vivo*, and suggest that STI-571 may have efficacy against MPX in prairie dogs, and possibly primates, against formation of pox, a prospect we are now testing.

STI-571 may also have utility when co-administered with other compounds under consideration as poxvirus therapeutics such as ST-246 and Cidofovir. ST-246 protects mice from lethal challenge when administered up to 3 days post-infection (2). ST-246 acts more distally to STI-571 by inhibiting F13 and interfering with IEV production and viral dissemination (36). Notably however, variants resistant to ST-246 have been described that result from a single base change in F13L (36). Similarly, resistance to Cidofovir is conferred by point mutations in E9L, the DNA polymerase gene (1). By contrast, STI-571 is less likely to engender resistant mutants because it targets host kinases. Moreover, when co-administered, STI-571 may reduce viral load and decrease the probablility of developing mutants resistant to ST-246 or cidofovir.

In summary, we describe a conserved mode of dissemination within the orthopoxvirus family, and the mechanism of actin tail formation and EEV release by MPX and VarV. In addition, we show that dual Src/Abl inhibitors effectively limit both actin tail based motility and EEV release *in vitro*. However, their utility against poxvirus infections *in vivo* is precluded by their immunosuppressive activity. By contrast, we show that STI-571 can be used in a therapeutic context,

and does not interfere with the acquisition of immune memory, which may warrant further testing in animal models of poxvirus infection.

Acknowledgements

This work was supported by NIH R01A107246201A2 to DK. We thank Jay Hooper (USAMRIID), Bernard Moss (NIH) and Stewart Isaacs (University of Pennsylvania) for sharing antibodies.

Author Contributions

PMR, ID, and DK conceived and designed experiments. PMR, VO, and SKS performed the experiments: WB contributed reagents/materials/analysis tools. PMR and DK analyzed the data. : PMR and DK wrote the paper.

References

1. **Becker, M. N., M. Obraztsova, E. R. Kern, D. C. Quenelle, K. A. Keith, M. N. Prichard, M. Luo, and R. W. Moyer.** 2008. Isolation and characterization of cidofovir resistant vaccinia viruses. Virol J **5:**58.
2. **Berhanu, A., D. S. King, S. Mosier, R. Jordan, K. F. Jones, D. E. Hruby, and D. W. Grosenbach.** 2009. ST-246(R) inhibits in vivo poxvirus dissemination, virus shedding, and systemic disease manifestation. Antimicrob Agents Chemother.
3. **Bray, M., M. Martinez, D. F. Smee, D. Kefauver, E. Thompson, and J. W. Huggins.** 2000. Cidofovir protects mice against lethal aerosol or intranasal cowpox virus challenge. J Infect Dis **181:**10-9.
4. **Carter, G. C., G. Rodger, B. J. Murphy, M. Law, O. Krauss, M. Hollinshead, and G. L. Smith.** 2003. Vaccinia virus cores are transported on microtubules. J Gen Virol **84:**2443-58.
5. **CDC.** 2003. Smallpox Vaccination and Adverse Reactions Guidance for Clinicians 52(RR04). CDC.
6. **CDC.** 2001. Vaccinia (Smallpox) Vaccine

Recommendations of the Advisory Committee on Immunization Practices (ACIP), 2001 50(RR10). CDC.

7. **Chen, Z., P. Earl, J. Americo, I. Damon, S. K. Smith, F. Yu, A. Sebrell, S. Emerson, G. Cohen, R. J. Eisenberg, I. Gorshkova, P. Schuck, W. Satterfield, B. Moss, and R. Purcell.** 2007. Characterization of chimpanzee/human monoclonal antibodies to vaccinia virus A33 glycoprotein and its variola virus homolog in vitro and in a vaccinia virus mouse protection model. J Virol **81:**8989-95.
8. **EMEA, E. M. A.** 2006. Sprycel European Public Assessment Report, p. 46. *In* E. M. A. EMEA (ed.). European Medicines Agency, London.
9. **Esposito, J., and Fenner, F.** 1999. Poxviruses, p. 2 v. (xix, 2336). *In* B. N. Fields and D. M. Knipe (ed.), Fields Virology, 2nd ed. Raven Press, New York.
10. **Hollinshead, M., G. Rodger, H. Van Eijl, M. Law, R. Hollinshead, D. J. Vaux, and G. L. Smith.** 2001. Vaccinia virus utilizes microtubules for movement to the cell surface. J Cell Biol **154:**389-402.
11. **Huggins, J., A. Goff, L. Hensley, E. Mucker, J. Shamblin, C. Wlazlowski, W. Johnson, J. Chapman, T. Larsen, N. Twenhafel, K. Karem, I. K. Damon, C. M. Byrd, T. C. Bolken, R. Jordan, and D. Hruby.** 2009. Nonhuman primates are protected from smallpox virus or monkeypox virus challenges by the antiviral drug ST-246. Antimicrob Agents Chemother **53:**2620-5.
12. **Kalman, D., O. D. Weiner, D. L. Goosney, J. W. Sedat, B. B. Finlay, A. Abo, and J. M. Bishop.** 1999. Enteropathogenic E. coli acts through

WASP and Arp2/3 complex to form actin pedestals. Nat Cell Biol **1:**389-91.

13. **Lacy, S. A., M. J. Hitchcock, W. A. Lee, P. Tellier, and K. C. Cundy.** 1998. Effect of oral probenecid coadministration on the chronic toxicity and pharmacokinetics of intravenous cidofovir in cynomolgus monkeys. Toxicol Sci **44:**97-106.
14. **Lowell, C. A.** 2004. Src-family kinases: rheostats of immune cell signaling. Mol Immunol **41:**631-43.
15. **Mortimer, P. P.** 2003. Can postexposure vaccination against smallpox succeed? Clin Infect Dis **36:**622-9.
16. **Moss, B.** 1999. Poxviridae: The Viruses and Their Replication, p. 2 v. (xix, 2336). *In* B. N. Fields and D. M. Knipe (ed.), Fields Virology, 2nd ed. Raven Press, New York.
17. **Mustelin, T., and K. Tasken.** 2003. Positive and negative regulation of T-cell activation through kinases and phosphatases. Biochem J **371:**15-27.
18. **National Research Council, I. o. M.** 1999. Assessment of Future Scientific Needs for Live Variola Virus. National Academy Press, Washington, D.C.
19. **Olson, V. A., K. L. Karem, S. K. Smith, C. M. Hughes, and I. K. Damon.** 2009. Smallpox virus plaque phenotypes: genetic, geographical and case fatality relationships. J Gen Virol **90:**792-8.
20. **Parker, S., A. Nuara, R. M. Buller, and D. A. Schultz.** 2007. Human monkeypox: an emerging zoonotic disease. Future Microbiol **2:**17-34.
21. **Ploubidou, A., V. Moreau, K. Ashman, I. Reckmann, C. Gonzalez, and M. Way.** 2000. Vaccinia virus infection disrupts microtubule organization and centrosome function. Embo J **19:**3932-44.
22. **Prevention, C. F. D. C. a.** 2003. Multistate outbreak of monkeypox--Illinois, Indiana, and Wisconsin, 2003. MMWR Morb Mortal Wkly Rep **52:**537-40.
23. **Quenelle, D. C., R. M. Buller, S. Parker, K. A. Keith, D. E. Hruby, R. Jordan, and E. R. Kern.** 2007. Efficacy of delayed treatment with ST-246 given orally against systemic orthopoxvirus infections in mice. Antimicrob Agents Chemother **51:**689-95.
24. **Reeves, P. M., B. Bommarius, S. Lebeis, S. McNulty, J. Christensen, A. Swimm, A. Chahroudi, R. Chavan, M. B. Feinberg, D. Veach, W. Bornmann, M. Sherman, and D. Kalman.** 2005. Disabling poxvirus pathogenesis by inhibition of Abl-family tyrosine kinases. Nat Med **11:**731-9.
25. **Rietdorf, J., A. Ploubidou, I. Reckmann, A. Holmstrom, F. Frischknecht, M. Zettl, T. Zimmermann, and M. Way.** 2001. Kinesin-dependent movement on microtubules precedes actin-based motility of vaccinia virus. Nat Cell Biol **3:**992-1000.

26. **Scaplehorn, N., A. Holmstrom, V. Moreau, F. Frischknecht, I. Reckmann, and M. Way.** 2002. Grb2 and Nck act cooperatively to promote actin-based motility of vaccinia virus. Curr Biol **12:**740-5.
27. **Smith, G. L., B. J. Murphy, and M. Law.** 2003. Vaccinia virus motility. Annu Rev Microbiol **57:**323-42.
28. **Smith, G. L., A. Vanderplasschen, and M. Law.** 2002. The formation and function of extracellular enveloped vaccinia virus. J Gen Virol **83:**2915-31.
29. **Smith SK, O. V., Karem KL, Jordan R, Hruby DE, Damon IK.** 2009. In vitro efficacy of ST246 against smallpox and monkeypox. Antimicrob Agents Chemother **53:**1007-12.
30. **Swedlow, J. R., J. W. Sedat, and D. A. Agard.** 1997. Deconvolution in Optical Microscopy, p. 284-307. *In* P. A. Jansson (ed.), Deconvolution of Images and Spectra. Academic Press, Inc., San Diego.
31. **Swimm, A., B. Bommarius, Y. Li, D. Cheng, P. Reeves, M. Sherman, D. Veach, W. Bornmann, and D. Kalman.** 2004. Enteropathogenic Escherichia coli use redundant tyrosine kinases to form actin pedestals. Mol Biol Cell **15:**3520-9.
32. **Tolomeo, M., F. Dieli, N. Gebbia, and D. Simoni.** 2009. Tyrosine Kinase Inhibitors for the Treatment of Chronic Myeloid Leukemia. Anticancer Agents Med Chem.
33. **Tsygankov, A. Y., S. Mahajan, J. E. Fincke, and J. B. Bolen.** 1996. Specific association of tyrosine-phosphorylated c-Cbl with Fyn tyrosine kinase in T cells. J Biol Chem **271:**27130-7.
34. **Ward, B. M., and B. Moss.** 2001. Vaccinia virus intracellular movement is associated with microtubules and independent of actin tails. J Virol **75:**11651-63.
35. **Wolf, D., and H. Rumpold.** 2009. A benefit-risk assessment of imatinib in chronic myeloid leukaemia and gastrointestinal stromal tumours. Drug Saf **32:**1001-15.
36. **Yang, G., D. C. Pevear, M. H. Davies, M. S. Collett, T. Bailey, S. Rippen, L. Barone, C. Burns, G. Rhodes, S. Tohan, J. W. Huggins, R. O. Baker, R. L. Buller, E. Touchette, K. Waller, J. Schriewer, J. Neyts, E. DeClercq, K. Jones, D. Hruby, and R. Jordan.** 2005. An orally bioavailable antipoxvirus compound (ST-246) inhibits extracellular virus formation and protects mice from lethal orthopoxvirus Challenge. J Virol **79:**13139-49.

Figure Legends

Figure 1. VarV recruits host cell factors required for actin polymerization. (**a**) Image of 3T3 cell infected with VarV BSH and stained with FITC-phalloidin to visualize actin (green), pY mAb (red) and DAPI to visualize DNA (blue). (**b-i) I**mages of actin tails on 3T3 cells infected with VarV strain BSH or SLN stained with FITC-phalloidin (green) and antibodies against cellular or viral proteins (red): (**b**) B5R mAb (**c**) Src pAb, (**d**) Fyn mAb, (**e**) Yes mAb, (**f**) Abl1 mAb, (**g**) Grb2 pAb, (**h**) Nck mAb, (**i**) Abl2 mAb. Panels **j-l** depict DAPI (blue) at tip of tails from **g-i**. Scale bars represent 5 μm (**a**) and 1μm (**b-i**).

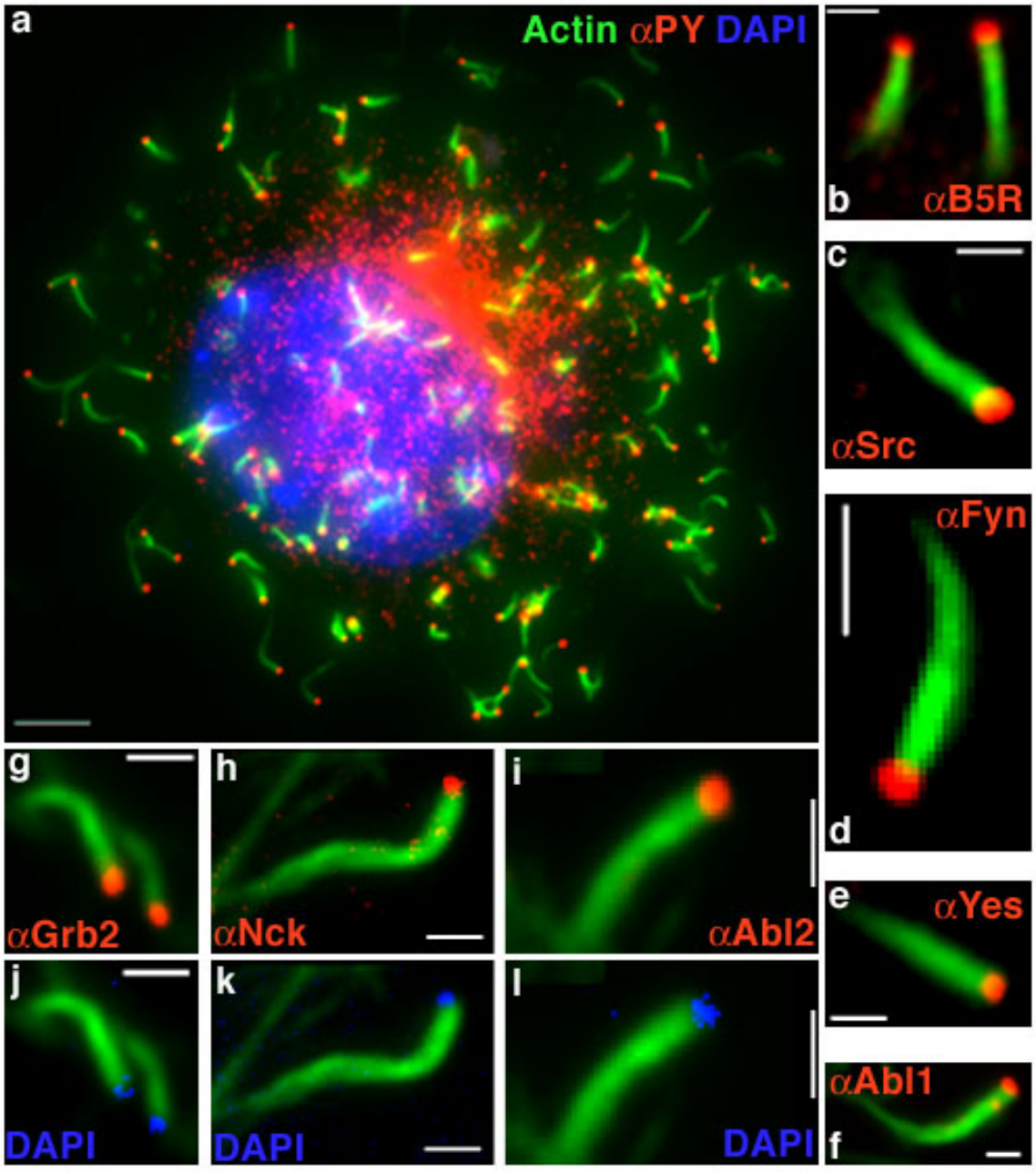

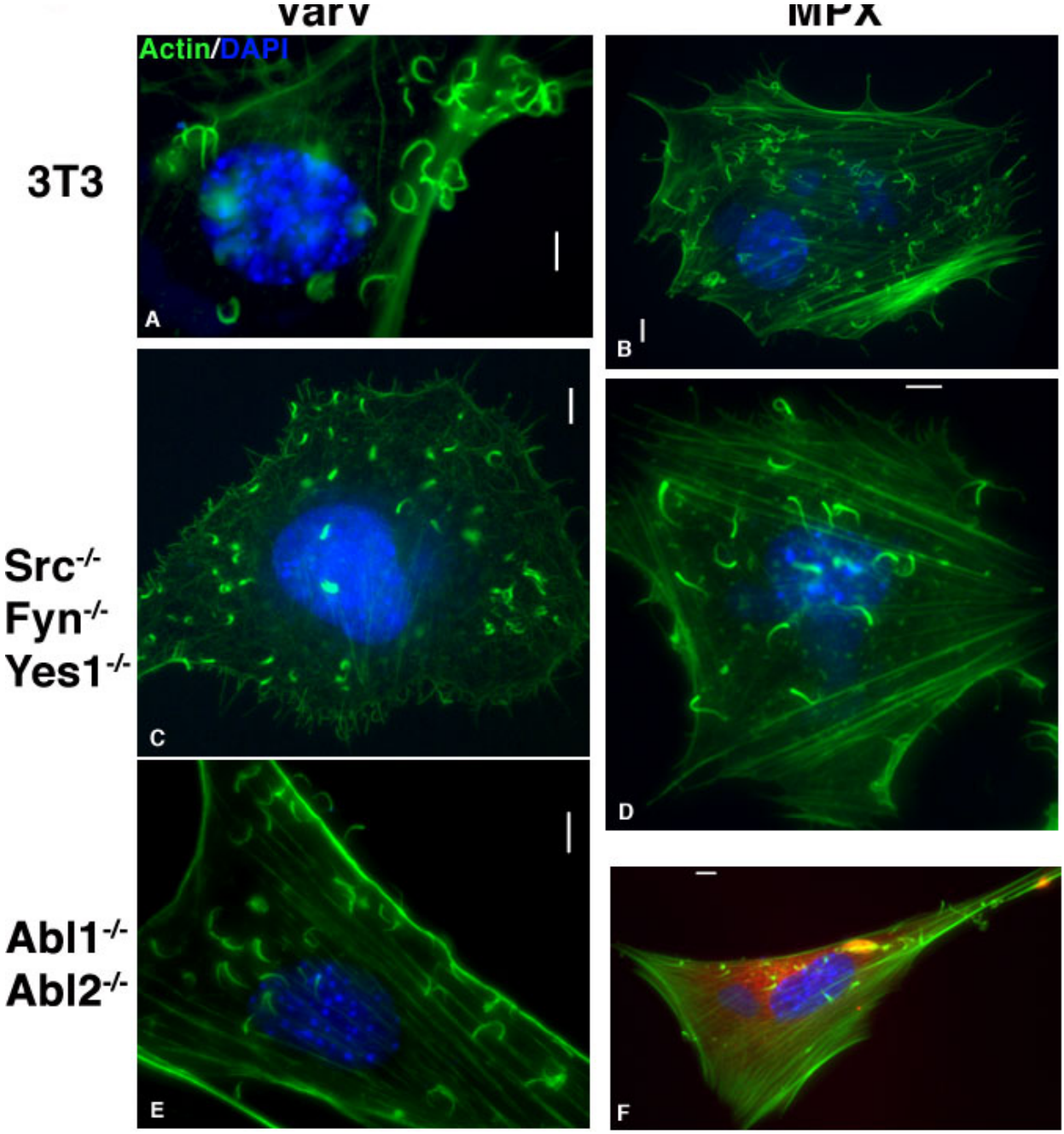

Figure 2. VarV and MPX form actin tails. (**a–f**) Images of fibroblast cell lines derived from WT mice (3T3)(**a,b**), *Src*$^{-/-}$*Fyn*$^{-/-}$*Yes1*$^{-/-}$ mice (**c,d**), or *Abl1*$^{-/-}$*Abl2*$^{-/-}$ mice (**e,f)**, infected with VarV strain BSH (**a, c, e**) or MPX (**b,d,f**) for 24 h, fixed, and stained with DAPI (blue) and FITC-phalloidin (green) to recognize DNA and actin, respectively. Scale bars represent 5 μm.

Figure 3. Actin tails formed by VarV and MPX require Abl and Src-family tyrosine kinases. (**a–h**) Images of fibroblast cell lines derived from WT mice (3T3) (**a-f**) or *Src*$^{-/-}$*Fyn*$^{-/-}$*Yes1*$^{-/-}$ mice (**g,h**) infected with VarV strain BSH (**a, c, e, g**) or MPX (**b, d, f, h**) for 24 h, and treated with STI-571 (a, b, g, h), PD-166326 (c,d) or BMS-354285 (e, f), each at 10 μM, and then fixed and stained with DAPI (blue) and FITC-phalloidin (green) to recognize DNA and actin, respectively. Scale bars represent 5 μm.

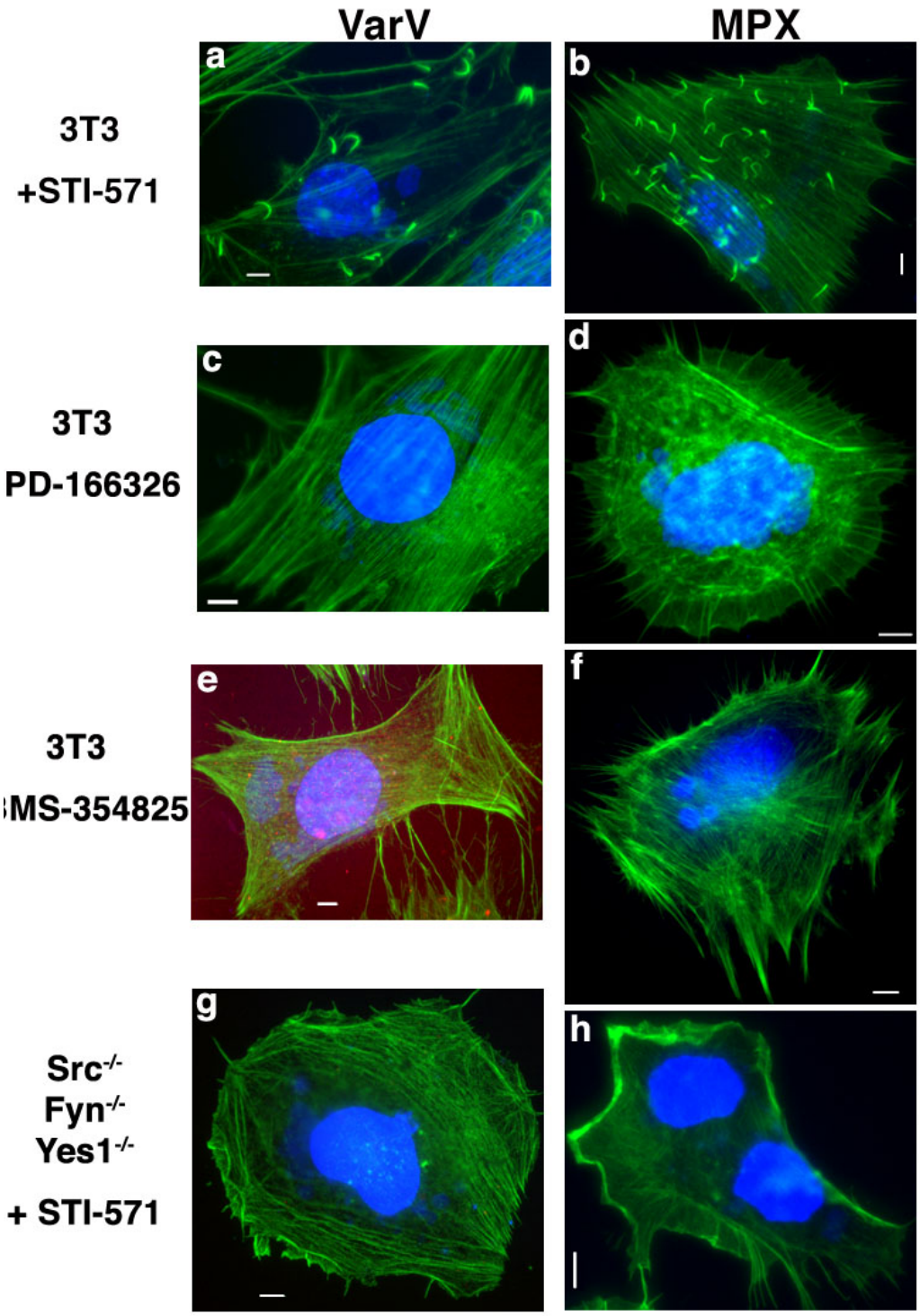

Figure 4. Comet assays. BSC-40 cells were infected with VarV virus strain BSH. Cells were left untreated or treated with either PD-166326, BMS-354825, STI-571, or AMN-107, each at 10 μM, 1 μM, or 100 nM. Drugs were added 1 h after infection. Cells were incubated for 4 d, fixed, and stained with VarV pAb to recognize infected cells.

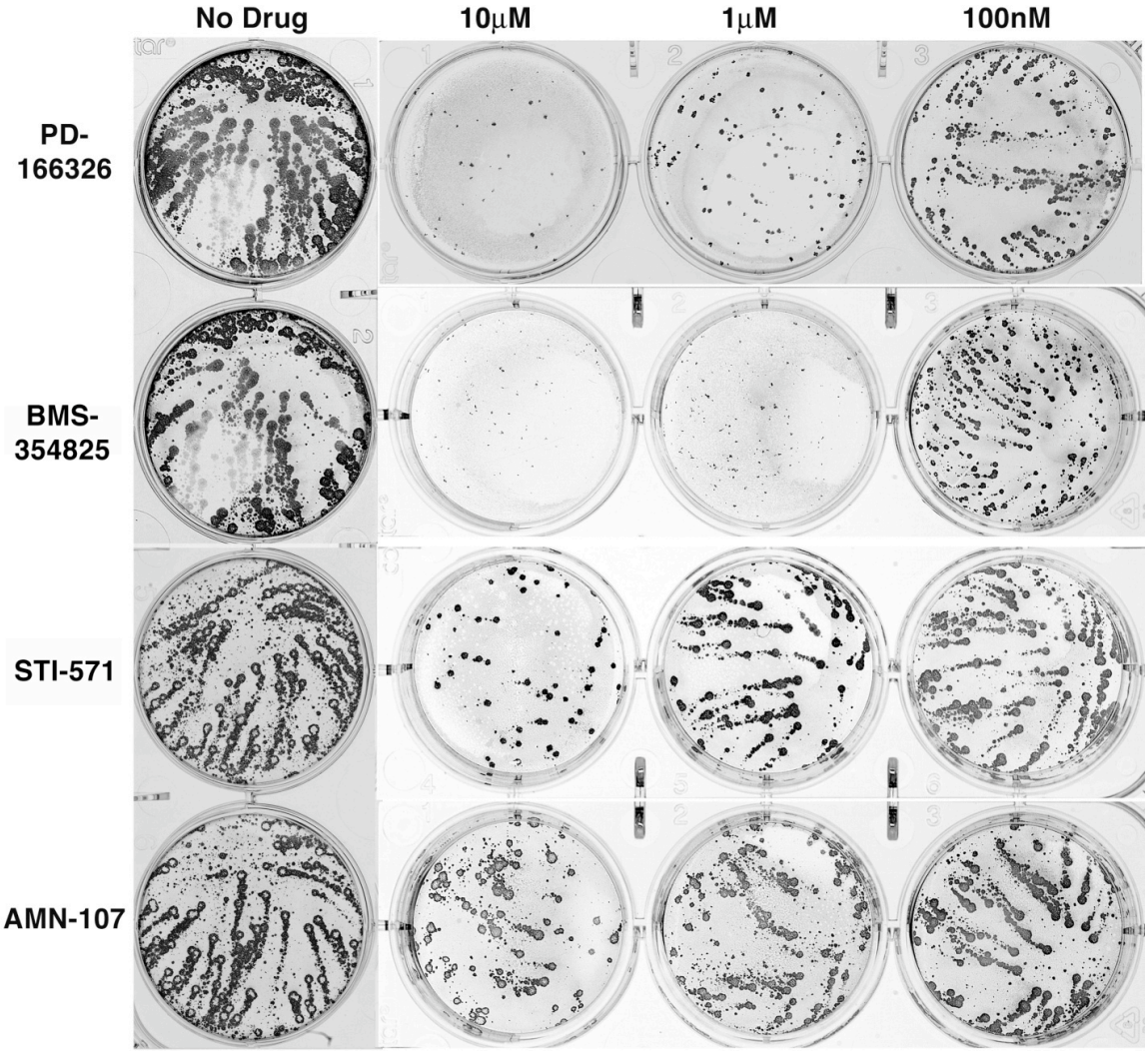

Figure 5. EEV & CAV Assay. Quantification of EEV from supernatant and CAV from lysates of BSC-40 cells infected with VarV strain BSH or strain SLN (**a,d**) MPX (**b,e**), or VacV strain WR (**c,f**) infected at MOI or 5. Inoculum was removed 1h post infection and replaced with media containing STI-571, BMS-354285, or PD-166326 (at 10μM). After 24h supernatant was removed and cells were lysed and titres measured on naïve BSC-40 cells.

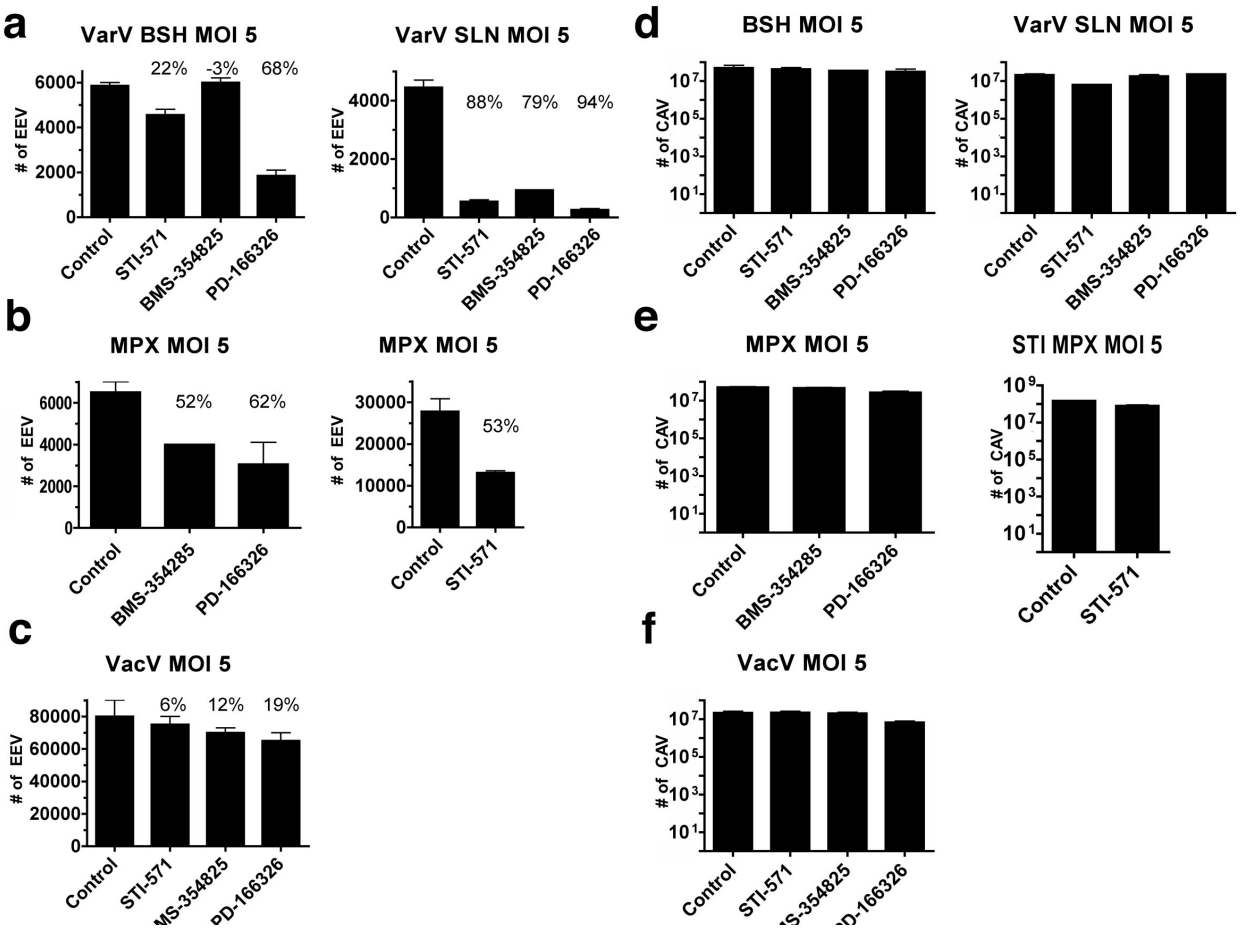

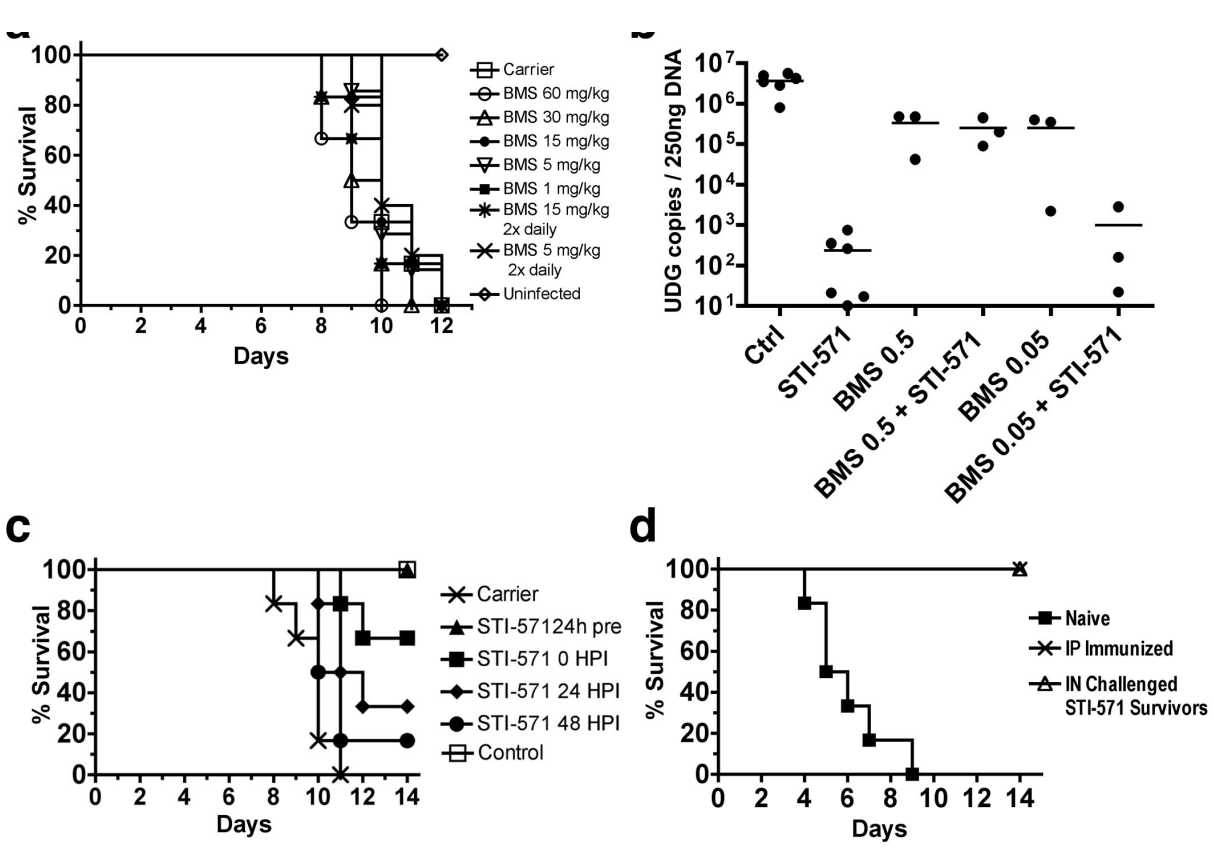

Figure 6. Effects of tyrosine kinase inhibitors on VacV infection in mice. (**a**) Beginning 24 h prior to infection, 6-week-old C57/B6 mice received, PBS (carrier) or BMS-354825 continuously via subcuanteous osmotic pump, or twice daily by IP injection, at concentrations indicated. Mice were infected IN with 2 x10^4 PFU VacV IHD-J (N=6 mice per condition). (**b**) One day prior to infection, mice were implanted with subcutaneous osmotic pumps to deliver STI-571 (200mg/kg/d) or BMS-354825 (0.5mg/kg/d or 0.05 mg/kg/d) or both drugs in a single pump. Control mice received PBS (carrier). Four days after IP infection, viral genome copies were quantified by Q-PCR. Each mouse is represented as a data point. The line represents the median number of viral genome copies for each condition. (**c**) Effects of STI-571 (200mg/kg/d) delivered 24 h before, at the time of (0 hrs), or 24 or 48 hours after IN infection with 2 x10^4 PFU VacV IHD-J . Carrier mice received PBS. Control mice were left uninfected. (**d**) Age matched naïve controls, IP immunized mice, or mice treated with STI-571 (200mg/kg/day) that survived a previous challenge with the LD_{100} (2 x10^4 PFU) VacV IHD-J, were injected IP with 10^8 PFU of VarV IHD-J. The percentage survival is plotted as a function of time after infection.

Supplemental Figure Legends

Supplemental Figure 1. (**a**) Image of 3T3 cell infected with MPX and stained with FITC-phalloidin to visualize actin (green), pY mAb (red) and DAPI to visualize DNA (blue). (**b-i) I**mages of actin tails on 3T3 cells infected with VarV strain BSH or SLN stained with FITC-phalloidin (green) and antibodies against cellular or viral proteins (red): (**b**) B5R mAb, (**c**) Nck mAb, (**d**) Grb2 pAb, (**e**) Src pAb, (**f**) Fyn mAb, (**g**) Yes mAb, (**h**) Abl1 mAb, (**i**) Abl2 mAb. Scale bars represent 5 μm (**a**) and 1μm (**b-i**).

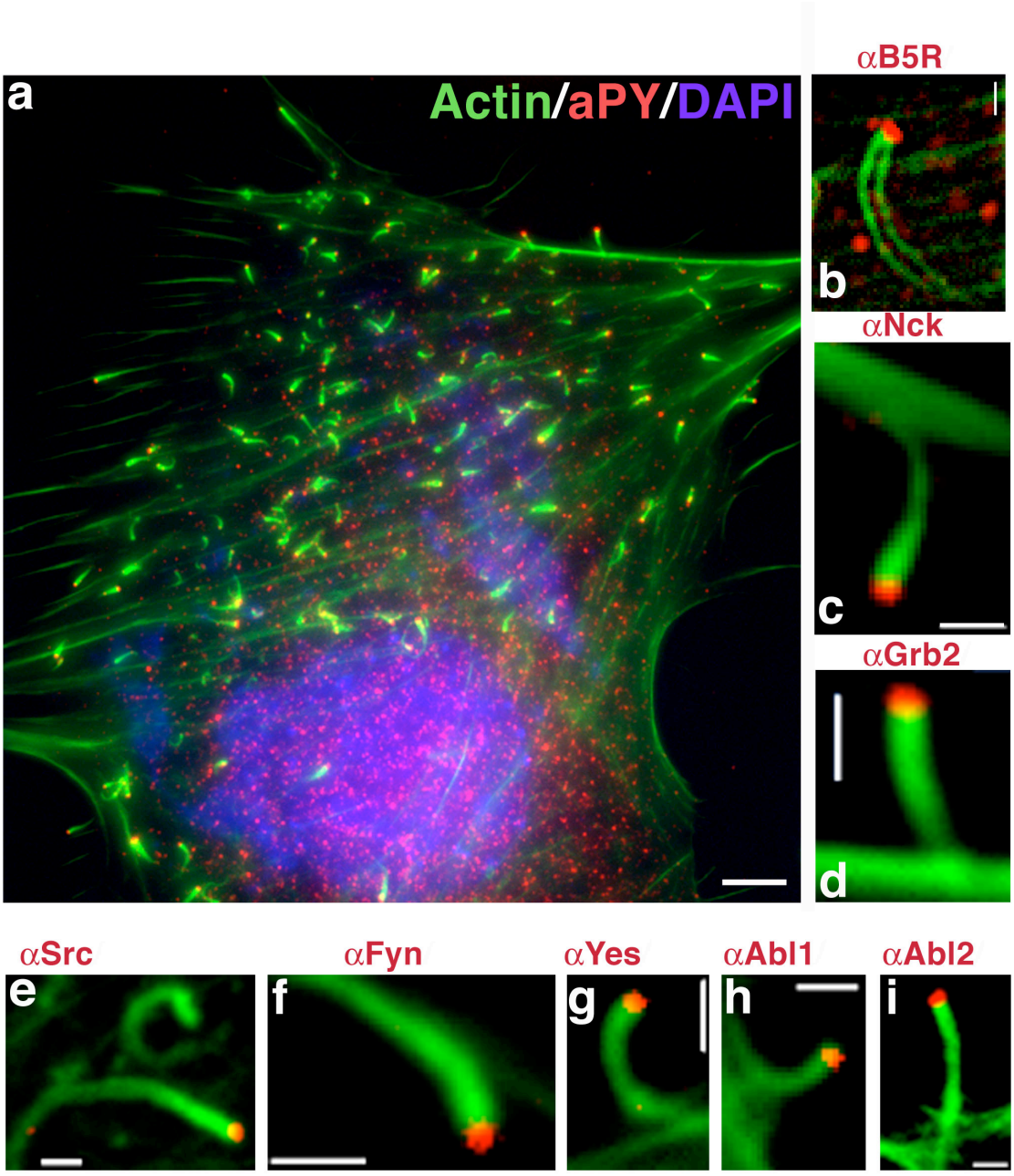

Supplemental Figure 2. BMS-354825 blocks VacV actin tails. (**a–b**) Images of 3T3 cells left untreated (**a**) or treated with 10 μM BMS354825 (**b**) and infected with VacV strain B5R-GFP WR for 18 h, fixed, and stained with DAPI (blue), and Cy3-phalloidin (red) to recognize actin. GFP is shown in green. Scale bars represent 5 μm.

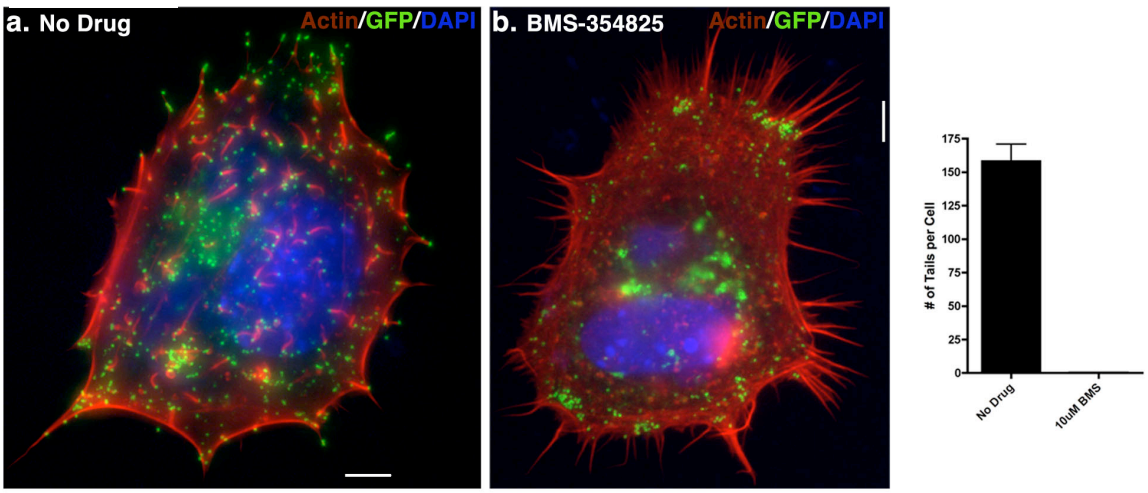

Supplemental Figure 3. MPX & VacV comet assay. BSC-40 cells were infected with MPX virus (**a**), VacV strain IHD-J (**b**) or VacV strain WR (**c**). Cells were left untreated or treated with PD-166326, BMS-354825, STI-571, or AMN-107, each at 10 μM, 1 μM, or 100 nM. Drugs were added 1 h after infection. Cells were incubated for 2 (VacV) or 3 (MPX) d, fixed, and stained with VarV pAb or VacV L1R mAb to recognize infected cells.

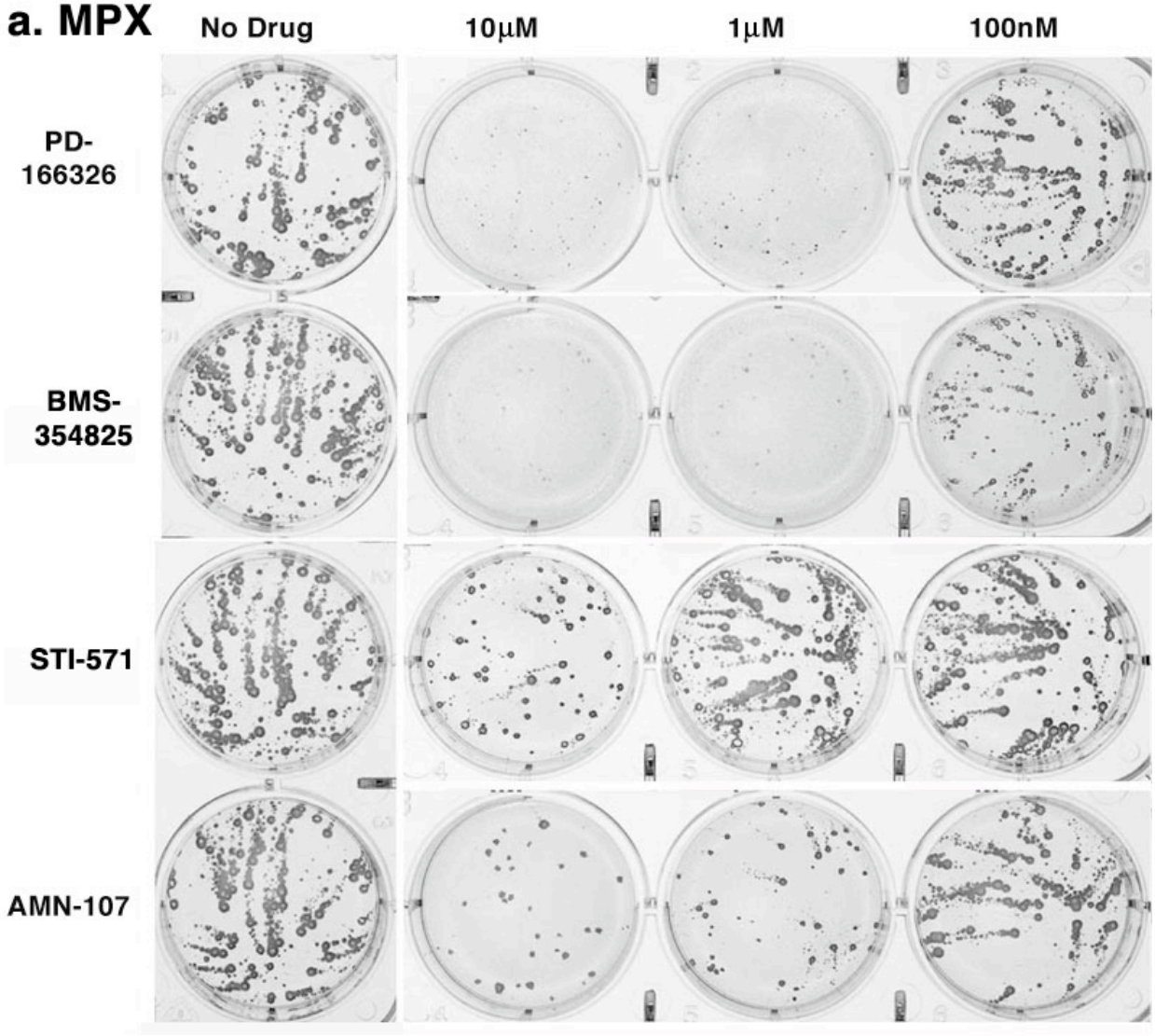

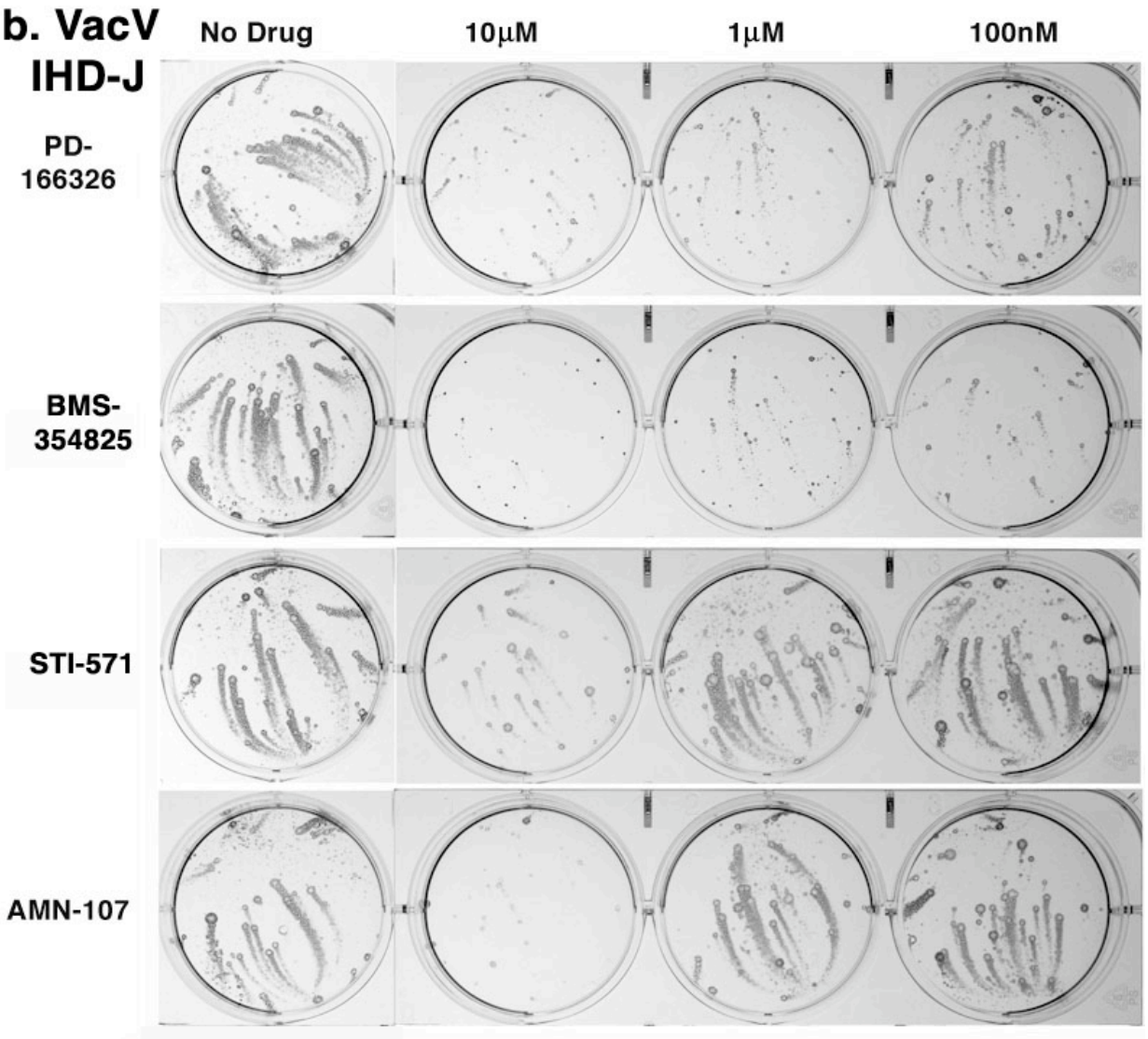
b. VacV
IHD-J
No Drug
10μM
1μM
100nM
PD-166326
BMS-354825
STI-571
AMN-107

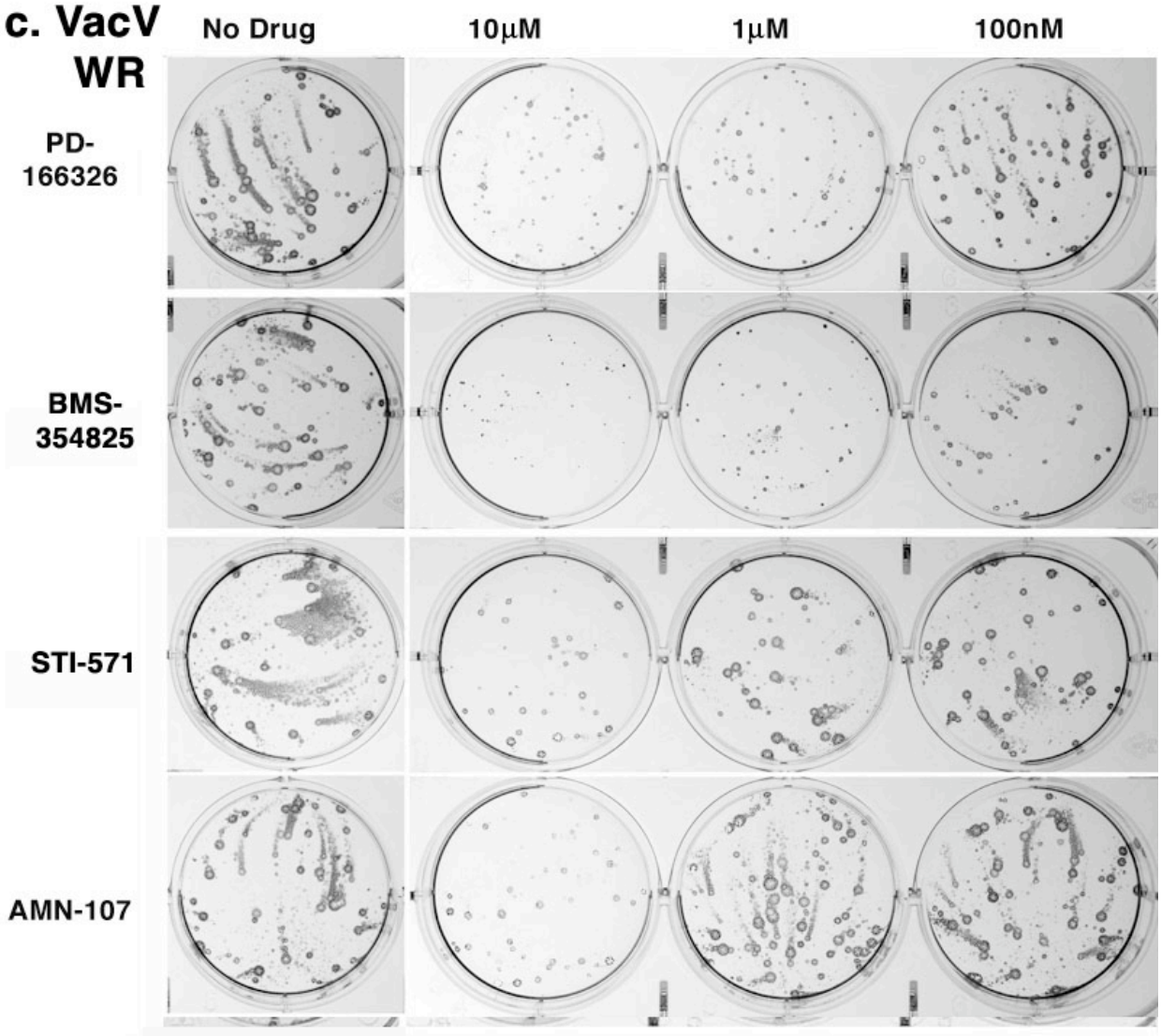
c. VacV WR
No Drug
10μM
1μM
100nM
PD-166326
BMS-354825
STI-571
AMN-107

Supplemental Figure 4. CMC Plaque Assay. BSC-40 cells were infected with VarV virus strain BSH and overlayed with CMC. PD-166326, BMS-354825, STI-571, or AMN-107 were added to a final concentration of 5μM, 0.5μM, or 50 nM 1h after infection. Cells were incubated for 4d fixed, and stained with a VarV pAb to recognize infected cells.

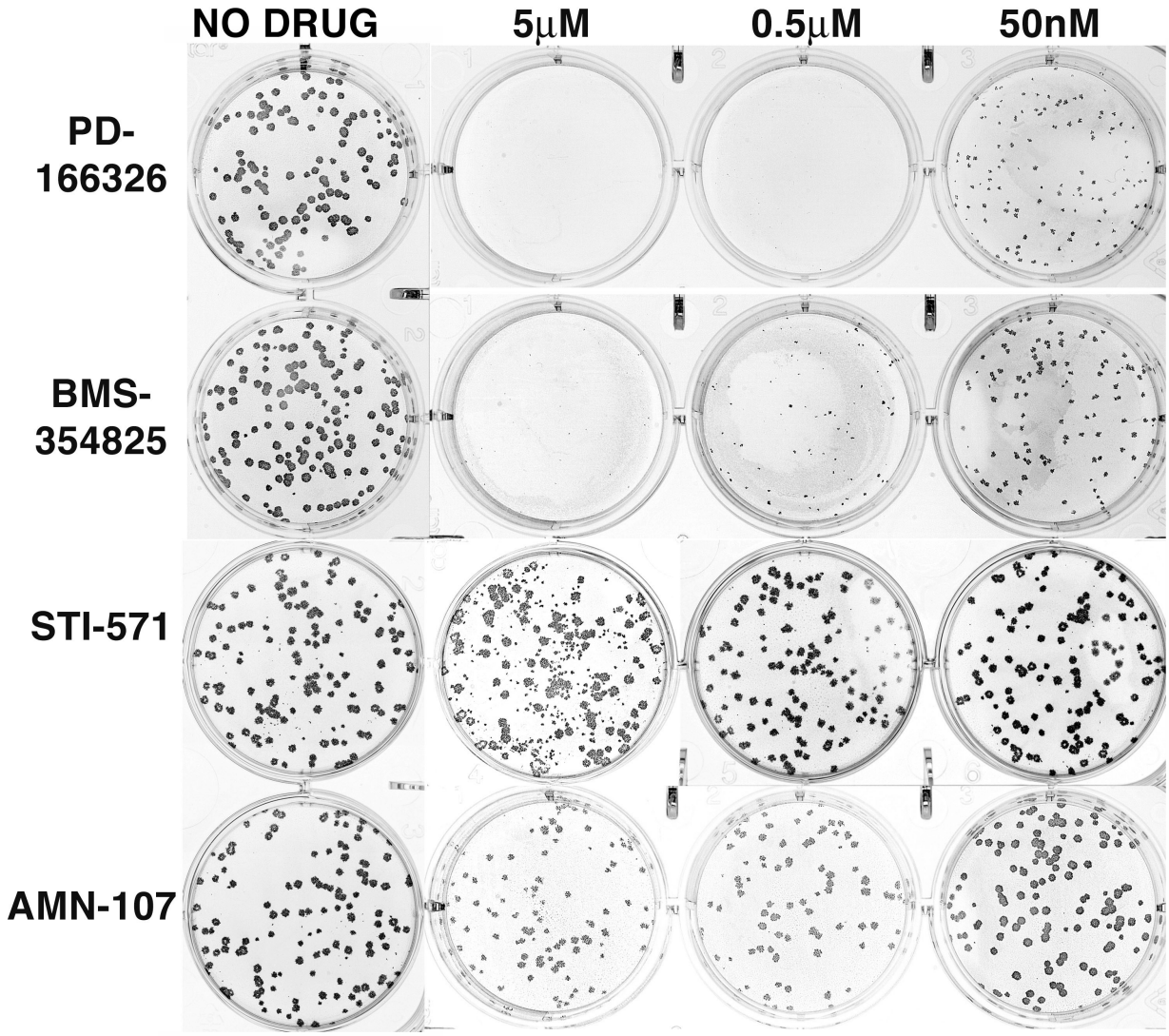

Supplemental Figure 5. BMS-354825 *In Vivo*. Quantification of viral genomes and spleen weight from VacV infected mice (**a**) Mice received 0.05 to 240 mg/kg/d BMS-354825 via osmotic pump and were infected IP with 10^4 PFUVacV IHD-J. Total number of viral genome copies was determined 4 d post infection. (**b**) Spleen weights were determined for mice left untreated or treated with various drugs.

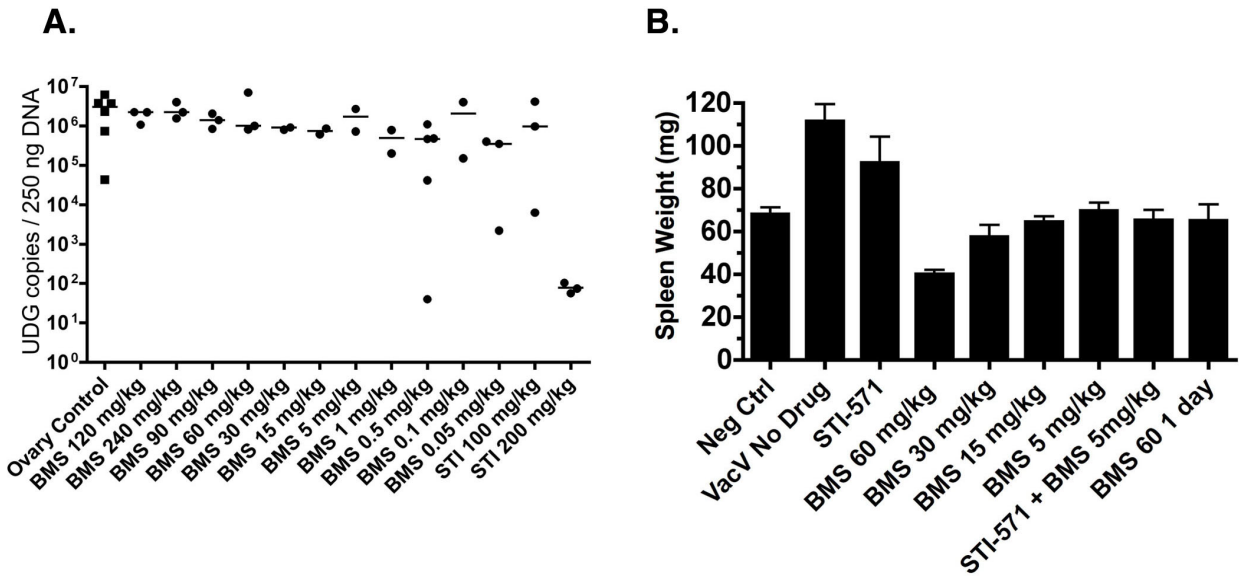

Chapter 5

Future Directions

Future Directions

Why might the virus make use of multiple kinases? In healthy cells the activity and specificity of tyrosine kinases is tightly regulated (5). However, several pathogens bypass the stringent controls on tyrosine kinases as part of their pathogenic program (3). In the case of vaccinia, phosphorylation of the viral protein A36R is critical for efficient viral dissemination (11). It is plausible that those virions bearing the most readily phosphorylated sequences were most likely to spread to and infect neighboring cells. This positive selection may have engendered sequences that enable A36R to act as promiscuous substrate. Poxviruses infect a variety of cell types and in the case of variola and monkeypox, several distinct host species. Therefore, sequences facilitating the phosphorylation by a diverse group of kinases may offer a growth and/or host range advantage. In light of the numerous and varied cellular functions associated with Abl- and Src-family kinases, (stress response, immune-signaling, motility, and differentiation) it is conceivable that the use of multiple kinases confers as yet un-described benefits to poxviruses. Indeed, both Src- and Abl-family kinases contribute in various aspects of immune signaling including inflammation, antigen receptor signaling, and natural killer cell (NK) development (4, 6, 8). Interfereing with NK cells or antigen presentation via tyrosine kinase

interactions may facilitate immune-evasion. To usurp host kinase activity and induce actin polymerization, the virus must first recruit kinase and overcome kinase specificity requirements. The mechanism by which vaccinia accomplishes this task remains an open area of investigation. However, work with EPEC has illustrated one possible method.

Previous work from our lab using EPEC demonstrated the redundant use of kinases by a pathogen (10). However, we were unable to identify all of the kinases responsible. Subsequent work demonstrated that Tec-family kinases in addition Abl-family kinases could suffice for actin pedestal formation by EPEC(2). The same study also illuminated the mechanism by which EPEC recruits host tyrosine kinases. In a series of elegant experiments, the criteria for functional localization were illustrated. First, it was demonstrated that mutants of Abl lacking the SH3 domain were able to localize to pedestals but were unable to support pedestal formation. Second, the preference for Abl-family kinases was exchanged for the Src-family. To accomplish this a series of mutations were introduced into the EPEC protein Tir. The polyproline region (PPR) and phosphorylation sequences of Tir were exchanged for sequences recognized by Src. Together, these two changes conferred the ability of Src but not Abl-family kinases to induce actin pedestals. Thus, EPEC Tir can recruit Abl- and Tec-family kinases via its PPR and subsequently activates the kinase via SH2-binding. This model is in agreement with models of host mediated c-Src regulation.

Vaccinia recapitulates many aspects of EPEC pedestal formation. Like Tir, the phosphorylation of the viral protein A36R initiates actin polymerization. However, unlike Tir, A36R does not possess sequences consistent with known SH3 binding motifs. How then does vaccinia recruit and activate host tyrosine kinases? Perhaps viral proteins other than A36R contribute to the recruitment and activation of host tyrosine kinases. Evidence in support of this possibility can be found in work with the viral protein B5R. Both A36R and B5R are located in the outer membrane of virus and are retained beneath the virion upon reaching the plasma membrane. Importantly, the extra-cellular region of B5R contains four short-census repeats (SCR1-4) that are required for the formation actin tails (9). Further, removal or mutation of SCR4 from B5R is sufficient to prevent kinase activation, A36R phosphorylation and actin tail formation (7). It is not known how the extracellular portion B5R activates the kinase or how B5R stimulates the localized activation of the kinase. Additionally, it is not clear whether B5R is sufficient for recruitment or only serves to activate kinase following recruitment.

How does vaccinia recruit host tyrosine kinases? Perhaps a second viral protein acts as “bait” and facilitates the recruitment of the kinase. Subsequently, B5R can activate the kinase to facilitate the phosphorylation of A36R. Unpublished data from our lab suggests that another viral protein F13L is tyrosine phosphorylated (figure 1). F13L is located in the same membrane as A36R and B5R. *In silico* analysis predict several SH2 and SH3 binding sites for both Abl and Grb2, in addition to Src phosphorylation sites (figure 1). However,

such analysis is highly speculative. Previous work indicates that deletion or mutation of F13L can disrupt morphogenesis and blocks actin tails (1). To test the role of F13L phosphorylation in morphogenesis or dissemination we generated a series of Y to F point mutations in residues implicated by the *in silico* analysis. Preliminary analysis demonstrates that all mutants grow normally and retain the capacity to form actin tails (figure 2 and 4). However, two mutants exhibit strong phenotypes with regard to EEV production. The Y335F mutant is enhanced in EEV release, while the Y252F mutant is diminished (figure 3). Further studies will attempt to identify the tyrosine residue(s) phosphorylated on F13L and assess the *in vivo* consequences of these mutations. The observations with F13L highlight another area of active investigation. The substrate of Abl-family kinases that governs EEV release remains unknown. In light of the mutant phenotypes with F13L and EEV release and the recognition of at least one phosphotyrosine residue via western blot, F13L may well participate in EEV release. However, treatment with STI-571 to block Abl kinases does not block F13L phosphorylation, while BMS-354825 inhibition of Src and Abl does (figure 1). Perhaps several residues on F13L are phosphorylated, as with A36R. Further analysis of current F13L mutations as well as the creation of additional mutant alleles is likely necessary to ascertain any contribution to actin tails and EEV release. Unfortunately, the resolution of western blot analysis is not sufficient to distinguish between a single and multiple phosphorylations. However, future analysis of the mutant alleles via western blot may shed further light on the issue.

Additional analysis via mass-spectrometry is likely necessary to perform a complete investigation. Regardless of which F13L site(s) is phosphorylated, the phenotypes of the mutants generated suggest several interesting avenues of investigation.

Work to determine the effects of the F13L mutations on dissemination and pathogenesis *in vivo* is of particular interest. Other methods are tempered by caveats. Vaccination with EEV specific proteins or introduction of EEV antibodies can also lead to recognition of infected cells as well as virions on the tips of actin tails. To date no other mutants have been generated that affect EEV release without demonstrating epistatic effects. Treatment with STI-571 does limit EEV without effect on replication, morphogenesis or actin tail formation. However, we cannot exclude the possibility that STI-571 may have additional off-target effects that may help curtail pathogenesis. These mutants offer a unique opportunity to investigate the contribution of EEV to pathogenesis.

Of particular interest are tests to explore the effect of F13L mutations either enhancing or limiting EEV release on the disease course in mice. We expect that the EEV decreased mutant will be attenuated *in vivo*. However, we are uncertain if the mutant enhanced in EEV release is likely to exhibit no change, attenuation, or enhanced pathogenesis. The outcome of this experiment will be important information regardless of the result. To gain further insights on the effect of these mutations on the kinetics of spread, we have developed a strain of vaccinia that expresses luciferase. In collaboration with Steve Thorne,

we will infect mice with luciferase expressing virus carrying F13L-WT or the F13L mutants that enhance or diminish EEV release and observe the dissemination of the virus. In another set of experiments we will measure the effect of STI-571 administration of viral spread. These experiments will provide a chronological analysis of the effects of the F13L mutations or STI-571 on spread. Together, these experiments may help to illuminate the relative contributions of EEV and actin tails to pathogenesis *in vivo*.

References

1. Blasco, R., and B. Moss. 1991. Extracellular vaccinia virus formation and cell-to-cell virus transmission are prevented by deletion of the gene encoding the 37,000-Dalton outer envelope protein. J Virol 65:5910-20.
2. Bommarius, B., D. Maxwell, A. Swimm, S. Leung, A. Corbett, W. Bornmann, and D. Kalman. 2007. Enteropathogenic Escherichia coli Tir is an SH2/3 ligand that recruits and activates tyrosine kinases required for pedestal formation. Mol Microbiol 63:1748-68.
3. Frischknecht, F., and M. Way. 2001. Surfing pathogens and the lessons learned for actin polymerization. Trends Cell Biol 11:30-38.
4. Gadue, P., N. Morton, and P. L. Stein. 1999. The Src family tyrosine kinase Fyn regulates natural killer T cell development. J Exp Med 190:1189-96.
5. Hantschel, O., and G. Superti-Furga. 2004. Regulation of the c-Abl and Bcr-Abl tyrosine kinases. Nat Rev Mol Cell Biol 5:33-44.
6. Kim, J. Y., Y. G. Lee, M. Y. Kim, S. E. Byeon, M. H. Rhee, J. Park, D. R. Katz, B. M. Chain, and J. Y. Cho. 2009. Src-mediated regulation of inflammatory responses by actin polymerization. Biochem Pharmacol.

7. **Newsome, T. P., N. Scaplehorn, and M. Way. 2004. SRC mediates a switch from microtubule- to actin-based motility of vaccinia virus. Science 306:124-9.**

8. **Phipps, D. J., S. Yousefi, and D. R. Branch. 1997. Increased enzymatic activity of the T-cell antigen receptor-associated fyn protein tyrosine kinase in asymptomatic patients infected with the human immunodeficiency virus. Blood 90:3603-12.**

9. **Rodger, G., and G. L. Smith. 2002. Replacing the SCR domains of vaccinia virus protein B5R with EGFP causes a reduction in plaque size and actin tail formation but enveloped virions are still transported to the cell surface. J Gen Virol 83:323-32.**

10. **Swimm, A., B. Bommarius, Y. Li, D. Cheng, P. Reeves, M. Sherman, D. Veach, W. Bornmann, and D. Kalman. 2004. Enteropathogenic Escherichia coli use redundant tyrosine kinases to form actin pedestals. Mol Biol Cell 15:3520-9.**

11. **Wolffe, E. J., A. S. Weisberg, and B. Moss. 1998. Role for the vaccinia virus A36R outer envelope protein in the formation of virus-tipped actin-containing microvilli and cell-to-cell virus spread. Virology 244:20-6.**

Figure Legends

Figure 1

a. Schematic of A36R and F13L

b. Western blot of F13L-GFP immunoprecipitated with polyclonal anti-GFP and probed for p-Tyr with monoclonal antibody 4G10

Figure 2

F13L mutant viral growth and EEV production. BSC-40 cells were infected with a moi of 0.1 or 5. Cells were incubated for 24 hours; both cells and supernatant were harvested. **A**. The cells were lysed and total viral progeny measured. **B.** The supernatant was treated with anti-IMV antibody and infectious EEV determined on naïve monolayers.

Figure 3

BSC-40 cells were infected with ~50 pfu and incubated for 48 hours. Cells were fixed and stained with crystal violet. Note the extent of satellite "comet" plaque formation

Figure 4

NIH-3T3 cells were infected for 18 hours and fixed in paraformaldehyde. FITC-phalloidin was used to label the actin (green) and DAPI labeling of DNA is evident in blue.

c. **Figure 1**

A

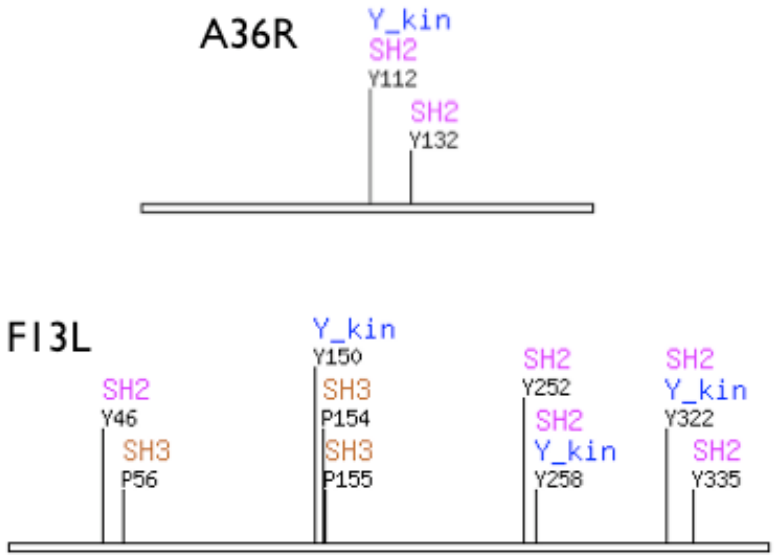
A36R
Y_kin
SH2
Y112
SH2
Y132
F13L
SH2
Y46
SH3
P56
Y_kin
Y150
SH3
P154
SH3
P155
SH2
Y252
SH2
Y_kin
Y258
SH2
Y_kin
Y322
SH2
Y335

B

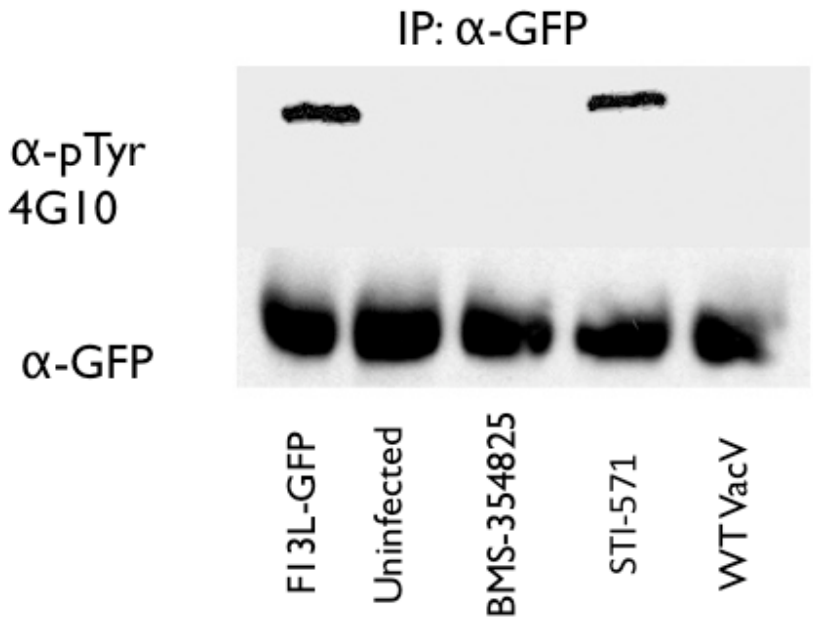
IP: α-GFP
α-pTyr
4G10
α-GFP
F13L-GFP
Uninfected
BMS-354825
STI-571
WT VacV

Figure 2

A.

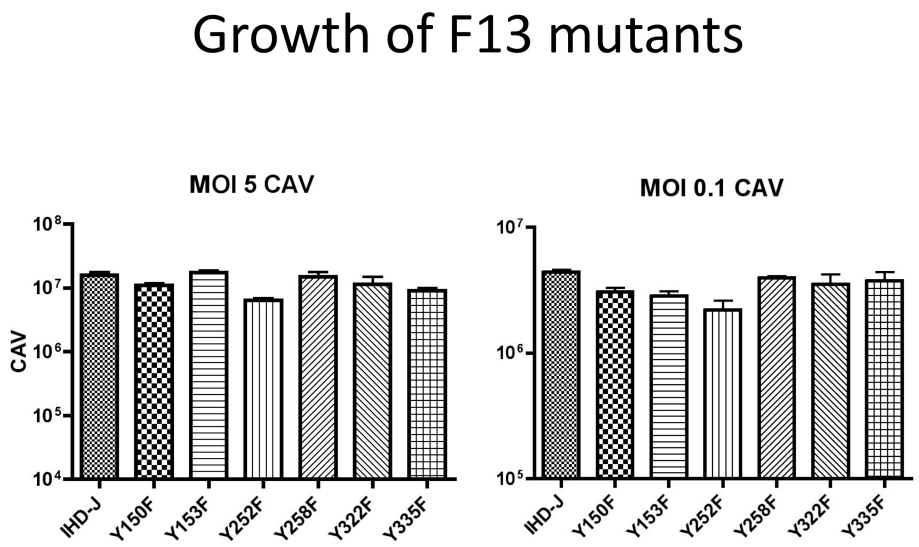
Growth of F13 mutants
MOI 5 CAV
MOI 0.1 CAV
CAV
10^8
10^7
10^6
10^5
10^4
10^7
10^6
10^5
IHD-J
Y150F
Y153F
Y252F
Y258F
Y322F
Y335F

B.

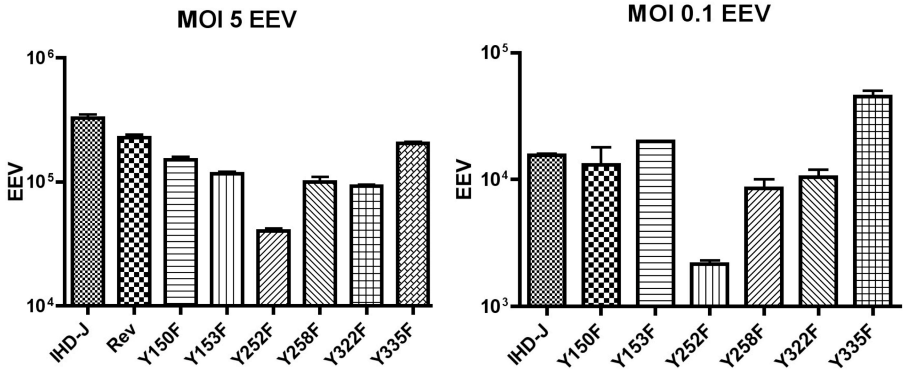
F13 Mutant EEV production
MOI 5 EEV
MOI 0.1 EEV
EEV
10^6
10^5
10^4
10^5
10^4
10^3
IHD-J
Rev
Y150F
Y153F
Y252F
Y258F
Y322F
Y335F

Figure 3

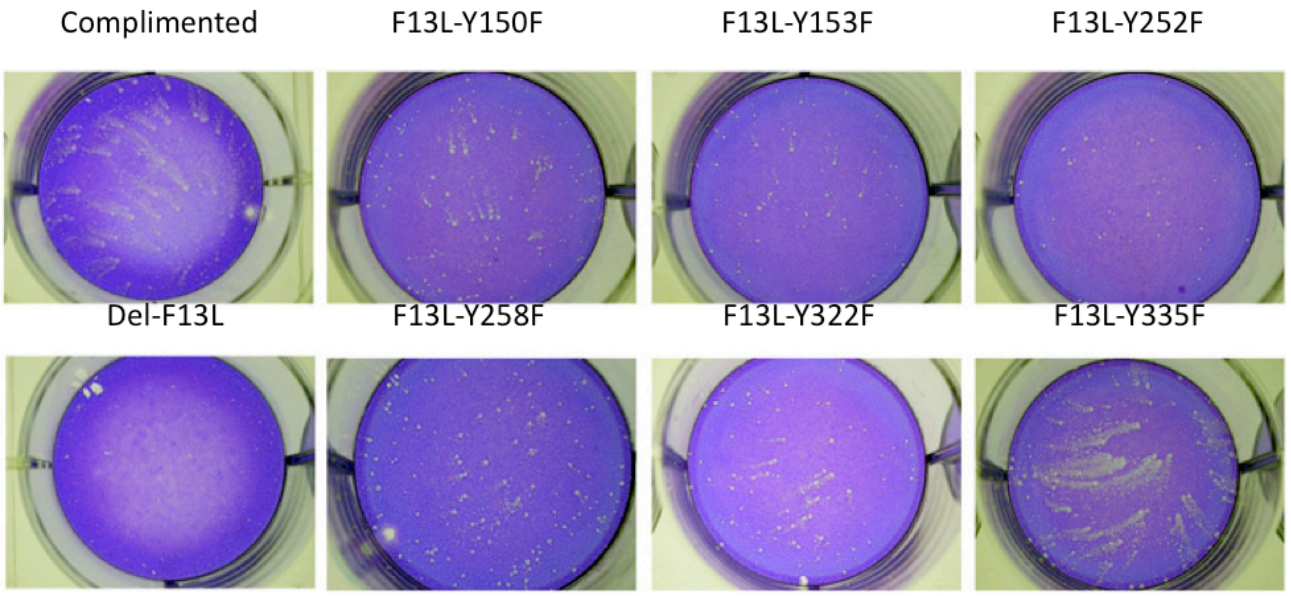
Complimented
F13L-Y150F
F13L-Y153F
F13L-Y252F
Del-F13L
F13L-Y258F
F13L-Y322F
F13L-Y335F

Figure 4

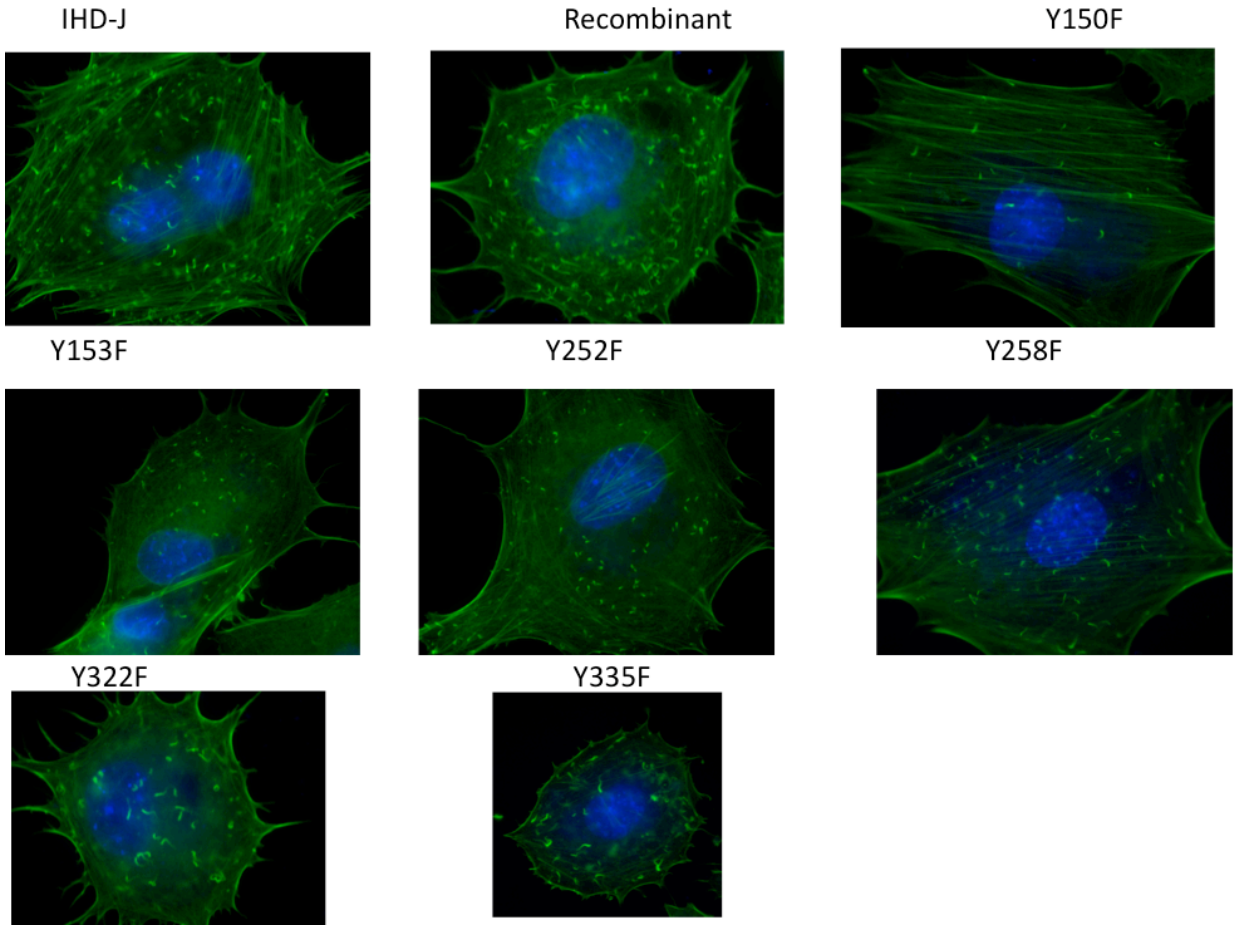

Chapter 5

CONCLUSION

The studies presented were conceived within the context of utilizing microbes to probe mechanisms of pathogenesis and basic cellular functions. Of particular interest to our group was the similarity between the actin polymerizing mechanisms described for EPEC and vaccinia virus (8, 13). In an effort to extend our observations with EPEC, we undertook experiments to explore the role of host tyrosine kinases in the poxvirus pathogenic program.

The study presented in chapter 2 directly tests the possibility that, like EPEC, the poxvirus vaccinia uses host tyrosine kinases in a redundant manner. Using fluorescent deconvolution microscopy, we screened for kinase localization at the tips of actin tails using a panel of antibodies raised against a diverse set of mammalian tyrosine kinases. We observed that members of both the Abl- and Src-family of kinases, but not members of other kinase families, localized to the tips of actin tails. Utilizing cell lines derived from knockout mice we showed that neither Src-family nor Abl-family kinases alone were necessary for the formation of actin tails. To define the kinases responsible for actin tail formation we treated cells lacking Src-family kinases with the small molecule inhibitor of Abl-family kinases, STI-571. We found that STI-571 treated Src-family deficient cells did not support actin tail formation. Similarly, use of the dual Src/Abl inhibitor PD-166326 also blocked the appearance of actin tails. Finally, we tested the sufficiency of each kinase using small molecule inhibitors of tyrosine kinases in combination with cells lacking specific kinases or expressing drug-resistant alleles. We

observed that with vaccinia, Abl2, Src, Fyn, or Yes can suffice for the formation of actin tails. Thus, like EPEC, vaccinia can redundantly use several kinases. Our observations confirmed previous reports that suggested the kinase Src could support vaccinia actin tails. However, previous reports were incomplete, as they failed to note the participation of Abl2, or the Src-family members Fyn or Yes(8).

Vaccinia virus actin tails are an important determinant of plaque size, an *in vitro* measure of viral dissemination. Mutations that prevent actin tail formation reduce plaque size and attenuate *in vivo* pathogenesis. We sought to test the contribution of the various kinases to plaque formation. As our microscopy data would predict, small molecule inhibition of both Src- and Abl-family kinases dramatically reduced plaque size, while inhibition of Abl-family kinases with STI-571 did not reduce plaque size. Surprisingly, while STI-571 did not reduce the size of primary plaques, it did prevent the appearance of the secondary plaques, or comets.

Unlike many other viruses, plaque assays with vaccinia do not utilize an overlay to help preserve the monolayer. Without an overlay, particles released into the media can freely disperse and infect both neighboring and distant cells. When this occurs, plaques can take on the appearance of a comet. Adjacent to the larger primary plaque, several small plaques form as the result of secondary and tertiary infections. It is thought that the release of extracellular enveloped virus (EEV) is responsible for the appearance of comets. Indeed, addition of EEV neutralizing antibody to the media can likewise prevent comet appearance.

Additionally, *in vivo* EEV are thought to mediate the dissemination of the virus to distal tissues. This raised the possibility that STI-571, an FDA approved anti-cancer drug, could be used to limit the spread of vaccinia *in vivo*.

To test the possible utility of STI-571, we infected mice intraperitoneally and after 4 days measured the amount of the virus in the ovaries, where the virus is known to accumulate. Using a Q-PCR analysis, we observed that treatment of mice with STI-571 decreased viral load by nearly 5 logs relative to the infected controls. In light of these findings, we tested the ability of STI-571 to protect mice from lethal challenge. We observed that STI-571 treatment protected mice from an otherwise lethal infection.

Through experiments originally intended to explore the cell biology of vaccinia virus actin motility, the study was extended in scope and several additional observations were made. Our results indicate: vaccinia uses host tyrosine kinases in a redundant manner to form actin tails, Abl-family kinases mediate the release of EEV, and use of STI-571 can protect mice from lethal challenge.

To achieve STI-571 protection in vaccinia infected mice, several factors were taken into consideration. STI-571 does not inhibit viral replication or prevent actin tail formation. Instead, inhibition of Abl-family kinase activity likely retains the virions on or near the surface of the cell, leading to an accumulation of virus. Therefore, if STI-571 drops below the inhibitory concentration, the “pre-loaded” cells can release the virus and dissemination can continue. Related to this

possibility, the half-life of STI-571 in mice is 5-6 hours, versus 12-16 hours in humans. It is not surprising that a twice-daily (2x day) dosing regimen was without benefit. To address this shortcoming, we made use of osmotic pumps implanted subcutaneously between the scapulae of the mice. The osmotic pumps contain a gel that polymerizes at a fixed rate to compress a reservoir. The pumps deliver continuously, enabling consistent levels of drug to be maintained. Additionally, our study utilized a pre-treatment period, in which the pumps were implanted 18-24 hours prior to infection. Steady state is usually achieved at 4.7 x half-life of the compound with continuous delivery, or ~ 25 hours for STI-571 in mice. In effect, the drug achieved steady state simultaneous to infection.

Additional consideration was given to the strain of vaccinia used in the study. Our initial experiments used the vaccinia strain Western Reserve (WR), the most common lab strain. Even with osmotic pump delivery, we were unable to achieve satisfactory protection. Vaccina WR was derived from the Wyeth vaccine strain by serial passage in mouse brains, and exhibits neurotropsim (22). Additionally, the time to death in WR infected mice is 7-8 days and STI-571 accumulation across the blood brain barrier is limited (5). Thus in an effort to mitigate the potential complications inherent to using vaccinia WR we chose to use another vaccinia strain, International Health Department Strain J (IHD-J). We chose IHD-J for a variety of reasons: no known neurotropism, the time to death is 10-14 days, and enhanced EEV release. IHD-J bears a mutation in the A34R gene that enhances EEV release 40 fold (2). We hypothesized that an

IHD-J model would robustly test STI-571, while providing a time to death closer to that of smallpox and providing a longer period for the drug and immune system to combat the infection.

In some regards, STI-571 acts to provide an advantage to the immune system. With IHD-J, the course of infection is sufficiently long to elicit both the innate and adaptive immune responses. Antibodies against core proteins appear after 6 days and neutralizing antibodies after 8 days (17). In this regard, it is critical to utilize mice with a sufficiently mature immune system; however, this requirement is tempered by amount of inoculum needed. We observed an incremental increase in the LD_{100} as mice age. Thus, using strain IHD-J of vaccinia the LD_{100} for 5-6 week old mice was $2.5x10^4$ pfu, and in 8-10 week old mice LD_{100} is $2.5x10^5$ pfu. The immune system of a 6 week-old mouse is sufficient to mount an adaptive response. Thus, our model was achieved: osmotic pump delivery of STI-571 to 6 week-old C57/Bl6 mice infected with $2.5x10^4$ pfu.

The work described in chapter 3 extends our *in vitro* and *in vivo* observations with variola. We again utilized immunofluoresecent deconvolution microscopy to ask if two other orthopoxviruses, monkeypox and variola, form actin tails. We observed that both monkeypox and variola form actin tails and recruit the identical set of host proteins as vaccinia. Additionally, monkeypox and vaccinia both can use Src- or Abl-family tyrosine kinases to form actin tails. Importantly, small molecule tyrosine kinase inhibitors can block variola and

monkeypox actin tail formation and EEV release. The use of dual Src/Abl inhibitors PD-166326 and BMS-354825 blocks actin tail formation and reduces plaque size. BMS-354825 is FDA approved to treat certain cancers. As with variola, STI-571 inhibition of Abl-family kinases does not block actin tail formation nor reduce plaque size in monkeypox or variola infected cells. Similarly, STI-571 treatment prevents the appearance of monkeypox or variola comets.

Collectively, these data demonstrate for the first time that Vaccinia, Monkeypox, and Variola share a conserved mechanism for actin tail formation and EEV release. Further, these findings suggest that drugs effective in limiting vaccinia dissemination and pathogenesis are likely to be effective against monkeypox and variola as well. Our previous study demonstrated the ability of STI-571 to protect mice when administered prior to infection. However, therapeutic value of STI-571 remained unknown. We administered STI-571 either simultaneous to, 24 hours or 48 hours following infection with a lethal dose of virus. Our results indicate administration STI-571 post infection does afford protection. However, as the time following infection increases the ability of STI-571 to protect diminishes. Similarly, increasing the dose to 10x the LD100 overcomes STI-571 protection. Increasing the quantity of tissue infected either with time or dose, limits the ability STI-571 to curtail pathogenesis. These findings are in line with the hypothesis that STI-571 acts to limit inter-tissue dissemination *in vivo*.

The dual Src/Abl inhibitor BMS-354825 inhibits both actin tail and EEV mediated dissemination *in vitro*. We sought to test the ability of BMS-354825 to limit spread and pathogenesis *in vivo*. Mice were either subjected to an intranasal lethal challenge or were inoculated intraperitoneally and viral loads measured. As with STI-571, the dose was determined by the concentrations used successfully in murine cancer studies (5-25 mg/kg/d). However, none of the doses tested afforded protection against lethal challenge. In a series of experiments we tested a range of concentrations from 200 to 0.5 mg/kg/d. Unexpectedly, none of the doses tested reduced viral load nor protected mice from lethal challenge. The studies with BMS-354825 were initiated while clinical trials were on going and the compound had yet to receive FDA approval. During the course of these studies, data was published describing immunosuppressive effects of BMS-354825 in mice, including suppression of both graft rejection and myeloproliferation (6). In agreement with these data, we observed splenopenia in BMS-354825 treated mice. Indeed, co-administration of BMS-354825 with STI-571 abrogated the benefit of STI-571. We were unable to find a concentration of BMS-354825 that limited viral spread, suggesting that the concentration sufficient to limit viral spread is greater than or equal to the immunosuppressive concentration.

In hindsight, the inability of BMS-354825 to limit viral spread *in vivo* is not unexpected. The inhibition of Src-family kinases was likely detrimental to both the innate and adaptive response of the mice. The participation of Src-family kinases, including Fyn, in immune signaling is well documented (12, 20). Notably, Fyn

has been implicated in a variety of immune functions including natural killer cell development and T-cell receptor signaling (4, 18). To form actin tails, poxviruses usurp molecules that can both recruit actin-polymerizing factors and participate in immune signaling. Perhaps poxviruses recruit host kinases to not only spread from cell to cell, but also to disrupt immune system signaling. The disruption or redirection of immune-signaling pathways may modify the host response to viral infection. Other examples of poxvirus immune-modulation are known, the poxvirus protein CrmA was the first viral protein shown to inhibit cytotoxic T-cell mediated apoptosis (21). An intriguing possibility is that poxviruses use kinases to hijack interactions between immune cells as part of their pathogenic program. Interestingly, the Src-family member Lck is tethered to CD4, and participates in its signal transduction (15). Further investigation exploring the interface between infected cells and immune cells may shed light upon this possibility.

What other animal models of monkeypox and variola infection are available? No model system recapitulates all aspects of monkeypox or variola infection of humans. Each model has caveats and particular advantages. Recent reviews describe the utility of two excellent small animal models: ectromelia infection of mice and the rabbitpox or vaccinia infection of rabbits (1, 7). Both systems recapitulate several aspects of smallpox pathology and powerful investigative tools. However, both systems utilize orthopoxvirus family members as surrogates rather than testing monkeypox or variola directly. Until recently, non-human primates were the only models available for the study of monkeypox

or variola. However, the recent appearance of monkeypox in the United States has given rise to another model (3). It was observed that prairie dogs that had previously been in contact with monkeypox infected Gambian rats were one of the vectors likely responsible for spreading monkeypox to humans. From these observations, a prairie dog model of monkeypox infection has recently been described (11). Previous models of monkeypox infection relied on non-human primates and therefore were not readily amenable to the investigation and development of new therapeutic approaches. Monkeypox infection of prairie dogs follows a time course consistent with that of smallpox in humans. Additionally, prairie dogs infected with monkeypox exhibit many symptoms of smallpox infection, including fever, appearance of a rash or pocks. Infected prairie dogs can be analyzed for antibody production, viral titre, and clinical signs of illness. Dissemination can be monitored through the appearance of pocks and evaluated on the number, distribution, and size of the lesions. Thus, the prairie dog model offers an excellent system for evaluating compounds such as STI-571 that limit viral spread. Success in the prairie dog model would suggest that STI-571 warrants investigation in non-human primate models of poxvirus infection.

Collectively, data presented here demonstrate that Vaccinia, Monkeypox, and Variola share conserved mechanisms of actin tail formation and EEV release that depend on the activity of host tyrosine kinases. Additionally, we demonstrate that small-molecule tyrosine kinase inhibitors such as STI-571 can limit dissemination and provide both prophylactic and therapeutic benefit to mice

lethally challenged with vaccinia virus. Together these data suggest STI-571 may exhibit *in vivo* activity against both Monkeypox and Variola virus. These studies provide insight into mechanisms of microbial dissemination and pathogenesis and explore the potential use of kinase inhibitors as therapeutics for microbial infections.

References

1. **Adams, M. M., A. D. Rice, and R. W. Moyer.** 2007. Rabbitpox virus and vaccinia virus infection of rabbits as a model for human smallpox. J Virol **81:**11084-95.
2. **Blasco, R., J. R. Sisler, and B. Moss.** 1993. Dissociation of progeny vaccinia virus from the cell membrane is regulated by a viral envelope glycoprotein: effect of a point mutation in the lectin homology domain of the A34R gene. J Virol **67:**3319-25.
3. **CDC.** 2003. Multistate Outbreak of Monkeypox --- Illinois, Indiana, and Wisconsin, 2003. MMWR **52:**537-540.
4. **Coyne, C. B., and J. M. Bergelson.** 2006. Virus-induced Abl and Fyn kinase signals permit coxsackievirus entry through epithelial tight junctions. Cell **124:**119-31.
5. **Dai, H., P. Marbach, M. Lemaire, M. Hayes, and W. F. Elmquist.** 2003. Distribution of STI-571 to the brain is limited by P-glycoprotein-mediated efflux. J Pharmacol Exp Ther **304:**1085-92.
6. **EMEA.** 2006. Sprycel European Public Assessment Report, p. 46. *In* E. M. Agency (ed.). European Medicines Agency, London.
7. **Esteban, D. J., and R. M. Buller.** 2005. Ectromelia virus: the causative agent of mousepox. J Gen Virol **86:**2645-59.
8. **Frischknecht, F., V. Moreau, S. Rottger, S. Gonfloni, I. Reckmann, G. Superti-Furga, and M. Way.** 1999. Actin-based motility of vaccinia virus mimics receptor tyrosine kinase signalling. Nature **401:**926-9.
9. **Gadue, P., N. Morton, and P. L. Stein.** 1999. The Src family tyrosine kinase Fyn regulates natural killer T cell development. J Exp Med **190:**1189-96.
10. **Hantschel, O., and G. Superti-Furga.** 2004. Regulation of the c-Abl and Bcr-Abl tyrosine kinases. Nat Rev Mol Cell Biol **5:**33-44.
11. **Hutson, C. L., V. A. Olson, D. S. Carroll, J. A. Abel, C. M. Hughes, Z. H. Braden, S. Weiss, J. Self, J. E. Osorio, P. N. Hudson, M. Dillon, K. L. Karem, I. K. Damon, and R. L. Regnery.** 2009. A prairie dog animal model of systemic orthopoxvirus disease using West African and Congo Basin strains of monkeypox virus. J Gen Virol **90:**323-33.
12. **Johnson, P., and J. L. Cross.** 2009. Tyrosine phosphorylation in immune cells: direct and indirect effects on toll-like receptor-induced proinflammatory cytokine production. Crit Rev Immunol **29:**347-67.

13. **Kalman, D., O. D. Weiner, D. L. Goosney, J. W. Sedat, B. B. Finlay, A. Abo, and J. M. Bishop.** 1999. Enteropathogenic E. coli acts through WASP and Arp2/3 complex to form actin pedestals. Nat Cell Biol **1:**389-91.
14. **Kim, J. Y., Y. G. Lee, M. Y. Kim, S. E. Byeon, M. H. Rhee, J. Park, D. R. Katz, B. M. Chain, and J. Y. Cho.** 2009. Src-mediated regulation of inflammatory responses by actin polymerization. Biochem Pharmacol.
15. **Kim, P. W., Z. Y. Sun, S. C. Blacklow, G. Wagner, and M. J. Eck.** 2003. A zinc clasp structure tethers Lck to T cell coreceptors CD4 and CD8. Science **301:**1725-8.
16. **Newsome, T. P., N. Scaplehorn, and M. Way.** 2004. SRC mediates a switch from microtubule- to actin-based motility of vaccinia virus. Science **306:**124-9.
17. **Novembre, F. J., K. Raska, Jr., and J. A. Holowczak.** 1989. The immune response to vaccinia virus infection in mice: analysis of the role of antibody. Arch Virol **107:**273-89.
18. **Phipps, D. J., S. Yousefi, and D. R. Branch.** 1997. Increased enzymatic activity of the T-cell antigen receptor-associated fyn protein tyrosine kinase in asymptomatic patients infected with the human immunodeficiency virus. Blood **90:**3603-12.
19. **Rodger, G., and G. L. Smith.** 2002. Replacing the SCR domains of vaccinia virus protein B5R with EGFP causes a reduction in plaque size and actin tail formation but enveloped virions are still transported to the cell surface. J Gen Virol **83:**323-32.
20. **Salmond, R. J., A. Filby, I. Qureshi, S. Caserta, and R. Zamoyska.** 2009. T-cell receptor proximal signaling via the Src-family kinases, Lck and Fyn, influences T-cell activation, differentiation, and tolerance. Immunol Rev **228:**9-22.
21. **Tewari, M., W. G. Telford, R. A. Miller, and V. M. Dixit.** 1995. CrmA, a poxvirus-encoded serpin, inhibits cytotoxic T-lymphocyte-mediated apoptosis. J Biol Chem **270:**22705-8.
22. **Williamson, J. D., R. W. Reith, L. J. Jeffrey, J. R. Arrand, and M. Mackett.** 1990. Biological characterization of recombinant vaccinia viruses in mice infected by the respiratory route. J Gen Virol **71 (Pt 11):**2761-7.